

2010

Using an autothrottle to compare techniques for saving fuel on a regional jet aircraft

Rebecca Marie Johnson
Iowa State University

Follow this and additional works at: <https://lib.dr.iastate.edu/etd>

 Part of the [Electrical and Computer Engineering Commons](#)

Recommended Citation

Johnson, Rebecca Marie, "Using an autothrottle to compare techniques for saving fuel on a regional jet aircraft" (2010). *Graduate Theses and Dissertations*. 11358.
<https://lib.dr.iastate.edu/etd/11358>

This Thesis is brought to you for free and open access by the Iowa State University Capstones, Theses and Dissertations at Iowa State University Digital Repository. It has been accepted for inclusion in Graduate Theses and Dissertations by an authorized administrator of Iowa State University Digital Repository. For more information, please contact digirep@iastate.edu.

**Using an autothrottle to compare techniques for saving fuel on
A regional jet aircraft**

by

Rebecca Marie Johnson

A thesis submitted to the graduate faculty
in partial fulfillment of the requirements for the degree of
MASTER OF SCIENCE

Major: Electrical Engineering

Program of Study Committee:
Umesh Vaidya, Major Professor
Qingze Zou
Baskar Ganapathayasubramanian

Iowa State University

Ames, Iowa

2010

Copyright © Rebecca Marie Johnson, 2010. All rights reserved.

DEDICATION

I gratefully acknowledge everyone who contributed to the successful completion of this research. Bill Piche, my supervisor at Rockwell Collins, was supportive from day one, as were many of my colleagues. I also appreciate the efforts of my thesis committee, Drs. Umesh Vaidya, Qingze Zou, and Baskar Ganapathayasubramanian. I would also like to thank Dr. Robert Throne, for sparking my interest in controls as an undergraduate student at Rose-Hulman Institute of Technology. Finally, my deepest gratitude to my parents, Ken and Jean, who through their own hard work have shown me the value of persistence and patience.

TABLE OF CONTENTS

LIST OF TABLES	v
LIST OF FIGURES	vii
ABSTRACT	viii
CHAPTER 1. OVERVIEW	1
1.1 Hypotheses	2
1.2 Significance to industry	3
1.3 Background	4
1.3.1 Aerodynamics	4
1.3.2 Practical flight	9
1.3.3 Autothrottle	11
CHAPTER 2. CONTROLLER AND REFERENCE DESIGN	17
2.1 Gain programming control laws	17
2.2 Gain programming control law design	24
2.3 Optimal control laws	28
2.4 Optimal control law design	29
2.5 Proposed methods to calculate reference input	30
2.5.1 Maximum lift-to-drag	31
2.5.2 Mach number for minimum thrust	31
2.5.3 Mach number for maximum velocity times lift-to-drag	31
2.5.4 Mach number for maximum velocity times lift-to-drag divided by TSFC	32
2.5.5 Average Mach number to maximize range	32
CHAPTER 3. METHODS AND PROCEDURES	34
3.1 Model used	34
3.2 Simulation procedures	37
3.3 Implementation of proposed references	37
3.3.1 Determination of constants	37
3.3.2 Calculation of TSFC	38
3.3.3 Maximum lift-to-drag	40
3.3.4 Mach number for minimum thrust	41
3.3.5 Mach number for maximum velocity times lift-to-drag	44
3.3.6 Mach number for maximum velocity times lift-to-drag divided by TSFC	44
3.3.7 Average Mach number to maximize range	46
3.3.8 Optimal control with a singular arc	47
3.4 Disturbances added	51
3.4.1 Winds	52
3.4.2 Variation of Mach number	52

3.4.3	Airspeed reference rounding	52
CHAPTER 4.	RESULTS	54
CHAPTER 5.	DISCUSSION AND SUMMARY	68
5.1	Discussion	68
5.2	Limitations of the method	73
5.3	Practical implementation	74
5.4	Future Work	75
5.5	Summary	75
APPENDIX A.	NOMENCLATURE	76
APPENDIX B.	ALL RESULTS	78
APPENDIX C.	MATLAB CODE	88
BIBLIOGRAPHY	100

LIST OF TABLES

Table 1.1	Basic Autothrottle Functions Over the Flight Profile	10
Table 3.1	Aircraft constant parameters	38
Table 3.2	Numerical values for speed at the maximum lift-to-drag ratio	41
Table 3.3	Numerical values for $U_{minThrust}$	42
Table 3.4	Numerical values for the speed corresponding to maximum $U(L/D)$	44
Table 3.5	Numerical values for the speed corresponding to maximum $U(L/D)/c_T$ at the weight for the start of cruise	45
Table 3.6	Numerical values for the speed corresponding to maximum $U(L/D)/c_T$ at the weight for the end of cruise	45
Table 3.7	Numerical values for the average speed corresponding to maximum $U(L/D)/c_T$ over the weight range for cruise	46
Table 3.8	Numerical values for the average speed corresponding to maximum range	46
Table 3.9	Numerical values for the speed on the singular arc at the weight for the start of cruise	47
Table 3.10	Numerical values for the speed on the singular arc at the weight for the end of cruise	48
Table 3.11	Numerical values for the average speed on the singular arc	48
Table 4.1	Fuel used (nmi/lb) for each method at each altitude	56
Table 4.2	Fuel used (nmi/lb) for each rounding method at 30,000 feet	56
Table 5.1	Rank of top six methods at each altitude with the Mach number rounded to the nearest hundredth	69
Table 5.2	Rank of top six methods at each altitude with the Mach number rounded to the nearest thousandth	70
Table B.1	Fuel used (nmi/lb) for each method with the Mach number rounded to the nearest hundredth at 20,000 feet	78
Table B.2	Fuel used (nmi/lb) for each method with the Mach number rounded to the nearest hundredth at 25,000 feet	79
Table B.3	Fuel used (nmi/lb) for each method with the Mach number rounded to the nearest hundredth at 30,000 feet	79
Table B.4	Fuel used (nmi/lb) for each method with the Mach number rounded to the nearest hundredth at 35,000 feet	80
Table B.5	Fuel used (nmi/lb) for each method with the Mach number rounded to the nearest hundredth at 40,000 feet	80
Table B.6	Fuel used (nmi/lb) for each method with the Mach number rounded to the nearest thousandth at 20,000 feet	81

Table B.7	Fuel used (nmi/lb) for each method with the Mach number rounded to the nearest thousandth at 25,000 feet	81
Table B.8	Fuel used (nmi/lb) for each method with the Mach number rounded to the nearest thousandth at 30,000 feet	82
Table B.9	Fuel used (nmi/lb) for each method with the Mach number rounded to the nearest thousandth at 35,000 feet	82
Table B.10	Fuel used (nmi/lb) for each method with the Mach number rounded to the nearest thousandth at 40,000 feet	82
Table B.11	Fuel used (nmi/lb) for three methods with small Mach variations from the calculated value rounded to the nearest hundredth at 20,000 Feet .	83
Table B.12	Fuel used (nmi/lb) for three methods with small Mach variations from the calculated value rounded to the nearest hundredth at 25,000 Feet .	83
Table B.13	Fuel used (nmi/lb) for three methods with small Mach variations from the calculated value rounded to the nearest hundredth at 30,000 Feet .	84
Table B.14	Fuel used (nmi/lb) for three methods with small Mach variations from the calculated value rounded to the nearest hundredth at 35,000 Feet .	84
Table B.15	Fuel used (nmi/lb) for three methods with small Mach variations from the calculated value rounded to the nearest hundredth at 40,000 Feet .	85
Table B.16	Fuel used (nmi/lb) for three methods with small Mach variations from the calculated value rounded to the nearest thousandth at 20,000 Feet	85
Table B.17	Fuel used (nmi/lb) for three methods with small Mach variations from the calculated value rounded to the nearest thousandth at 25,000 Feet	86
Table B.18	Fuel used (nmi/lb) for three methods with small Mach variations from the calculated value rounded to the nearest thousandth at 30,000 Feet	86
Table B.19	Fuel used (nmi/lb) for three methods with small Mach variations from the calculated value rounded to the nearest thousandth at 35,000 Feet	87
Table B.20	Fuel used (nmi/lb) for three methods with small Mach variations from the calculated value rounded to the nearest thousandth at 40,000 Feet	87

LIST OF FIGURES

Figure 1.1	Aircraft axes of rotation	5
Figure 1.2	TECS block diagram	14
Figure 1.3	SISO autothrottle block diagram	15
Figure 2.1	Maximum thrust (lbs) of one engine at each altitude	25
Figure 2.2	Representation of the nonlinear control law used to control airspeed	27
Figure 3.1	Screen shot of the top level Simulink model of the aircraft	36
Figure 3.2	TSFC data at 35,000 feet with best fit line in the form of Equation 1.15	39
Figure 3.3	TSFC data at 35,000 feet with best fit line in the form of Equation 3.5	40
Figure 3.4	Screen shot of Simulink model used to calculate the Mach number references in real time	43
Figure 3.5	Singular arc at 20,000 feet based on Equation 2.38	49
Figure 3.6	Singular arc at 25,000 feet based on Equation 2.38	49
Figure 3.7	Singular arc at 30,000 feet based on Equation 2.38	50
Figure 3.8	Singular arc at 35,000 feet based on Equation 2.38	50
Figure 3.9	Singular arc at 40,000 feet based on Equation 2.38	51
Figure 3.10	Plot of wind speed and airspeed at 20,000 feet in turbulence	53
Figure 4.1	Comparison of methods at 20,000 feet	57
Figure 4.2	Comparison of methods at 25,000 feet	58
Figure 4.3	Comparison of methods at 30,000 feet	59
Figure 4.4	Comparison of methods at 35,000 feet	60
Figure 4.5	Comparison of methods at 40,000 feet	61
Figure 4.6	Comparison best fuel consumption at each altitude	62
Figure 4.7	Comparison of methods with winds at 20,000 feet	63
Figure 4.8	Comparison of methods with winds at 25,000 feet	64
Figure 4.9	Comparison of methods with winds at 30,000 feet	65
Figure 4.10	Comparison of methods with winds at 35,000 feet	66
Figure 4.11	Comparison of methods with winds at 40,000 feet	67

ABSTRACT

With rising fuel costs there is an initiative to conserve fuel during flight. Several methods have been proposed to calculate an optimum speed to fly during cruise flight to maximize the range of a particular aircraft. This paper compares 11 of these methods using the same aircraft model and discusses how to implement these techniques in an autothrottle. Alternative implementations also include adding the algorithm to the Flight Management System to use during flight planning, or to including it in the databases to use during dispatch calculations. The results show that the speeds calculated by these methods are more fuel efficient than the usual cruise operating speed.

Since flying at the optimum speed is not always practical, this research also looked at the design of the industry autothrottle. Improvements to the industry autothrottle speed control law were implemented to see if improvements to fuel consumption could be achieved at any speed. The results show that the improvements proposed did not improve the fuel consumption during the conditions simulated.

CHAPTER 1. OVERVIEW

Just as a car's fuel-mileage is important to the driver's budget, an airplane's fuel consumption is important to each commercial airline's budget. Rising fuel costs have impacted everyone and greenhouse gas emissions are increasing the impact of global warming around the world. Decreasing the fuel consumption will help both of these problems. Additionally, as some cars have cruise control, some airplanes have automatic throttle control as well. The automatic throttle control in an airplane is called an autothrottle and is usually included as part of the Automatic Flight Control System (AFCS). The AFCS also includes the flight guidance, autopilot, and yaw damper computers. The flight guidance computer calculates commands to help the crew navigate through each phase of flight. The autopilot and yaw damper take the commands from the flight guidance computer and adjust the airplane's surfaces to follow the commands. More detail about the control references of the autothrottle, flight guidance, and autopilot modes is included in Section 1.3.2.

The longest phase of flight for most commercial airplanes is the cruise phase at a constant altitude; in this phase the autothrottle is the AFCS function that is responsible for tracking the speed command input from the crew. Research to improve the range of the aircraft has also been concentrated to this phase of flight as well. The methods proposed have included finding an airspeed corresponding to the maximum point in the range equation, finding an optimal controller to follow a singular arc, and finding an optimal bang-bang controller.

The maximum range equation has several terms; it is used to find the speed corresponding to the maximum point. Several different speeds have been found by assuming that some terms in the range equation are not dependent on speed. These proposed methods take more information into consideration than the normal cruise speed currently specified by the aircraft manufacturer. The constant speeds calculated with this method could be used in current

aircraft and in controlled airspace, provided they are within a range to maintain spacing in traffic.

The two optimal controllers, singular arc and bang-bang, are also designed to maximize range. The singular arc is a curve of weight vs. speed to define a similar speed as the previous equations for the constant speeds corresponding to maximum range [27]. The thrust to fly this curve is also determined. However, in controlled airspace the varying speed in this model may not be practical. The bang-bang controller sets the throttles to minimum thrust or maximum thrust based on switching points [18]. This controller design allows the speed and altitude to vary which is also not practical for controlled airspace. From the published research, it is not evident that either of these approaches has been implemented in a practical system.

This research focuses on implementing 11 methods proposed in the literature on the same airframe using the same techniques that are currently used in industry. The results of several of the methods presented can be implemented on a current system by adjusting the appropriate constants to match to the target airframe. Additionally, modifications to the current industry autothrottle were investigated to try to improve fuel consumption at any speed.

1.1 Hypotheses

The first hypothesis to be tested is that there is one particular airspeed for an airplane to fly that is more efficient than any other. There have been several different methods proposed in the literature for calculating an optimum speed for an airplane. To test this hypothesis each of these methods will be compared using the same aircraft simulation. The practical implementation and automation of these methods will also be considered, including tracking the speed with an industry autothrottle.

The second hypothesis to be tested is that improvements can be made to an industry autothrottle that can help save fuel at any speed. Reducing the amount of throttle activity may increase decrease fuel consumption. To test this hypothesis, techniques to reduce throttle activity will be applied to the industry standard autothrottle control law. To account for one of the nonlinearities of this system, gain scheduling is used in the design of this control law.

1.2 Significance to industry

The outcomes of these hypotheses are important because the air transport industry is extremely competitive and rising fuel costs have impacted every operator. Even small changes in aircraft performance and fuel efficiency can have a cumulative large impact on operating costs. Approximately 81.5 billion US dollars were spent on fuel for aviation in 2006 [17]. The data in [4] shows that there were 10.2 million domestic and international flights operated by U.S. carriers in 2008. This number dropped 6.6 percent in 2009, for a total of 9.6 million domestic and international flights operated by U.S. carriers [5]. In addition to fuel costs, carbon trading schemes for aircraft will be implemented, mostly in Europe, by 2012 [17].

For commercial flights, the majority of flight time is spent in the cruise phase, and as a result, much research has been focused on fuel savings during this phase of flight. Yet, most of this research has been theoretical and has not been applied in industry. One proposed fuel saving method is to use an optimal singular arc flight path. This path would increase the range of the aircraft by seven percent, however, it is not practical to fly using this method in controlled airspace because of the changing airspeed [27]. The ideal solution for controlled airspace is a flight path with constant altitude and an optimum Mach number [26], [18], [10]. Such a Mach number can increase the range from two percent [26], [18] to six percent [10].

An autothrottle is a feature that may be included in an Automatic Flight Control System (AFCS) of an airplane. According to Bader, “the purpose of the Autothrottle is to enhance the ease, economy, and safety of flight operations” [8]. The autothrottle is designed to control the throttle position from takeoff through landing to reduce pilot workload. Since the autothrottle is controlling speed during the cruise phase of flight, allowing the autothrottle to compute the optimum Mach number and hold that value could be a practical way to implement this proposed fuel saving technique.

Jet engines, like other combustion engines, emit carbon dioxide into the atmosphere [17]. This CO₂ can remain in the atmosphere for approximately 100 years [17]. The other major emissions are nitrogen oxides, water vapor, sulphur oxides, and soot [25]. From 1990-2005, the emissions from international aviation decreased by 40 percent [25]. Three changes led to this

decrease: air traffic management, improvements of aircraft and engine design, and an increase in load factors (using an aircraft to capacity) [25]. Because of the growth in the industry during the same period, the total amount of emissions still increased during this same period [25]. The aviation industry is projected to continue to grow about five percent per year until 2025 [25]. While aviation is not presently a significant contributor to the total amount of greenhouse gases, steps to reduce emissions should still be considered [25].

1.3 Background

To understand the system to be controlled, background information on the aerodynamics of an airplane, the uses in practical flight, and existing autothrottle control systems was reviewed. The aerodynamics of the airplane describes the physical characteristics of the plant to be controlled. Additionally, a metric used to calculate fuel consumption is the range an aircraft can travel. The practical flight background provides constraints on the system based on how a typical commercial flight is flown. The existing autothrottle controllers provide a starting point for this research.

1.3.1 Aerodynamics

Both aerodynamic and engine performance equations combine to fully describe aircraft performance. In addition to the aircraft manufactures' published speed and maximum range for a particular model, much research has been done to try to improve the advertised performance of cruise flight. For instance, the research in [26] and [12], focused on the flight conditions that could increase the cruise range performance.

Two coordinate systems that are used when studying aircraft. The first system is the traditional, right-handed earth coordinate system with the x-axis pointing north, the y-axis pointing east, and the z-axis pointing down. The second coordinate system rotates with the aircraft. The x-axis points out the nose, the y-axis out the right wing, and the z-axis points down. Rotation of the aircraft about the x-axis is called roll; rotation about the y-axis is called pitch; and rotation around the z-axis is called yaw. A depiction of this rotation is shown in Figure 1.1 [6].

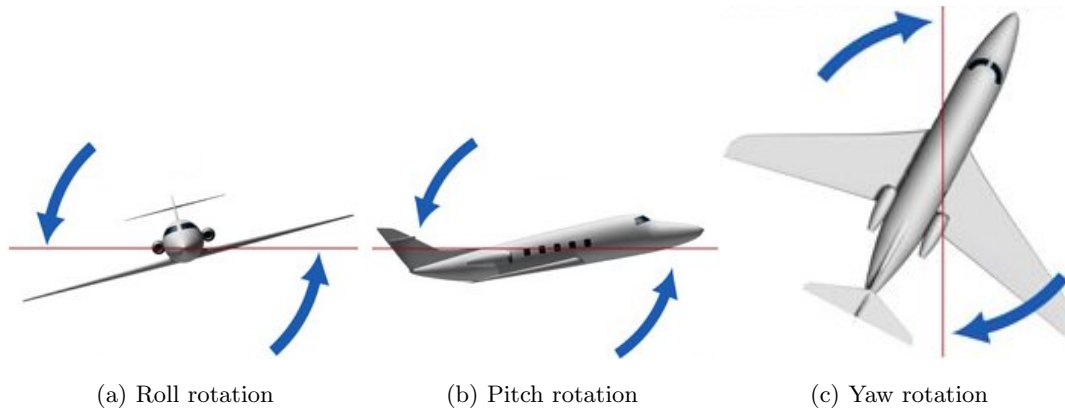


Figure 1.1: Aircraft axes of rotation

The equations to define the aerodynamics of the cruise phase of flight can be split into equations of motion and range equations. The equations of motion define physics-based equations of the flight condition and the range equations define the range the aircraft can fly under current conditions.

1.3.1.1 Equations of motion

The forces acting on an airplane can be classified into four groups. The first is the weight of the aircraft and the direction is down in earth coordinates. The opposing force to weight is the aerodynamic lift on the airplane, in the negative direction of the aircraft z -axis. The lift force is produced by the airfoil-shaped wings and tail on the aircraft. The third force is produced by the jet engines attached to the airframe. Some airplanes have their engines attached to the wings, however in the case studied here the engines are attached to the rear of the fuselage near the tail, symmetrically placed on either side of the x -axis. If both engines are operating, the direction of the thrust force is approximately parallel to the fuselage, in the positive x -direction of the aircraft. Opposing this force is the aerodynamic drag. Drag force is produced by the aircraft and changes in the position of the surfaces, such as elevators, ailerons, spoilers, and stabilizers.

The equations for the forces in each direction acting on the airplane are [28]:

$$\begin{aligned}
 m(\dot{U} - VR + WQ) &= -mg\sin\Theta + F_{A_x} + F_{T_x} \\
 m(\dot{V} + UR - WP) &= mg\sin\Phi\cos\Theta + F_{A_y} + F_{T_y} \\
 m(\dot{W} + UQ - VP) &= mg\cos\Phi\cos\Theta + F_{A_z} + F_{T_z}
 \end{aligned} \tag{1.1}$$

In these equations F_A is the aerodynamic force in the direction specified by the subscript, including both lift and drag, F_T is the force of thrust in the direction specified by the subscript. The speeds in the x, y, and z direction are U , V , and W respectively. The rates of rotation are P , Q , and R , which represent roll rate, pitch rate, and yaw rate respectively. The acceleration due to gravity is g and the mass of the aircraft is m . The pitch angle is represented by Θ and the roll angle by Φ . The equations for the moments about each axis of the airplane are [28]:

$$\begin{aligned}
 I_{xx}\dot{P} - I_{xz}\dot{R} - I_{xz}PQ + (I_{zz} - I_{yy})RQ &= L_A + L_T \\
 I_{yy}\dot{Q} + (I_{xx} - I_{zz})PR + I_{xz}(P^2 - R^2) &= M_A + M_T \\
 I_{zz} - I_{xz}\dot{P} + (I_{yy} - I_{xx})PQ + I_{xz}QR &= N_A + N_T
 \end{aligned} \tag{1.2}$$

In these equations, I is the inertia and the variables L , M , and N are the aerodynamic and thrust moments about the x, y, and z-axis respectively.

For aircraft flying in the cruise phase, the aircraft is assumed to be in rectilinear flight [28]. In this phase several rates and moments can be assumed to be small. The rates of rotation (P , Q , and R) are approximately zero. The flight is assumed to be with wings level (not turning), therefore $\Phi = 0$. In this case the engines are parallel to the x-axis, therefore $F_{T_z} = 0$. Altitude is also assumed to be constant, so V is also zero. With these assumptions, the equations of motion in 1.1 and 1.2 can be simplified to be the forces in the x-direction. In some cases the change in weight can be neglected, although when looking at long flight durations weight change as fuel is used can be a factor. When considering the change in weight a second equation can be added. In this condition, [27] defines the equations of motion as follows:

$$\begin{aligned}
 \dot{U} &= (F_{T_x} - F_{A_x})/m \\
 \dot{m}_{ac} &= -\dot{m}_f
 \end{aligned} \tag{1.3}$$

where the fuel flow rate is \dot{m}_f . The following assumptions were used when deriving the equations of motion in [27]:

$$\begin{aligned} F_{T_x}(U) &= \delta T_M(U, h) \\ \dot{m}_f(U) &= c_T(U) F_{T_x}(U) \\ F_{A_x} &= AU^2 + BL^2/U^2 \end{aligned} \quad (1.4)$$

here

$$\begin{aligned} L &= mg = W \\ A &= C_{D_0}(\rho S/2) \\ B &= (2K/\rho S) \end{aligned} \quad (1.5)$$

In these equations, C_{D_0} is the zero-lift drag coefficient, K is the induced drag factor, ρ is the air density, and S is the wing area, all assumed to be positive constants during cruise flight. The throttle setting is defined as δ , where $\delta_{min} \leq \delta \leq 1$ and T_M is the maximum thrust. The induced drag factor, K , is defined as [26]:

$$K = \frac{1}{\pi e AR} \quad (1.6)$$

In this equation, the aspect ratio of the wing, AR , is defined as the wing span squared divided by the wing area (b^2/S) and e is the Oswald span efficiency factor.

1.3.1.2 Definition of range

In addition to the plant model, a measure of the performance of the aircraft should also be derived, in this case the desired output is the range traveled by the aircraft. In [26], range in nautical miles is a defined function of true airspeed in knots, U , lift-to-drag ratio, L/D , thrust specific fuel consumption (TSFC) in pound per hour per pound, c_T , and aircraft weight, W , as follows:

$$R = \int_{W_{initial}}^{W_{final}} \frac{U}{c_T} \left(\frac{L}{D} \right) \frac{dW}{W} \quad (1.7)$$

If speed, lift-to-drag ratio, and TSFC are assumed to be constant with respect to weight, Equation 1.7 can be simplified to:

$$R = \frac{U}{c_T} \left(\frac{L}{D} \right) \ln \left(\frac{W_{initial}}{W_{final}} \right) \quad (1.8)$$

In [27] and [12] variations of Breguet equation are used for range. The derivation of this range equation starts with the following definition of lift-to-drag ratio:

$$\frac{L}{D} = 2E_{m_0} \frac{\mu^2 w}{\mu^4 - 2k_2 E_{\mu_0} w \mu^2 + w^2} \quad (1.9)$$

where w is the ratio of the current aircraft weight to the aircraft weight at the start of cruise, E_{m_0} is the maximum lift-to-drag ratio defined by [12]:

$$E_{m_0} = \frac{1}{2\sqrt{k_1 C_{D_0}}}, \quad E_m = \frac{1}{2\sqrt{k_1 C_{D_0} - k_2}} \quad (1.10)$$

and $\mu = M/M_{md_0}$, where M_{md_0} is the minimum drag Mach number for the initial conditions of cruise flight defined as [12]:

$$M_{md_0} = \left(\frac{k_1}{C_{D_0}} \right)^{\frac{1}{4}} \left(\frac{2W_0}{\gamma p S} \right)^{\frac{1}{2}} \quad (1.11)$$

In these equations, k_1 and k_2 are both induced drag factors, and γ is the specific heat ratio for air. For a stable condition, $\mu \geq 1$ can be used. Equation 1.9 can be substituted in to Equation 1.7. After solving the resulting integral, the non-dimensional range is [12]:

$$R = \mu^{1-\beta} \left[\tan^{-1} \sqrt{\frac{E_m}{E_{m_0}} \frac{\zeta \mu^2 \sqrt{1+k_2+E_{m_0}}}{\mu^4 - (2-\zeta)k_2 E_{m_0} \mu^2 + (1-\zeta)}} \right] \quad (1.12)$$

where ζ is the cruise fuel weight fraction defined as:

$$\zeta = (W_0 - W_1)/W_0 \quad (1.13)$$

A third definition of range is found in [10]:

$$R = \frac{2UE_{max}}{c_T} \tan^{-1} \left[\frac{\zeta E_0}{2E_{max}(1 - KC_{L_0}\zeta E_0)} \right] \quad (1.14)$$

Here E is the lift-to-drag ratio, the subscript 0 indicates the initial condition and the subscript *max* indicates the maximum value. The variable U is the airspeed, and C_{L_0} is the initial coefficient of lift.

1.3.1.3 Engine

The engine is also an important part of the plant of this system, as such its characteristics are also important. In some situations TSFC is assumed to be constant for all thrust levels [9].

Actual engine data provided in [26] indicates that this is really not the case. This data shows that at full throttle TSFC does not vary much with speed, but at lower throttle settings TSFC varies considerably with speed. TSFC is the fuel consumption rate in pounds per hour for each pound of thrust produced. Both [26] and [10] define TSFC as follows:

$$c_T = c_{T_0} M^\beta \quad (1.15)$$

where β , for turbofan engines, varies from 0.4 to 0.7 for high-bypass ratios and from 0.2 to 0.4 for low-bypass ratios. The term c_{T_0} is the reference TSFC for the current altitude, [10] defines this parameter as follows:

$$c_{T_0} = c_T^* (M_{CR}^*)^{-\beta} (\theta/\theta^*)^{1/2} \quad (1.16)$$

where θ is the relative temperature and the ‘*’ superscript indicates the cruise TSFC, Mach number, and relative temperature specified by the engine manufacturer.

1.3.2 Practical flight

Since the practical implementation of this system was considered in this research, background information on the practical application is included. A description of the phases of flight that the AFCS is used and what term is being controlled by that system during that time is included. Also, there are restrictions placed on aircraft flying in controlled airspace by Air Traffic Control (ATC).

1.3.2.1 Phases of flight

Business jet autothrottle application design goals were established to maximize passenger comfort and minimize unneeded response to temporary environmental variations [8]. Table 1.1 below, is a description of autothrottle and the interaction with the other AFCS functions for each phase of flight [8].

Table 1.1: Basic Autothrottle Functions Over the Flight Profile

	Flight Phase	Flight Director Mode	Autothrottle Function	Autopilot Function
1	Takeoff	Takeoff	Maximum rated thrust	N/A
2	Climb-out	Flight Level Change	Takeoff to Climb thrust transition	Airspeed Control
3	Small-step Climb	Flight Level Change	Reduced climb thrust for smooth transition	Airspeed Control
4	Large-step Climb	Flight Level Change	Full climb thrust	Airspeed Control
5	Top-of-Climb	Altitude Capture	Transition to airspeed control	Altitude Capture
6	Cruise	Altitude Hold	Airspeed control	Altitude Hold
7	Top-of-Descent	Flight Level Change	Transition to minimum thrust	Airspeed Control
8	Descent	Flight Level Change	Maintain minimum thrust	Airspeed Control
9	Approach	Glideslope Track	Airspeed control	Glideslope Track
10	Landing	N/A	Disengage	Disengage
11	Go-Around	Go-Around	Maximum rated thrust	Disengage

The timing of each of these phases of flight is usually imposed by ATC when the flight plan is filed and with enroute instructions. These enroute instructions can have an impact on fuel consumption.

1.3.2.2 Air traffic control

It is the responsibility of ATC to provide clearances to the crew based on known traffic and physical airport conditions. Section 4 of [16], states that ATC may clear an aircraft to a different altitude or route due to traffic conditions. In certain congested areas, ATC may also reroute an aircraft onto a preferred route in order to increase traffic capacity. Each pilot is expected to follow the clearances provided by ATC, unless an amendment to the clearance is obtained. In section 4-4-12, it is explained that ATC may issue speed adjustments to maintain required spacing between aircraft. While complying with a speed adjustment from ATC, the crew must maintain a speed within plus or minus 0.02 Mach number of the speed specified, unless this is outside the safe operating speed of the aircraft.

Changes to this policy could improve fuel efficiency. Approximately 6-12 percent of fuel burned could be saved by more efficient flight plans and decreasing holding patterns [13]. In [11] the impact on fuel consumption when a faster airplane follows a slower airplane is analyzed for a range of 100 nautical miles and three different altitudes. This research showed that an aircraft's performance can be reduced by up to 11 percent when forced to follow a slower airplane. The Federal Aviation Administration (FAA) has proposed a new set of rules for air traffic management that will be rolled out completely by 2025 [14]. These new rules include "Reduce interaction between dependent flows in multiplex airspace," which means that the slower aircraft would be flying in a different traffic flow from the faster airplanes helping to address the impact of faster aircraft following slower aircraft [14].

1.3.3 Autothrottle

Now that the types of controllers, the plant that is being controlled, and the practical use of the system have been described some background on the current autothrottle implementations are provided. There are two types of throttle control proposed in literature. First is a Total Energy Control System (TECS) that combines pitch and throttle control into one multi-input multi-output (MIMO) control law. The second is a single-input single-output (SISO) architecture that has two separate control laws for pitch and throttle. The thrust output of these control laws is a throttle rate command, which is sent to a servo inside the throttle quadrant

assembly (TQA) to move each throttle [20]. This gives the pilot visibility as to what the autothrottle is commanding. This visual feedback was not provided on the A320, a survey of the pilots of this aircraft was conducted, while not having back driving the throttles had some advantages, it was concluded that providing movement of the throttles was preferred [23]. For both types of thrust control, the FAA defines the normal performance criteria to be “smooth and accurate control of thrust without significant or sustained oscillatory power changes or excessive overshoot of the required power setting” [15]. Each of these systems has different design approaches as well as some advantages and disadvantages.

1.3.3.1 Total energy control system

The multi-input multi-output control design is based on a philosophy of controlling all of the energy in the longitudinal axis with one control law, because thrust and pitch changes are tightly coupled [19]. If the elevator is used to hold flight path and the throttle is used to hold speed independently, a movement of the elevator can cause a speed deviation if the throttle is held constant and conversely a movement of the throttle can cause a pitch deviation if the elevator is held constant. This inter dependency has led to research of the MIMO system that controls both elevator and throttle concurrently with the same control law, allowing both to coordinate movement for each maneuver. In the longitudinal axis of the aircraft the energy of the system is the sum of kinetic and potential energy [19]:

$$E_{total} = PE + KE = mgh + 1/2mv_T^2 \quad (1.17)$$

where v_T is the true airspeed of the aircraft and h is the height of the aircraft. The rate of change of energy can be found by taking the derivative of the above equation [19]:

$$\frac{\partial E_{total}}{\partial t} = mg\dot{h} + mv_T\dot{v}_T \quad (1.18)$$

Then this equation can be normalized with weigh and velocity [19]:

$$E_{totalnorm} = \frac{\dot{h}}{v} + \frac{\dot{v}_T}{g} = \gamma + \frac{\dot{v}_T}{g} \quad (1.19)$$

From this equation the thrust required is derived, assuming a point mass equation of motion [19]:

$$T_{req} = mg \left(\sin\gamma + \frac{\dot{v}_T}{g} \right) + D \quad (1.20)$$

To simplify this equation, assume a small flight path angle, γ , and steady level flight. Therefore thrust equals drag and the equation can be expressed using the change in thrust required for a maneuver [19]:

$$\Delta T_{req} = mg \left[\Delta\gamma + \Delta \left(\frac{\dot{v}_T}{g} \right) \right] \quad (1.21)$$

In the TECS the throttle is used to control the change in total energy and elevator is used to control the distribution between kinetic and potential energy [19]. The coordination of these two controls brings the total energy rate and energy distribution rate to zero at the same time. When the airplane is holding altitude and a change in speed is requested, the two commands work together to change the state of kinetic energy while the potential energy remains constant. The potential energy remains the same in this case because the altitude should remain constant. A block diagram of this system is provided in Figure 1.2 [19]. The TECS is designed to allow for situations when the system has reached a thrust limitation. Each phase of flight is designed to have pitch or speed as a priority so that when both cannot be achieved within the thrust limits the term that is most important can be controlled using pitch. In the system described: approach and go around used pitch priority and altitude and pitch modes used speed priority. When the system is in speed priority mode, the cross-term is cut allowing the pitch controller to control to the target speed and pitch angle is open loop, conversely, in pitch priority the pitch controller is used to control glideslope or go around path while speed remains open loop. As soon as thrust is back within the limits of the engine controller, the TECS returns to the original configuration.

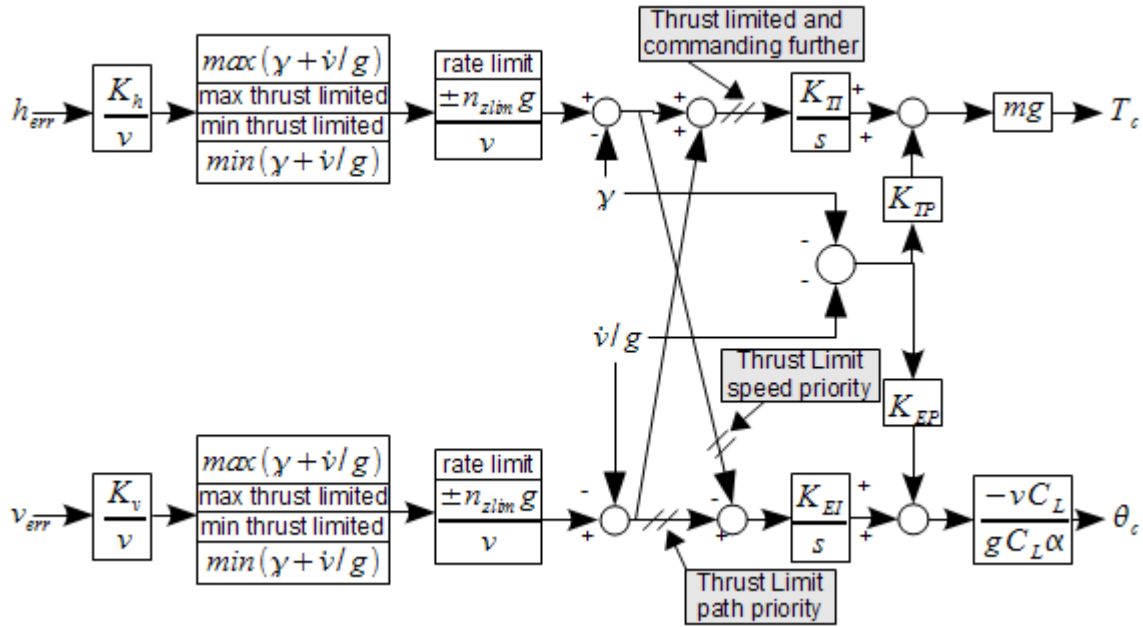


Figure 1.2: TECS block diagram

In [7] a modification to the above system is proposed to deal with significant nonlinearities in the system, including sudden maneuvers and significant winds such as microbursts and wind gusts. To analyze this system, equations to balance the energy of the aircraft, engine, and the surroundings was derived. In the first TECS changes in drag were neglected, the modified energy control system (MECS) proposes that a ΔD term be added as a corrective term. The simulated results of the MECS show that there is improved performance with this corrective term, especially when tracking the glideslope on an approach [7].

1.3.3.2 Separate autothrottle control system

There are two basic closed-loop functions in the SISO autothrottle: thrust control and airspeed control. During the cruise phase of flight, the autothrottle is in a speed-hold mode. In this mode the autothrottle control law commands the throttles to hold the selected airspeed. Figure 1.3 shows a simple autothrottle airspeed loop. In Figure 1.3 K_u represents the autothrottle control law [29]. The throttle servo block is a model of the mechanical servo inside the TQA [29]. The engines are modeled with a gain, K_T , of throttle position to thrust

(lbs/degree) and a lag [29]. The last block of the plant is the transfer function of thrust to airspeed, which is a simplified model of the airplane dynamics [29]. The feedback of the airspeed includes another lag to model the filtering present inside the air data sensor [29]. In [8] the design of this control law for the Gulfstream IV is explained. Prior to the autothrottle control loop, the airspeed target is input into the speed command processor, ensuring that maximum speed limits are not violated and that target transitions are smooth. Within the closed loop airspeed controller, measured airspeed is complemented with inertial acceleration to reduce the effects of unwanted high frequency noise such as wind [8]. To compensate for changes in configuration, aircraft drag information is also included in the control law [8]. Another design parameter is acceleration and deceleration programming configured to smoothly capture the airspeed target [8]. A combination of these features, plus appropriate closed-loop gains, ensure minimal throttle activity with accurate speed control [8]. The last closed loop controller in this mode is an Engine Pressure Ratio (EPR) inner loop. This loop provides more stability and accuracy during speed hold. After applying a lead-lag compensation to the airspeed error, an EPR rate command is computed [8]. The EPR command is adjusted for changes in drag and flight path angle. After the adjustments are made, the EPR command is bounded by the engine limits [8]. From this EPR command a proportional throttle command is calculated. When a Full Authority Digital Engine Control (FADEC) is used a trim command could be sent directly to the engine control to make small adjustments to the EPR without moving the throttles [8]. Because of safety concerns, the authority of this command is limited [8].

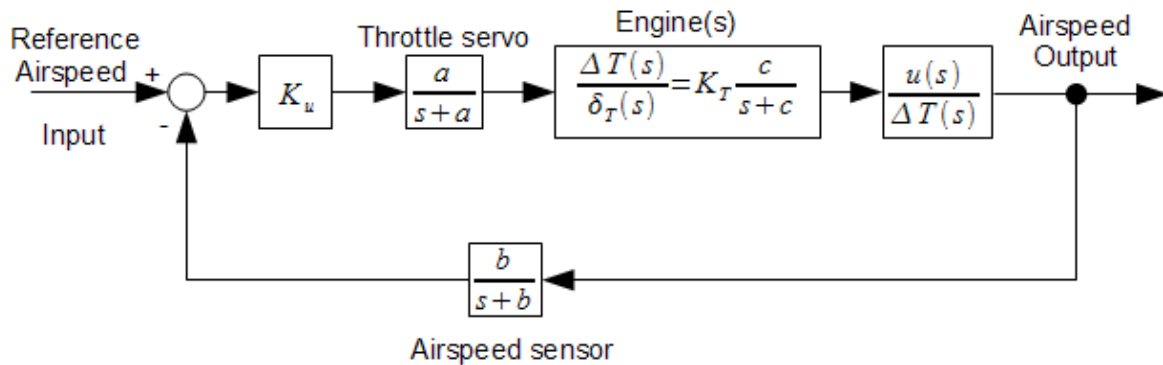


Figure 1.3: SISO autothrottle block diagram

According to [8], a major design compromise is represented by balancing control accuracy and dynamic response with throttle activity. A typical flight crew makes steady and infrequent movements of the throttles, and the autothrottle is expected to mimic this behavior. Passenger comfort is also taken into consideration, since they are able to hear adjustments to the engines and feel changes to aircraft accelerations. Since high-altitude cruise can be the longest phase of flight, passenger comfort and minimal throttle activity was considered to be the top priority. While controlling airspeed, a wind gust can create a speed error equal in magnitude to that of the gust. However, given the bandwidth of this loop, adjusting throttles to compensate for winds, especially turbulence, could cause continuous cycling of the throttles. In this situation the crew would set the throttle to a nominal position [8].

There are advantages and disadvantages of each type of system. The TECS results showed that in simulation, the system was stable and predictable for the conditions tested [19]. The speed was held within 1 knot during altitude changes and altitude deviation was only 10 feet during speed changes [19]. However, the TECS system would require a significant change from current industry designs [19]. For the separate autothrottle the system has a modular architecture and can operate independently of the pitch maneuvers and be developed independently of the flight guidance system [8]. Some coupling terms can be added to the SISO system such as flight path angle and flap position, this would move closer to the MIMO design but with the modular design of the separate autothrottle [8]. Even though the MIMO system has shown good performance in simulation, the separate autothrottle design has had acceptable performance in aircraft since the Gulfstream IV certification in December 1989 [8].

CHAPTER 2. CONTROLLER AND REFERENCE DESIGN

As discussed, the airline industry is interested in saving fuel and reducing pilot workload. The autothrottle is part of the AFCS that helps reduce pilot workload by controlling each engine's throttle. The system that is controlled by the autothrottle is nonlinear; one method considered for autothrottle control law is gain programming. Optimal control is another design methodology used in this research. The design for this application using each of these control methodologies is described. Additionally, the speeds proposed to maximize the range of the aircraft are used to calculate the reference signal used by the autothrottle airspeed control law.

2.1 Gain programming control laws

Gain scheduling is one technique of nonlinear control law design that is used in the flight control and automotive industries [30]. Gain scheduling in autopilots has been used since World War II due to the stability problems in jet aircraft, and increased operating envelopes. One form of gain scheduling is switching gains based on a predetermined time or operating condition. Another form of gain scheduling is to continuously change the controller coefficients based on a scheduling variable or signal. These scheduling variables may be external to the system or feedback from the plant. One feature of gain scheduling is the ability to use well-known linear design techniques. Another feature is that exact definition of the plant does not need to be determined for the entire operating envelope. Additionally, the computational resources required to calculate a control law with scheduling techniques are usually less than with other nonlinear approaches. The scheduled gains can change quickly with the changing parameters of the plant. Also, most performance criteria is defined by frequency and time-domain parameters that can be easily determined from a gain-scheduled control law.

In autopilot design, the loop gain is dependent on the effectiveness of the control surfaces

(elevators, ailerons, and rudder) [30]. These surfaces lose effectiveness as altitude and Mach number increase. Gain scheduling is used in this case to maintain the same loop gain despite the change in effectiveness. Additionally switching to a default value can be used when sensors required for scheduling have an unacceptable failure rate. In the event of a failure, reduced but safe performance is preferred to the loss of the function.

The steps for gain scheduling design are as follows [21]:

1. Compute a model for the plant, then linearize the model about a set of operating points, expressed in terms of the scheduling variable. These linear models will be used as a basis for linearization scheduling.
2. Use linear design techniques to find a control law for each of the linear models. This results in a set of linear controllers with fixed gains for each operating point.
3. Combine the set of controllers into one controller with varying controller gains to cover the operating points.
4. Evaluate the performance at each operating point as well as at other points within the operating envelope of the plant.

To illustrate this process, start with a nonlinear plant model [30]:

$$\begin{aligned}\dot{x} &= a(x, u, w, v) \\ z &= c_1(x, y, w, v) \\ y &= c_2(x, w, v)\end{aligned}\tag{2.1}$$

here x is the state, u is the input, z is the error signal to be controlled, and y is a measured output available to the control law. The measured output can include, penalized variables, tracking commands, and some of the states. The variables w and v are exogenous inputs to the plant, the difference is that w depends on parameters from the plant whereas v is based on external inputs, such as disturbances, noises, and references. An additional distinction is that during the design the system will be linearized with respect to v , but not w [30].

From the nonlinear plant model two different approaches can be used to define the linear models: linear parameter-varying (LPV) model and the quasi-LPV model. In the LPV model,

the equilibrium point of the system defined in Equation 2.1 is defined as x_e , u_e , v_e , and w_e where $a(x_e, u_e, w_e, v_e) = 0$ [30]. The set of equilibrium points, S , is defined as $x_e(\sigma)$, $u_e(\sigma)$, $v_e(\sigma)$, and $w_e(\sigma)$ where:

$$a(x_e(\sigma), u_e(\sigma), w_e(\sigma), v_e(\sigma)) = 0, \quad \sigma \in S \quad (2.2)$$

This set is commonly referred to as an equilibrium family. From this equilibrium family and error equilibrium family can be defined as:

$$z_e(\sigma) = c_1(x_e(\sigma), y_e(\sigma), w_e(\sigma), v_e(\sigma)), \quad \sigma \in S \quad (2.3)$$

Similarly, the measured output equilibrium family is defined as:

$$y_e(\sigma) = c_2(x_e(\sigma), w_e(\sigma), v_e(\sigma)), \quad \sigma \in S \quad (2.4)$$

One method of defining equilibrium points is from a specific $z_e(\sigma)$ called trim points. An example of this would be a system that is designed to track a constant reference, r , with zero steady-state error, then the equilibrium family would satisfy the condition in Equation 2.2 and Equation 2.3 would also be equal to zero. During the design process the scheduling variable, σ , is considered a parameter then it is a time-varying input to the final control law. The final input is defined as $\sigma(t) = g(y(t), w(t))$ [30].

The next part of the process is to define the Jacobian linearization of the plant based on the family of equilibrium points. The plant linearization family can be written in the form [30]:

$$\begin{bmatrix} \dot{x}_\delta \\ z_\delta \\ y_\delta \end{bmatrix} = \begin{bmatrix} A(\sigma) & B_1(\sigma) & B_2(\sigma) \\ C_1(\sigma) & D_{11}(\sigma) & D_{12}(\sigma) \\ C_2(\sigma) & D_{21}(\sigma) & 0 \end{bmatrix}, \quad \sigma \in S \quad (2.5)$$

where,

$$\begin{aligned}
A(\sigma) &= \frac{\partial a}{\partial x}(x_e(\sigma), u_e(\sigma), w_e(\sigma), v_e(\sigma)) \\
B_1(\sigma) &= \frac{\partial a}{\partial v}(x_e(\sigma), u_e(\sigma), w_e(\sigma), v_e(\sigma)) \\
B_2(\sigma) &= \frac{\partial a}{\partial u}(x_e(\sigma), u_e(\sigma), w_e(\sigma), v_e(\sigma)) \\
C_1(\sigma) &= \frac{\partial c_1}{\partial x}(x_e(\sigma), u_e(\sigma), w_e(\sigma), v_e(\sigma)) \\
D_{11}(\sigma) &= \frac{\partial c_1}{\partial v}(x_e(\sigma), u_e(\sigma), w_e(\sigma), v_e(\sigma)) \\
D_{12}(\sigma) &= \frac{\partial c_1}{\partial u}(x_e(\sigma), u_e(\sigma), w_e(\sigma), v_e(\sigma)) \\
C_2(\sigma) &= \frac{\partial c_2}{\partial x}(x_e(\sigma), w_e(\sigma), v_e(\sigma)) \\
D_{21}(\sigma) &= \frac{\partial c_2}{\partial v}(x_e(\sigma), w_e(\sigma), v_e(\sigma))
\end{aligned} \tag{2.6}$$

This completes the derivation of the plant linearization family.

Now, the quasi-LPV method starts by breaking up the plant model in Equation 2.1 into its linear and nonlinear part [30]:

$$x(t) = \begin{bmatrix} x_a(t) \\ x_b(t) \end{bmatrix} \tag{2.7}$$

The nonlinear part of $x(t)$, $x_a(t)$, is combined with the the time-varying scheduling variable:

$$\sigma(t) = \begin{bmatrix} x_a(t) \\ w(t) \end{bmatrix} \tag{2.8}$$

From these assumptions the plant model in Equation 2.1 is written in the quasi-LPV form:

$$\begin{bmatrix} \dot{x}_a \\ \dot{x}_b \\ z \\ y \end{bmatrix} = \begin{bmatrix} A_{11}(\sigma) & A_{12}(\sigma) & B_{1a}(\sigma) & B_{2a}(\sigma) \\ A_{21}(\sigma) & A_{22}(\sigma) & B_{1b}(\sigma) & B_{2b}(\sigma) \\ C_{1a}(\sigma) & C_{1b}(\sigma) & D_{11}(\sigma) & D_{12}(\sigma) \\ C_{2a}(\sigma) & C_{2b}(\sigma) & D_{21}(\sigma) & D_{22}(\sigma) \end{bmatrix} \begin{bmatrix} x_a \\ x_b \\ v \\ \hat{u}(\sigma, u) \end{bmatrix} \tag{2.9}$$

In this model, the value of $\sigma(t)$ is unknown a priori, but is measurable in the final system. The new control input, \hat{u} is invertible with respect to u , which means:

$$\hat{u}^{-1}(\sigma, \hat{u}(\sigma, u)) = u \tag{2.10}$$

From the \hat{u} found in the design with the above system, the actual control can be found using this equation . In this method the plant does not have to be linearized about a family of equilibrium points, just the origin. However, this model introduces additional behaviors that can increase the difficulty of finding the controller.

Each of these methods can be more clearly illustrated with a simple model of a missiles' longitudinal dynamics. The state model is [30]:

$$\begin{aligned}\dot{x} &= MC_n(\alpha, \delta, M)\cos(\alpha) + q \\ \dot{q} &= M^2C_m(\alpha, \delta, M)\end{aligned}\tag{2.11}$$

in this model the states are angle-of-attack, $\alpha(t)$, and pitch-rate, $q(t)$. The parameter $M(t)$ is an exogenous variable representing Mach number and $\delta(t)$ is the tail-fin deflection and the control input. The parameters C_n and C_m represent the aerodynamic coefficients which are assumed to be in the form:

$$\begin{aligned}C_n(\alpha, \delta, M) &= c_n(\alpha, M) + d_n\delta \\ C_m(\alpha, \delta, M) &= c_m(\alpha, M) + d_m\delta\end{aligned}\tag{2.12}$$

The output of this system is normal acceleration, $\eta(t)$, defined as:

$$\eta = KM^2C_n(\alpha, \delta, M)\tag{2.13}$$

here K is a constant. The usual control problem is to design a control with the objective of producing a $\delta(t)$ command such that $\eta(t)$ tracks a commanded $\eta_{com}(t)$, that is $z(t) = \eta_{com}(t) - \eta(t)$. If α and M are chosen as the scheduling parameters the system can be rewritten as:

$$\begin{aligned}\delta_e &= \frac{-c_m(\alpha, M)}{d_m} \\ q_e(\alpha, M) &= M \left[\frac{d_n c_m(\alpha, M)}{d_m} - c_n(\alpha, M) \right] \cos(\alpha) \\ \eta_e(\alpha, M) &= KM^2 \left[c_n(\alpha, M) - \frac{d_n c_m(\alpha, M)}{d_m} \right]\end{aligned}\tag{2.14}$$

From this, the corresponding linearization family is:

$$\begin{bmatrix} \dot{x}_\delta \\ \dot{q}_\delta \end{bmatrix} = \begin{bmatrix} M \frac{\partial c_n}{\partial \alpha} \cos(\alpha) - \left[M c_n - \frac{M d_n c_m}{d_m} \right] \sin(\alpha) & 1 \\ m^2 \frac{\partial c_m}{\partial \alpha} & 0 \end{bmatrix} \begin{bmatrix} x_\delta \\ q_\delta \end{bmatrix} + \begin{bmatrix} M d_n \cos(\alpha) \\ M^2 d_m \end{bmatrix} \delta_\delta \quad (2.15)$$

$$\eta_{delta} = \begin{bmatrix} K M^2 \frac{\partial c_n}{\partial \alpha} & 0 \end{bmatrix} \begin{bmatrix} x_\delta \\ q_\delta + (K M^2 d_n) \delta_\delta \end{bmatrix}$$

This completes the linearized plant description of this system. From this point a controller can be designed using the methods discussed later in this section.

Next, for the quasi-LPV method start with the same plant in Equation 2.11. Then perform a change of variables for q , δ , and η to represent the deviation from an equilibrium point, as follows [30]:

$$\begin{aligned} \hat{q} &= q - q_e(\alpha, M) \\ \hat{\delta} &= \delta - \delta_e(\alpha, M) \\ \hat{\eta} &= \eta - \eta_e(\alpha, M) \end{aligned} \quad (2.16)$$

The state equations become:

$$\begin{aligned} \dot{\alpha} &= \hat{q} + M d_n \cos(\alpha) \hat{\delta} \\ \dot{\hat{q}} &= -\frac{\partial q_e(\alpha, M)}{\partial \alpha} \hat{q} + \left(M^2 d_m - M d_n \cos(\alpha) \frac{\partial q_e(\alpha, M)}{\partial \alpha} \right) \hat{\delta} - \frac{\partial q_e(\alpha, M)}{\partial M} \dot{M} \\ \dot{\hat{\eta}} &= K M^2 d_n \hat{\delta} \end{aligned} \quad (2.17)$$

This moves the equilibrium point to the origin. The derivative of Mach number can be used as a new disturbance input [30]. The quasi-LPV model derived from these equations is:

$$\begin{bmatrix} \dot{\alpha} \\ \dot{\hat{q}} \\ \dot{\hat{\eta}} \end{bmatrix} = \begin{bmatrix} 0 & 1 & 0 & b_{2a}(\sigma_1, \sigma_2) \\ 0 & a_{22}(\sigma_2, \sigma_2) & b_{1b}(\sigma_2, \sigma_2) & b_{2b}(\sigma_2, \sigma_2) \\ 0 & 0 & 0 & d_{22}(\sigma_2) \end{bmatrix} \begin{bmatrix} \alpha \\ \hat{q} \\ \dot{M} \\ \hat{\delta} \end{bmatrix} \quad (2.18)$$

Now that the plant and its linear models have been defined, the next step is to define the parameterized linear controller family corresponding to the system in Equation 2.5. The notation used to describe this controller is [30]:

$$\begin{bmatrix} \dot{x}_\delta^c \\ u_\delta \end{bmatrix} = \begin{bmatrix} F(\sigma) & G(\sigma) \\ H(\sigma) & E(\sigma) \end{bmatrix} \begin{bmatrix} x_\delta^c \\ y_\delta \end{bmatrix}, \quad \sigma \in S \quad (2.19)$$

This leads to a family of controllers for each σ corresponding to the family of equilibrium points [30]. Normally this set of controllers are interpolated with respect to σ , in a continuous way. Interpolating between each $F(\sigma)$ is one to achieve a controller for every possible σ . The goal of gain programming is to design a linear control family, in the form of Equation 2.19, with the general form:

$$\begin{aligned}\dot{x}^c &= f(x^c, y, w) \\ u &= h(x^c, y, w)\end{aligned}\tag{2.20}$$

Combining Equations 2.1 and 2.20 at one of the equilibrium points leads to a function, $x_e^c(\sigma)$, such that:

$$\begin{aligned}0 &= f(x_e^c(\sigma), y_e(\sigma), w_e(\sigma)) \\ u_e(\sigma) &= h(x_e^c(\sigma), y_e(\sigma), w_e(\sigma)) \\ \sigma &\in S\end{aligned}\tag{2.21}$$

This means that the controller satisfies the equilibrium conditions. To relate this outcome back to the controller in Equation 2.19:

$$\begin{aligned}\frac{\partial f}{\partial x^c}(x_e^c(\sigma), y_e(\sigma), w_e(\sigma)) &= F(\sigma) \\ \frac{\partial h}{\partial y}(x_e^c(\sigma), y_e(\sigma), w_e(\sigma)) &= E(\sigma) \\ \sigma &\in S\end{aligned}\tag{2.22}$$

Using the equilibrium points, the controller in Equation 2.19 can also be defined in the form:

$$\begin{aligned}\dot{x}^c &= F(\sigma)[x^c - x_e^c(\sigma)] + G(\sigma)[y - y_e(\sigma)] \\ u &= H(\sigma)[x^c - x_e^c(\sigma)] + E(\sigma)[y - y_e(\sigma)] + u_e(\sigma) \\ \sigma &\in S\end{aligned}\tag{2.23}$$

As mentioned earlier, the final implementation of the controller sets $\sigma(t) = g(y(t), w(t))$, substituting this into the above equation leads to the final representation of the gain scheduled controller [30]:

$$\begin{aligned}\dot{x}^c &= F(g(y, w))[x^c - x_e^c(g(y, w))] + G(g(y, w))[y - y_e(g(y, w))] \\ u &= H(g(y, w))[x^c - x_e^c(g(y, w))] + E(g(y, w))[y - y_e(g(y, w))] + u_e(g(y, w))\end{aligned}\tag{2.24}$$

Now that these equations are no longer depending on σ when the plant and controller are linearized together hidden coupling terms may appear in the system. Reference [30] gives

Theorem 10 to determine if a system has hidden coupling terms, it states “Given the linear controller family (2.19), there exists a gain scheduled controller (2.24) with no hidden coupling terms if there exists a controller equilibrium function $x_e^c(\sigma)$ satisfying

$$\begin{aligned} F(\sigma) \frac{\partial x_e^c(\sigma)}{\partial \sigma} + G(\sigma) \frac{\partial y_e(\sigma)}{\partial \sigma} &= 0 \\ \frac{\partial u_e(\sigma)}{\partial \sigma} - H(\sigma) \frac{\partial x_e^c(\sigma)}{\partial \sigma} - E(\sigma) \frac{\partial y_e(\sigma)}{\partial \sigma} &= 0 \end{aligned} \quad (2.25)$$

for $\sigma \in S$ ”

Starting with the initial nonlinear plant a family of equilibrium points led to a family of linearized models. From each of these linear models a family of controllers was designed, then interpolation is used to connect the family of controllers into one smooth, continuous controller. Once this controller is designed simulation and analysis can be performed to check the performance of the controller at the equilibrium points and at various points in between. The interpolation technique may need to be adjusted to achieve the desired performance between the family of controllers. After the simulation and analysis is complete, the gain scheduled controller design is complete.

2.2 Gain programming control law design

As discussed in 2.1, gain programming is a method used to design non-linear control laws. The controller used in this research is a basic proportional-derivative control law that uses two different gain programmers and is designed to track airspeed. One programmer varies the command based on altitude, because as altitude increases thrust decreases. This decrease in thrust is shown in Figure 2.1. Adding a gain programmer allows for the command to be increased as altitude increases. The second gain programmer is programmed with the average throttle lever angle. At low thrust settings the engine takes longer to respond to thrust settings, so to help prevent excessive movement, lower gains are used at low throttle angles. Another compensation that is used in this control law is pitch angle. While tracking altitude, the pitch angle is not used because the changes in pitch angle are small. However, during other phases of flight, initial changes in pitch angle should be accounted for when controlling speed, because the angle of the force of thrust is changing. Once an initial compensation for pitch angle has

been added, it is washed out, so pitch angle does not create an unnecessary long term bias in the command. A representation of the autothrottle control law is included in Figure 2.2.

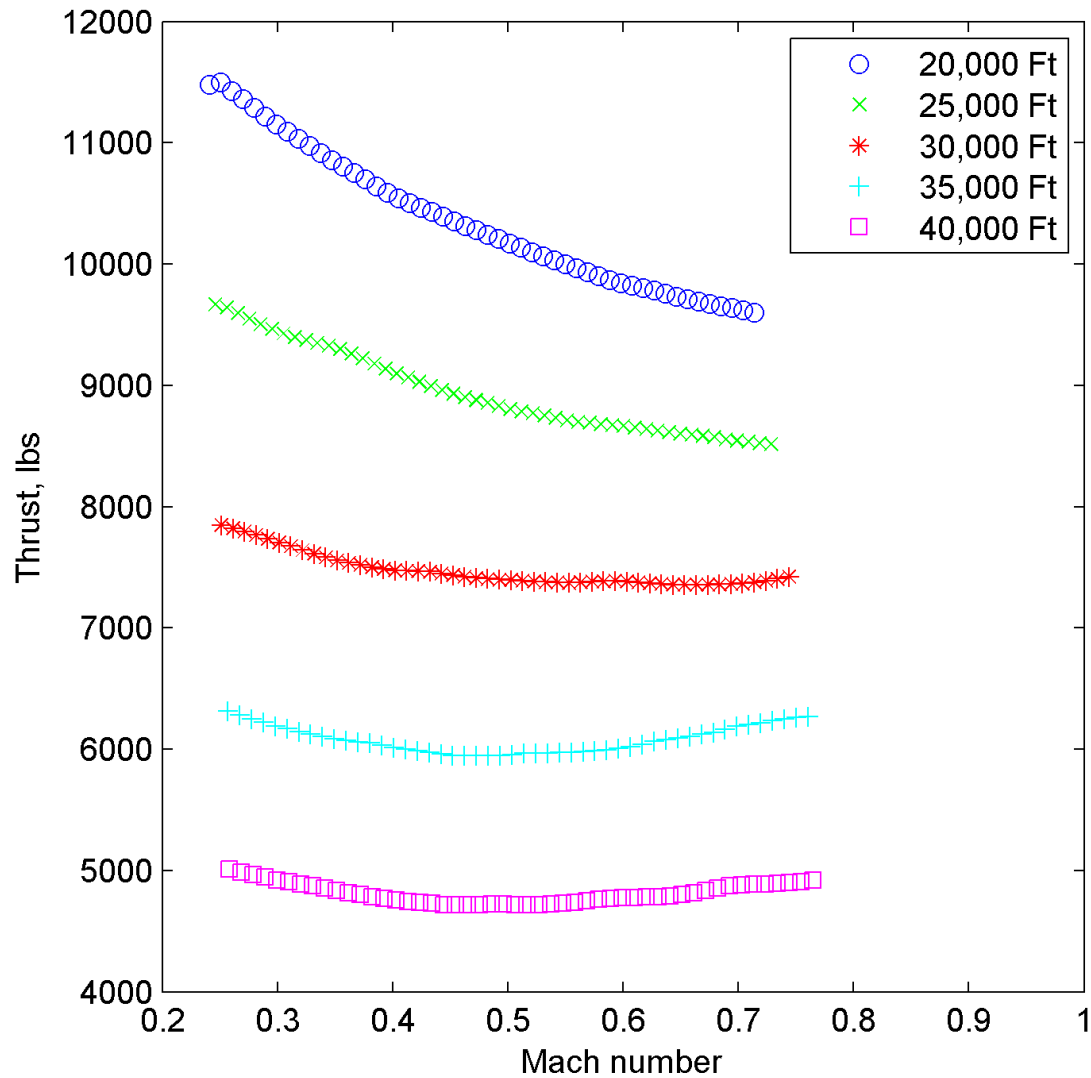


Figure 2.1: Maximum thrust (lbs) of one engine at each altitude

Several changes were made to this control law to reduce throttle activity and fuel consumption. The first change was to reduce the gains of the proportional and derivative paths of the control law. The second was to remove the fine control parameter that is sent directly to

the engine, staying with the original gains and the lower gains. By removing the fine control parameter, the amount of dead zone is increased before a change of thrust is commanded.

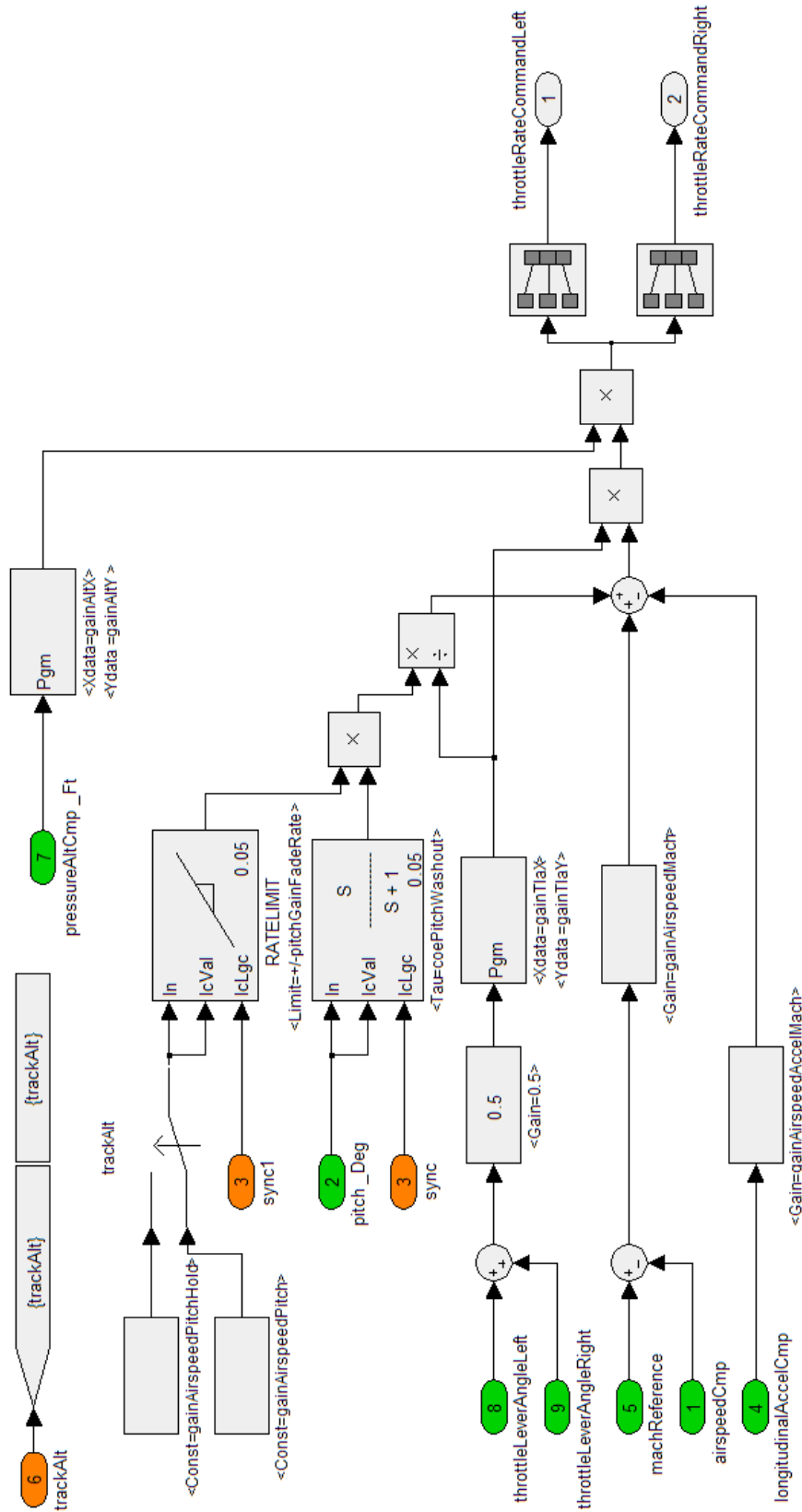


Figure 2.2: Representation of the nonlinear control law used to control airspeed

2.3 Optimal control laws

Another control theory that was used in this research was optimal control. The design of an optimal control is “to determine the control signals that will cause a process to satisfy the physical constraints and at the same time minimize (or maximize) some performance criterion” [22]. This section will define the generic continuous time optimal control problem. To start, define the plant as [24]:

$$\dot{x}(t) = f(x, u, t) \quad (2.26)$$

with the state $x(t) \in \mathfrak{R}^n$ and the control input $u(t) \in \mathfrak{R}^m$. The performance index of the system (the term to be maximized or minimized) is defined as [24]:

$$J(t_0) = \phi(x(T), T) + \int_{t_0}^T L(x(t), U(t), t) dt \quad (2.27)$$

the time interval considered in this problem is $[t_0, T]$ [24]. In Equation 2.27 the term $\phi(x(T), T)$ is the final weight term and only depends on the final state and time and the integral represents a weighting function that depends on all of the intermediate states on $[t_0, T]$. Next the Hamiltonian function is derived to combine the constraints of the system to the performance index [24]:

$$H(x, u, t) = L(x, u, t) + \lambda^T f(x, u, t) \quad (2.28)$$

. The necessary conditions to minimize Equation 2.27 for this system are derived from the Hamiltonian:

$$\begin{aligned} \dot{x} &= \frac{\partial H}{\partial \lambda} = f \\ -\dot{\lambda} &= \frac{\partial H}{\partial x} = \frac{\partial f^T}{\partial x} \lambda + \frac{\partial L}{\partial x} \\ 0 &= \frac{\partial H}{\partial u} = \frac{\partial L}{\partial u} + \frac{\partial f^T}{\partial u} \lambda \end{aligned} \quad (2.29)$$

The first of these equations corresponds to the state equation defined in 2.26, second equation is the costate equation, and the third is the stationarity condition [24]. To find the singular arc there are additional necessary conditions of the stationarity condition and its derivatives to also be zero [27]. This additional necessary condition is known as the Kelley condition [27]. Another way to compute the singular arc for two states is by using Green’s theorem [27]. The

state equations are:

$$\begin{aligned}\dot{x} &= f_x(x, y) + g_x(x, y)u \\ \dot{y} &= f_y(x, y) + g_y(x, y)u\end{aligned}\quad (2.30)$$

and the cost function is [27]:

$$J = \int_t^{t_f} f_0(x, y)dt \quad (2.31)$$

To solve for the singular arc, start by elimination the control in Equations 2.30 and substituting the result into Equation 2.31. Then solve for the minimum of the resulting integral, the associated curve from this integral is:

$$\frac{\partial A}{\partial y} - \frac{\partial B}{\partial x} = 0 \quad (2.32)$$

where A and B are:

$$\begin{aligned}A &= \frac{f_0 g_y}{f_x g_y - f_y g_x} \\ B &= \frac{f_0 g_x}{f_y g_x - f_x f_y}\end{aligned}\quad (2.33)$$

Solving Equation 2.32 is the same as solving the necessary equations (Equation 2.29) and the Kelley condition [27].

2.4 Optimal control law design

To maximize range, [27] derived a singular optimal controller. With the equations of motion defined in Section 1.3.1, the following equations define the optimal control problem from [27].

The cost function is [27]:

$$J = - \int_0^t U dt \quad (2.34)$$

The Hamiltonian and Euler-Lagrange equations are [27]:

$$\begin{aligned}H &= -U + \lambda_U \left(\frac{\delta T_M}{m} - \frac{AU^2}{m} - \frac{Bmg^2}{U^2} \right) - \lambda_m c_T \delta T_M \\ \dot{\lambda}_U &= 1 + \lambda_U \left(\frac{\delta T_M}{m} - \frac{2AU}{m} - \frac{2Bmg^2}{U^3} \right) + \left(\frac{dC}{dU} \delta T_M + c_T \delta \frac{dT_M}{dU} \right) \\ \dot{\lambda}_m &= \lambda_U \left(\frac{\delta T_M}{m^2} - \frac{AU^2}{m^2} - \frac{Bg^2}{U^2} \right)\end{aligned}\quad (2.35)$$

On the singular arc these equations are [27]:

$$\begin{aligned}\bar{H} &= -U + \lambda_U \left(-\frac{AU^2}{m} - \frac{Bmg^2}{U^2} \right) = 0 \\ S &= \frac{\lambda_U}{m} - \lambda_m c_T \\ \dot{S} &= 1 + \lambda_U \left(\frac{2AU}{m} - \frac{2Bmg^2}{U^3} + \frac{c_T AU^2}{m} - \frac{c_T Bmg^2}{U^2} \right) + \lambda_m \frac{dC}{dU} \left(AU^2 + \frac{Bm^2 g^2}{U^2} \right) = 0\end{aligned}\quad (2.36)$$

Solving these equations for mass, gives the singular arc [27]:

$$m = \frac{U^2}{g} \sqrt{\frac{A \left(1 + U c_T + \frac{U}{c_T} \frac{dC}{dU} \right)}{B \left(3 + U c_T - \frac{U}{c_T} \frac{dC}{dU} \right)}}\quad (2.37)$$

The term $U c_T$ can be assumed to be small compared to the rest of the terms, and with both sides of the equation multiplied by the acceleration due to gravity, the solution becomes an equation for weight as a function of airspeed [27]:

$$W = U^2 \sqrt{\frac{A[1 + (U/c_T)(dc_T/dU)]}{B[3 - (U/c_T)(dc_T/dU)]}}\quad (2.38)$$

To determine the thrust required to follow the arc, the equation for $\ddot{S} = 0$ must be formed [27]. This equation becomes difficult to manage algebraically. This equation can be solved if a couple of assumptions are made, i.e. the term $c_T U$ is small, and c_T is independent of U . Then the thrust on the arc is [27]:

$$F_{T_x} = \frac{4}{3} AU^2\quad (2.39)$$

2.5 Proposed methods to calculate reference input

As proposed in the first hypothesis there may be an optimum speed to fly an aircraft to reduce fuel, this section will derive each of these methods that have been proposed in literature. In section 1.3.1.2 equations are defined for the range of an aircraft. Much research has been done to find a particular speed to maximize the range equations. These methods include finding the speed corresponding to the maximum point of the range equation by assuming some terms do not depend on speed, and an average Mach number based on the Breguet equation. Another method proposed is an optimal controller to maximize the range of the aircraft.

2.5.1 Maximum lift-to-drag

For level flight lift L is equal to weight. Lift can be expressed in terms of the lift coefficient C_L [26]:

$$W = L = C_L \left(\frac{1}{2} \rho U^2 \right) S \text{ or } C_L = \frac{W}{\left(\frac{1}{2} \rho U^2 \right) S} \quad (2.40)$$

Here, the parenthetical term represents dynamic pressure, including atmospheric density for the flight altitude, ρ and S represents the wing area. To determine the drag coefficient C_D , the lift coefficient is substituted into the drag polar equation:

$$C_D = C_{D_0} + K C_L^2 = C_{D_0} + K \left[\frac{W}{\left(\frac{1}{2} \rho U^2 \right) S} \right]^2 \quad (2.41)$$

where K is the induced drag factor. Equations 2.40 and 2.41 can be divided to calculate the lift-to-drag ratio [26]:

$$\frac{L}{D} = \frac{C_L}{C_D} = \frac{W}{C_{D_0} \left(\frac{1}{2} \rho U^2 \right) S + K \frac{W^2}{\left(\frac{1}{2} \rho U^2 \right) S}} \quad (2.42)$$

The maximum lift-to-drag ratio is given by:

$$\left(\frac{L}{D} \right)_{max} = \sqrt{\frac{1}{4C_{D_0}K}} \quad (2.43)$$

2.5.2 Mach number for minimum thrust

In steady level flight, the required thrust is equal to the total drag, therefore the minimum thrust required is the same as the minimum drag. [26] Minimizing the drag equation and solving for speed, the result is a speed corresponding to the minimum thrust required for level flight [26]:

$$U_{minThrust} = \left[\frac{2}{\rho} \sqrt{\frac{K}{C_{D_0}}} \frac{W}{S} \right]^{1/2} \quad (2.44)$$

2.5.3 Mach number for maximum velocity times lift-to-drag

To maximize the range, $U(L/D)/c_T$ should be a maximum if initial and final weights are specified. If c_T is assumed to be constant with respect to velocity, then the range will be

maximized when $U(L/D)$ is maximized. The term $U(L/D)$ can be defined as follows [26]:

$$\begin{aligned}
 U \frac{L}{D} &= V \frac{W}{C_D \left(\frac{1}{2}\rho U^2\right) S} \\
 &= \frac{W}{C_D \left(\frac{1}{2}\rho U\right) S} \\
 &= \frac{\sqrt{W}}{C_D \sqrt{\left(\frac{1}{2}\rho U^2\right) S}} \left[\frac{\sqrt{W}}{\sqrt{\left(\frac{1}{2}\rho\right) S}} \right] \\
 &= \frac{C_L^{1/2}}{C_D} \left[\frac{\sqrt{W}}{\sqrt{\left(\frac{1}{2}\rho\right) S}} \right]
 \end{aligned} \tag{2.45}$$

In Equation 2.45, the term in brackets is fixed value for a given weight and flight altitude. Therefore by maximizing $C_L^{1/2}/C_D$, the value of $U(L/D)$ will also be maximized, this speed is defined in [26]:

$$U = 1.316U_{minThrust} \tag{2.46}$$

2.5.4 Mach number for maximum velocity times lift-to-drag divided by TSFC

For a constant altitude, c_T , L/D , and U , are not the same as weight changes [9]. If c_T , L/D , and U are assumed to vary with speed, maximize range for a set of initial and final weights, by maximizing $U(L/D)/c_T$ [26]. The speed for maximum $U(L/D)/c_T$ does not necessarily correspond to the same speed calculated in Equation 2.46 [26]. The equation to be maximized in this case is:

$$R = U \frac{W}{C_D \left(\frac{1}{2}\rho V^2\right) S} \tag{2.47}$$

At a specific weight and altitude, Equation 2.47 can be solved for a speed to produce the maximum range.

2.5.5 Average Mach number to maximize range

From Equation 1.12 an approximate average Mach number can be derived [12]:

$$\bar{\mu}^2 = \frac{\mu_0^2 + \mu_1^2}{2} = \frac{2 - \zeta}{2(1 + \beta)} \left[-(1 - \beta)k_2 E_{M_0} + \sqrt{(1 - \beta)k_2^2 E_{M_0}^2 + (1 + \beta)(3 - \beta)} \right] \tag{2.48}$$

If the wing has no camber, Equation 2.48 can be simplified to [12]:

$$\bar{\mu}^2 = \frac{2 - \zeta}{2(1 + \beta)} \left[\sqrt{(1 + \beta)(3 - \beta)} \right] \tag{2.49}$$

This specifies an average Mach number over the range of cruise weights to maximize range [12].

Two types of control law design have been presented: gain scheduling and optimal. The design of each of these controllers for this system have been described. Lastly each method for calculating an optimal speed reference has been derived.

CHAPTER 3. METHODS AND PROCEDURES

This chapter describes the methods and procedures used to complete this research. First the regional jet airplane model and the autothrottle control law design are described. Then the procedures used to run each simulation. After that the implementation of each of the methods described in Chapter 2 in simulation. The final area discussed is the disturbances that were added to the model to understand the performance in non-ideal conditions.

3.1 Model used

The airplane simulation is a six degree of freedom model of a regional jet implemented in Simulink. A screen shot of this model is shown in Figure 3.1. This jet is designed to transport about 50 passengers. It has two engines mounted at the rear of the fuselage. The throttle quadrant model includes two independent servos two back drive the throttle. The resulting throttle position from this model is the input to the engine. The simulation includes atmospheric parameters such as wind, temperature, and pressure. Models of sensors and other avionics have been added as interfaces to the autothrottle.

The Simulink model, shown in Figure 3.1, is broken into blocks that represent different functional areas of the aircraft. The throttle quadrant block is a model of the throttle quadrant assembly, including the servos that drive the throttles. The command calculated by the autothrottle is sent to these servos. The Aircraft block contains the models of the atmosphere, engines, aerodynamics, and weight of the airplane. The atmosphere block contains models of wind, atmospheric temperature, atmospheric pressure, and the speed of sound. The engine simulation takes the throttle position from the throttle quadrant model, fine trim commands from the autothrottle model and the atmosphere model to calculate the thrust produced. The aerodynamics model includes calculations of the aerodynamic forces (both lift and drag) on

the airplane, including the wings, tail, and movable surfaces. Two of the outputs of this model are the coefficients of lift and drag. The last model of this block is the weight model, representing the weight of the aircraft based on the weight entered, fuel used, location of the center of gravity, and attitude of the aircraft. All of the forces calculated inside of the aircraft are combined to calculate the total forces and moments of the aircraft. The sensors block contains models of the air data computer, inertial reference unit (measures attitude data), navigation data, and radio data. Simulations of panels, displays, and other avionics in the cockpit are included in the Avionics block. The simulation of the panels in the cockpit allow the simulation to set the same parameters as the crew, such as altitude and airspeed targets. The displays and other avionics system components also provide data that is required for simulation of the AFCS, such as flight plan information from the Flight Management System (FMS). The AFCS block contains models of the autothrottle and flight guidance computers used in the simulation. For this simulation, the autothrottle is setup to track a reference airspeed and the flight guidance is set to hold altitude and heading. The data recording block records the data from the simulation to be analyzed and plotted after the simulations are complete. The last block, SimControl, controls the initialization of the aircraft and other parameters needed in the simulation, such as wind speed and direction.

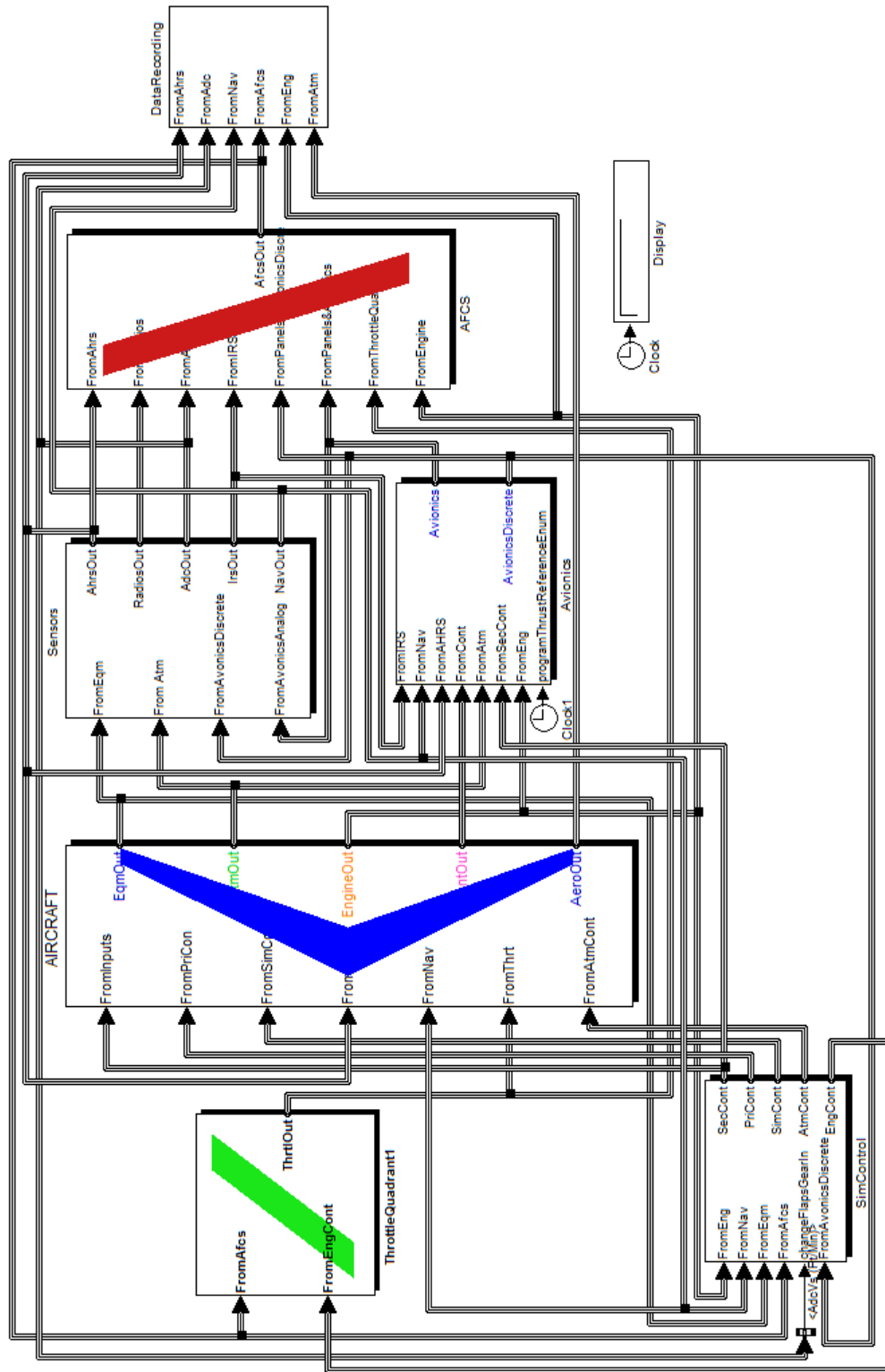


Figure 3.1: Screen shot of the top level Simulink model of the aircraft

3.2 Simulation procedures

Each of the methods described in 2.5 were simulated at 5 different altitudes lying within the normal range of altitudes for cruise flight: 20,000, 25,000, 30,000, 35,000, and 40,000 feet. As a baseline case, a simulation was initialized at Mach 0.78, the normal cruise speed of the regional jet simulation, and the airspeed control law described in Section 2.2 was used to track that speed for the duration of the cruise phase of flight. Each of the simulation variations proposed in this chapter were run for an equivalent of three hours of real time flight. These procedures are included in Appendix C.

3.3 Implementation of proposed references

The implementation of the proposed methods includes the determination of the constants and values for TSFC that are used in all of the methods proposed in literature. Additionally, for each method the calculation of initial values and the set up of the simulation are described.

3.3.1 Determination of constants

Before determining the numerical values of the equations in Chapter 2, several constant values were defined. The first group of constants is based on Earth's parameters on a standard day. For the troposphere, at altitudes less than 36,152 feet, the temperature (degrees Ferenheight), and atmospheric pressure (pounds per square feet) are defined as [1]:

$$\begin{aligned} Temp &= 590.00356h \\ p &= 2116 \left[\frac{Temp + 459.7}{518.6} \right]^{5.256} \end{aligned} \quad (3.1)$$

where h is the altitude in feet. For the lower stratosphere, including altitudes between 36,152 and 82,345 feet, the temperature and atmospheric pressure are defined as [1]:

$$\begin{aligned} Temp &= -70 \\ p &= 473.1e^{1.73-0.000048h} \end{aligned} \quad (3.2)$$

Based on the temperature and pressure found in 3.1 or 3.2 the atmospheric density, ρ , in slugs per cubic feet can be derived by [1]:

$$\rho = \frac{p}{1718(Temp + 459.7)} \quad (3.3)$$

The specific heat ratio, γ , of air on a standard day is estimated as 1.4 in [2]. From [3], the speed of sound, a , in feet per second is determined using the equation:

$$a = \sqrt{\gamma R Temp} * 3.28 \quad (3.4)$$

where R is the gas constant (286 m²/s²/K) and $Temp$ is the temperature in Kelvin. The acceleration due to gravity is defined as 32.174 feet per second squared.

The next group of constants is based on assumptions of the aircraft design. The values of these constants for the regional jet model used are defined in Table 3.1 below.

Table 3.1: Aircraft constant parameters

Variable	Description	Value	Units
b	Wing span	76.25	Feet
S	Wing area	760	Square Feet
AR	Aspect Ratio, b^2/S	7.65	
e	Oswald span efficiency factor	0.85	
K	Induced drag factor, $1/(\pi e AR)$	0.055478	
T_M	Maximum Thrust	12,670	Pounds
W_0	Weight at the start of cruise flight	72,300	Pounds
W_f	Weight at the end of cruise flight	63,100	Pounds
C_{D_0}	Coefficient of drag at zero-lift, $11.5/S$	0.0125	

3.3.2 Calculation of TSFC

As explained in Section 1.3.1.3, Equation 1.15 can be used to determine the TSFC for jet engines. The values of c_{T0} and β in the TSFC equation were empirically found using the jet

engine model of the simulation. First TSFC was calculated at different throttle positions at the speed for maximum lift-to-drag ratio. From this data, the throttle position corresponding to the thrust required the maximum lift-to-drag ratio. The TSFC over a range of Mach numbers was calculated at this thrust level. From this set of Mach numbers and calculated TSFC a best fit line was derived. While an equation in the form of Equation 1.15 was a good fit for the data, the author found that the following equation was a better fit for the data:

$$c_T = c_{T\alpha} e^{\alpha M} \quad (3.5)$$

The data at 35,000 feet is shown in Figures 3.2 and 3.3 to show an example of the difference. Figure 3.2 shows the data and best fit line from Equation 1.15 and Figure 3.3 shows the same data and best fit line from Equation 3.5.

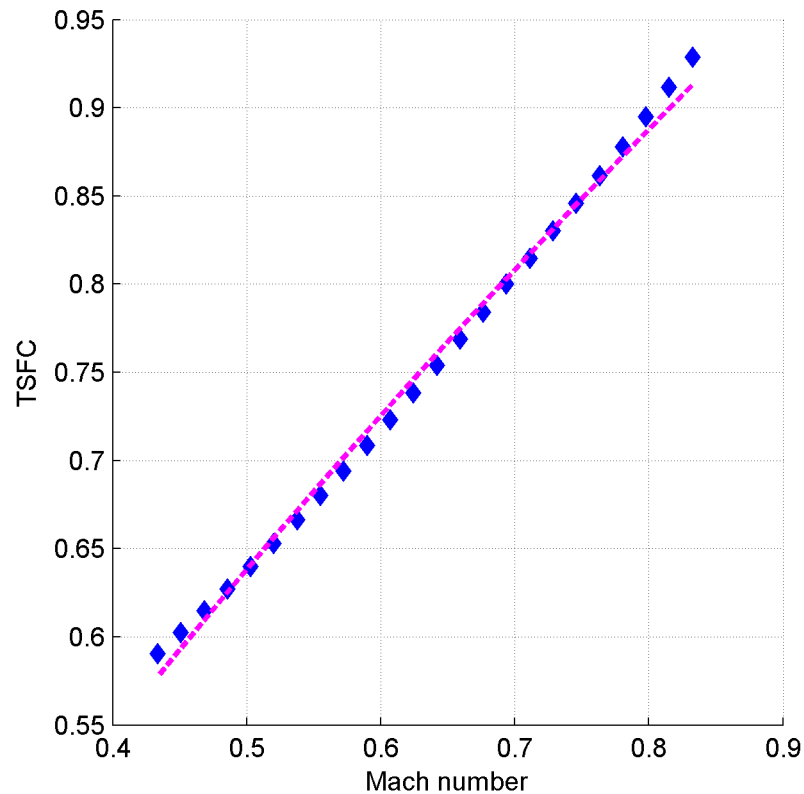


Figure 3.2: TSFC data at 35,000 feet with best fit line in the form of Equation 1.15

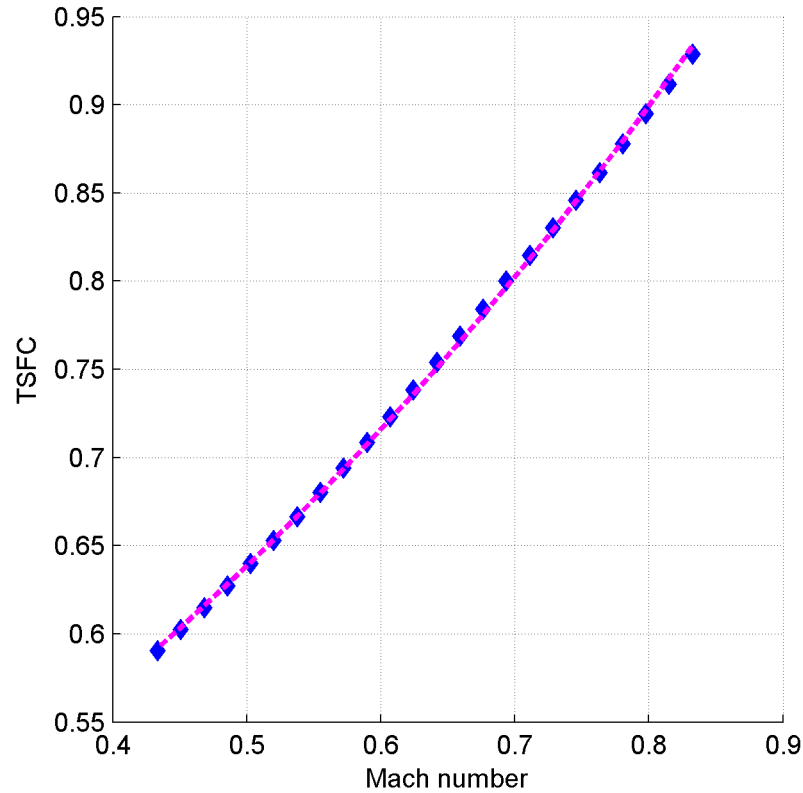


Figure 3.3: TSFC data at 35,000 feet with best fit line in the form of Equation 3.5

3.3.3 Maximum lift-to-drag

In section 2.5.1 the maximum lift-to-drag ratio is defined in Equation 2.43. Using the constants in Table 3.1 the value can be calculated. The speed at which the maximum lift-to-drag ratio is attained was also determined and is shown in Table 3.2. During level flight the thrust required is equal to the drag and the lift is equal to the weight. Therefore the thrust required to achieve the maximum lift-to-drag ratio is the weight divided by the value of maximum lift-to-drag. The value of thrust required at the start of cruise flight is 3807.89 pounds. To implement this scenario in the simulation, the same throttle position determined during the TSFC calculations was set as the constant throttle position for the duration of the cruise phase of flight. Since the amount of thrust needed changes with the weight, a second test case was included to reposition the throttles halfway through the flight to the new value

of thrust required. In both scenarios the simulation was initialized to a Mach number equal to the speed corresponding to a maximum lift-to-drag ratio.

Table 3.2: Numerical values for speed at the maximum lift-to-drag ratio

Altitude (Feet)	Speed (Feet/Second)	Mach Number
20,000	519.5096	0.501
25,000	566.3766	0.557
30,000	619.7324	0.623
35,000	680.8174	0.700
40,000	765.2544	0.790

3.3.4 Mach number for minimum thrust

In section 2.5.2 the equation for speed at the minimum thrust is shown in Equation 2.44. This equation was used to determine the speed for each altitude, shown in Table 3.3. The values in Tables 3.2 and 3.3 are the same, although they were arrived at through different methods. The values in Table 3.2 were determined from the speed vs. lift-to-drag ratio curve, by finding the speed corresponding to the point of maximum lift-to-drag ratio. The values in Table 3.3 were calculated from Equation 2.44 which was determined symbolically from the lift-to-drag equation in [26]. The simulation was initialized to this speed and a model of an industry autothrottle was used to hold the speed throughout the duration of the cruise flight. Since the parameters required to calculate this speed in real time are available to the avionics system, a simulation where the speed was constantly calculated (as weight changes) was also run and sent to the autothrottle as the speed reference. A screen shot of how this is modeled in Simulink is provided in Figure 3.4. The top path in this figure is the same as in Equation 2.44. The first part of the calculation is $2/\rho$. The result is multiplied by a constant that is equal to $\sqrt{K/C_{D_0}}$. The weight, which is constantly changing, is divided by a constant S and the result is multiplied by the previous result. After that the 'sqrt' block is used to calculate the square root of the result. This equation produces a speed in knots, and the last programmer is

used to convert the speed into a Mach number. A programmer is used for this since, the speed of sound changes with altitude. The other two programmers in the drawing will be explained as they are used. The switches, which pass the top input if the middle input is greater than 0.5, are used to select the desired type of Mach reference. To use this reference the parameter 'asRefMinThrustReq', is set to one and 'asRefMax' is set to zero.

Table 3.3: Numerical values for $U_{minThrust}$

Altitude (Feet)	Speed (Feet/Second)	Mach Number
20,000	519.5096	0.501
25,000	566.3766	0.557
30,000	619.7324	0.623
35,000	680.8174	0.700
40,000	765.2544	0.790

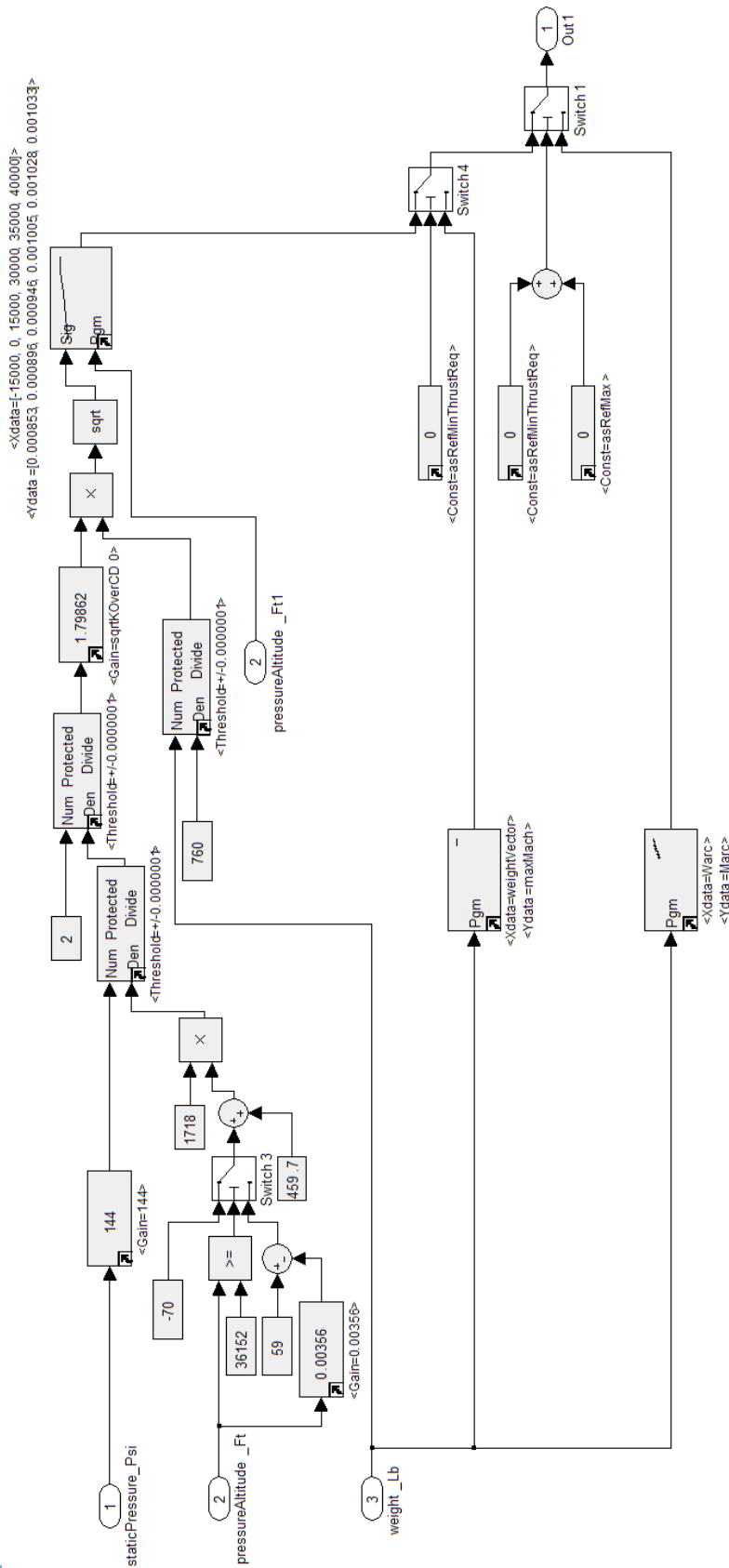


Figure 3.4: Screen shot of Simulink model used to calculate the Mach number references in real time

3.3.5 Mach number for maximum velocity times lift-to-drag

As described in section 2.5.3 the speed corresponding to the maximum $U(L/D)$ is defined by Equation 2.46. The numerical values for this speed are shown in Table 3.4. The simulation was initialized to this speed and a model of an industry autothrottle was used to hold the speed throughout the duration of the cruise flight. At 35,000 and 40,000 feet the speed for maximum $U(L/D)$ is greater than the maximum operating Mach number (0.85) of the airplane.

Table 3.4: Numerical values for the speed corresponding to maximum $U(L/D)$

Altitude (Feet)	Speed (Feet/Second)	Mach Number
20,000	683.6746	0.659
25,000	745.3516	0.734
30,000	815.5679	0.820
35,000	895.9557	0.921
40,000	1007.0748	1.040

3.3.6 Mach number for maximum velocity times lift-to-drag divided by TSFC

Section 2.5.4 demonstrated maximizing the equation for $U(L/D)/c_T$ was derived. The result is an equation for range, Equation 2.47. Using mathematical equation software, the maximum of Equation 2.47 was calculated numerically for the weights at the start and end of the cruise phase of flight. The speed corresponding to this value was also calculated. These speeds are shown in Tables 3.5 and 3.6. The average speeds over the weight range were also calculated, and the numerical values are shown in Table 3.7. Two implementations of this speed were considered in simulation. This first implementation is similar to the other constant speeds described, in which the simulation was initialized to the Mach number in Table 3.7 and the industry autothrottle was set to hold that speed for the duration of cruise flight. The other implementation was include a 2-dimensional look-up table, with weight as the input and the desired Mach number for that weight as the output. Two points were used in the table, with a linear interpolation in-between values. The first point is the ending weight for cruise, and the

corresponding speed from Table 3.6 and the second point is the starting weight for cruise and the corresponding speed from Table 3.5. This look-up table is the second path shown in Figure 3.4. To use this reference the parameter ‘asRefMinThrustReq’ is set to zero and parameter ‘asRefMax’ is set to one.

Table 3.5: Numerical values for the speed corresponding to maximum $U(L/D)/c_T$ at the weight for the start of cruise

Altitude (Feet)	Speed (Feet/Second)	Mach Number
20,000	556.4709	0.537
25,000	607.5852	0.598
30,000	665.8245	0.669
35,000	733.8104	0.754
40,000	824.8197	0.852

Table 3.6: Numerical values for the speed corresponding to maximum $U(L/D)/c_T$ at the weight for the end of cruise

Altitude (Feet)	Speed (Feet/Second)	Mach Number
20,000	519.9361	0.501
25,000	567.6945	0.559
30,000	622.1100	0.625
35,000	685.6324	0.705
40,000	770.6666	0.796

Table 3.7: Numerical values for the average speed corresponding to maximum $U(L/D)/c_T$ over the weight range for cruise

Altitude (Feet)	Speed (Feet/Second)	Mach Number
20,000	538.2035	0.519
25,000	587.6399	0.578
30,000	643.9672	0.647
35,000	709.7214	0.729
40,000	797.7432	0.824

3.3.7 Average Mach number to maximize range

In section 2.5.5 another method for calculating the average Mach number to maximize range is proposed. The average Mach numbers for each altitude were calculated from Equation 2.49, producing the values shown in Table 3.8. As in the previous scenarios, the simulation was initialized to the speed in table 3.8, and the industry autothrottle set to hold that speed. Even though the values for average Mach number in Tables 3.7 and 3.8 were determined differently, they are very close, and for most altitudes the difference occurs in the fourth or fifth decimal place.

Table 3.8: Numerical values for the average speed corresponding to maximum range

Altitude (Feet)	Mach Number
20,000	0.519
25,000	0.578
30,000	0.647
35,000	0.729
40,000	0.824

3.3.8 Optimal control with a singular arc

In Section 2.4, a singular arc was derived using optimal control theory to show the relationship of weight vs. speed to maximize the range. This arc is defined in Equation 2.38. Since the calculations in [27] are in SI units, dimensional analysis was performed on Equation 2.38 to verify the units. Using Equation 3.5 for TSFC, the numerical values for the arc were determined across the cruise weight range. The numerical values for the start and end cruise weights are shown in Tables 3.9 and 3.10 respectively. There are two implementations of the speed on the singular arc in the simulation. The first initializes and holds the average Mach number from the arc, similarly to the other methods described above. The second implementation included a 2-dimensional lookup table with the points of the singular arc across the weight range. A function in Matlab was created to generate the arrays for the programmer at each altitude, and this code can be found Appendix C. The look-up table is the third path shown in Figure 3.4. To use this reference the parameters ‘asRefMinThrustReq’ and ‘asRefMax’ are both set to zero. A third look-up table was used because 21 break points were used to define the singular arc at each altitude, whereas only two points were used in the other table. With this different number of break points, the simulation would have needed to recode and compile each time the number of break points was changed, so separating the look-up tables saved simulation time.

Table 3.9: Numerical values for the speed on the singular arc at the weight for the start of cruise

Altitude (Feet)	Speed (Feet/Second)	Mach Number
20,000	556.4709	0.537
25,000	607.5852	0.598
30,000	665.8245	0.669
35,000	733.8104	0.754
40,000	824.8197	0.852

Table 3.10: Numerical values for the speed on the singular arc at the weight for the end of cruise

Altitude (Feet)	Speed (Feet/Second)	Mach Number
20,000	519.9361	0.501
25,000	567.6945	0.559
30,000	622.1100	0.625
35,000	685.6324	0.705
40,000	770.6666	0.796

Table 3.11: Numerical values for the average speed on the singular arc

Altitude (Feet)	Speed (Feet/Second)	Mach Number
20,000	599.9503	0.579
25,000	649.9992	0.640
30,000	700.0408	0.704
35,000	749.9682	0.771
40,000	800.0378	0.826

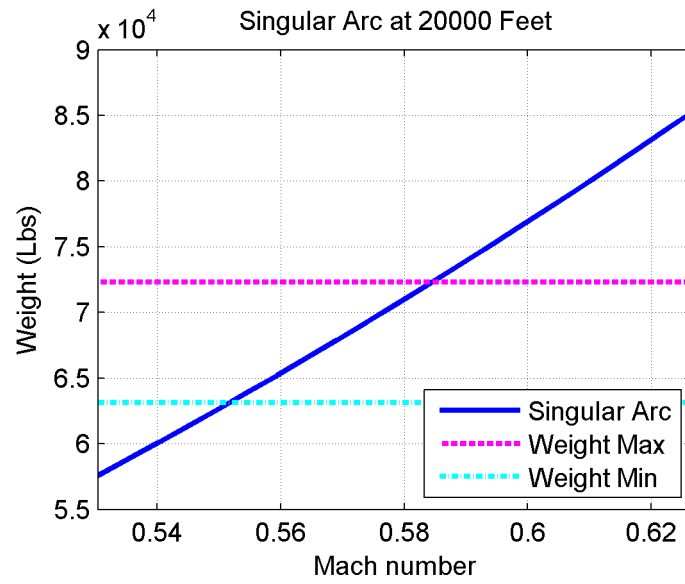


Figure 3.5: Singular arc at 20,000 feet based on Equation 2.38

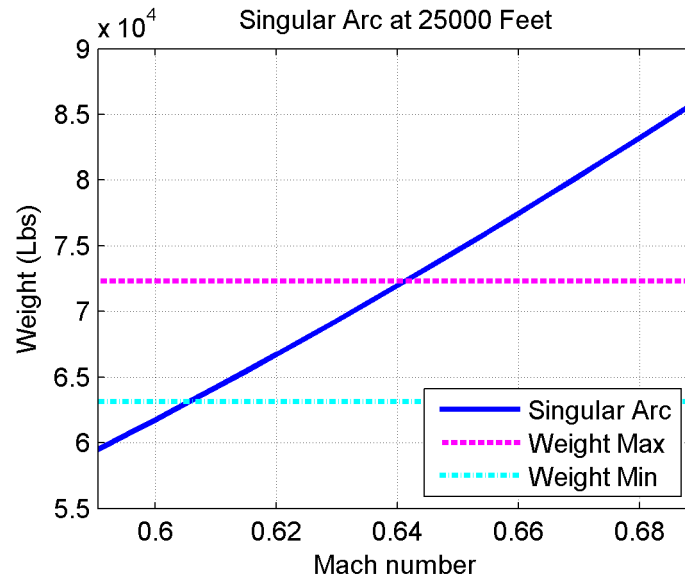


Figure 3.6: Singular arc at 25,000 feet based on Equation 2.38

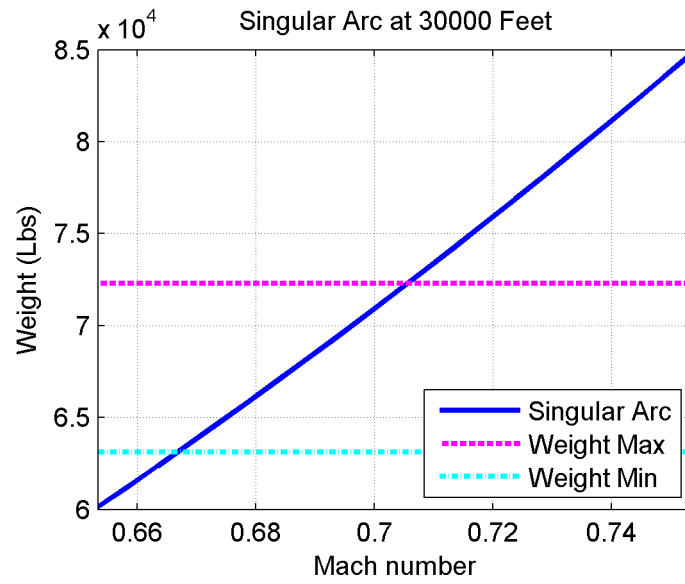


Figure 3.7: Singular arc at 30,000 feet based on Equation 2.38

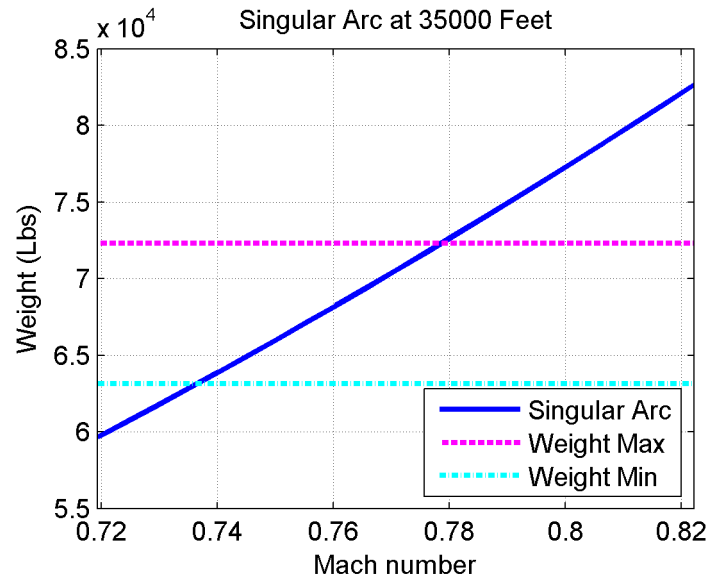


Figure 3.8: Singular arc at 35,000 feet based on Equation 2.38

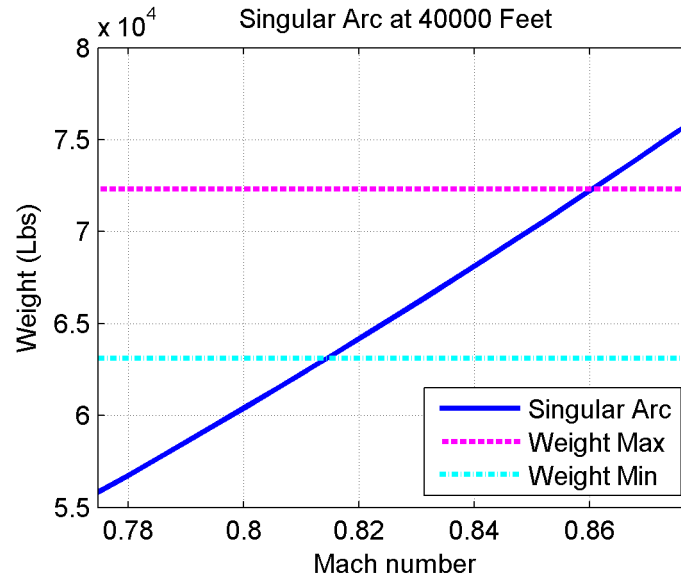


Figure 3.9: Singular arc at 40,000 feet based on Equation 2.38

To implement the thrust on the arc, the control δ was calculated based on the equation for F_{T_x} in Equation 1.4. This means that δ is derived by dividing Equation 2.39 by T_M . The simulation was initialized to the speed in Table 3.9 and the throttles were positioned based on the continuously-calculated value of δ throughout the duration of the simulation.

3.4 Disturbances added

The initial simulations were run at the speed calculated in steady winds, this is the ideal situation. To understand the impact of non-ideal equations several cases were added with winds. Additionally to understand the sensitivity of each Mach number simulations were run at various small differences away from the ideal value. Initially the simulation was run with a practical implementation including rounding of the reference airspeed to the nearest hundredth, since each of the methods proposed have more significant digits, additional simulations were run with more precision.

3.4.1 Winds

While still air is ideal, it rare to find, so three different types of winds were considered to understand the impact of non-ideal conditions. The first type of winds added was turbulence in all directions at 6 feet per second RMS. Turbulence is modeled as white noise, added to the airspeed signal used by the autothrottle. Next 30-knot bursts of head and tail winds were included in separate cases.

Figure 3.10 illustrates the impact of winds on the control law. This plot was generated from data recorded in a 20,000 ft test case. The first subplot shows the magnitude of the wind speed in turbulence. The magnitude is calculated from the longitudinal and lateral winds. The second subplot shows the actual Mach number in the solid line and the complemented Mach number in the dashed line. As mentioned in [8], airspeed is complemented with longitudinal airspeed to remove some of the unneeded high-frequency content. The ground speed of the aircraft is the sum of the airspeed and the wind speed (tail wind is positive wind speed). This means a tail wind increases the ground speed and a head wind decreases the ground speed. Because the destination of the aircraft is on the ground, range is usually calculated by the distance traveled relative to the ground. Therefore headwinds are detrimental to the range of the aircraft.

3.4.2 Variation of Mach number

In order to look at the sensitivity to a change in Mach number a second series of simulations were run on the average Mach numbers calculated in Tables 3.7, 3.8, and 3.11. For each of these Mach numbers, a simulation was run at a various small differences in Mach number, from -0.2 to 0.1 Mach. Each of these results were compared to the original speed.

3.4.3 Airspeed reference rounding

Human factors should always be taken into consideration when designing a system. In this case, because both the Mach number and the airspeed reference (in Mach number) are displayed to the crew to the nearest hundredth, the Mach number reference in the autothrottle is also rounded to the nearest hundredth. To allow the crew to verify that the autothrottle

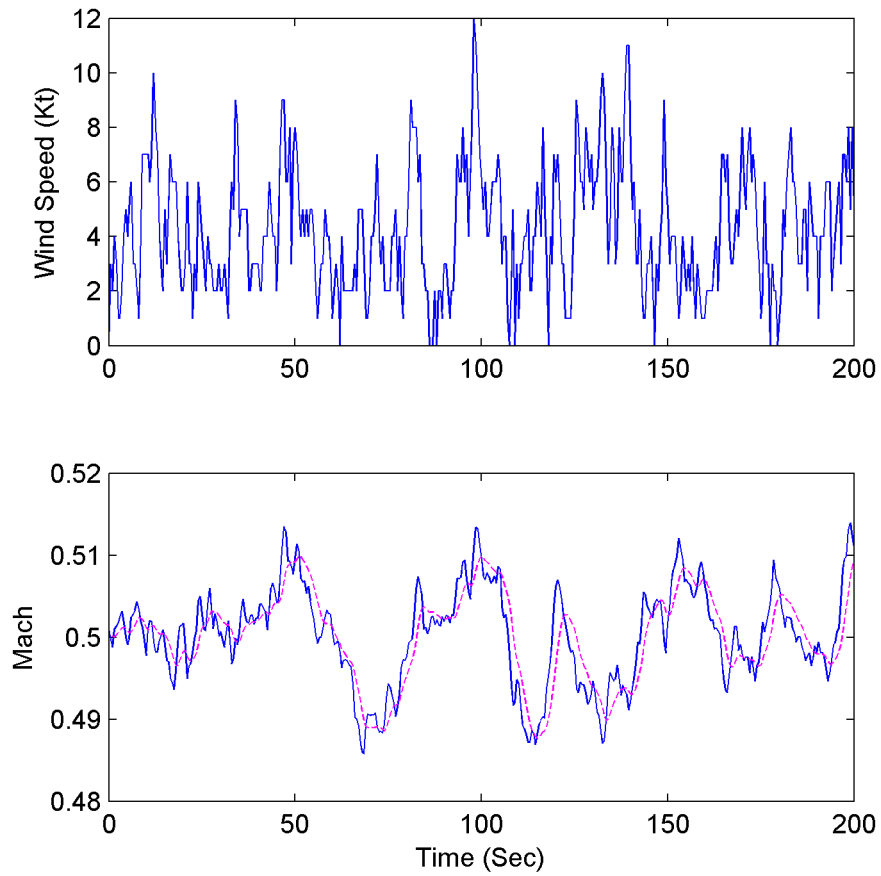


Figure 3.10: Plot of wind speed and airspeed at 20,000 feet in turbulence

is performing correctly, the reference input used by the autothrottle is the same value that is displayed in the cockpit. The data shown in this chapter was calculated using this rounding. However, both the airspeed-based cases in the original simulation and the delta simulations were run with rounding to the thousandth as well.

The model of the regional jet aircraft and the procedures to run this model have been reviewed. Additionally the implementation of each method and the disturbances added to the simulation have been discussed. This provides a foundation for the results that were found during this research.

CHAPTER 4. RESULTS

After each method was simulated at each altitude, they were compared using the average number of nautical miles, nmi, flown per pound of fuel. To understand the sensitivity to each Mach number that was calculated, another series of simulations was run at varying small deviations from the calculated Mach number. From this run of simulations it was determined that some of the original constants were not accurate, so they were adjusted and all simulations were repeated. The constants and Mach numbers provided in Chapter 3 are the final values. The data provided in this chapter were collected using those values as well. These new constants were verified by comparing the calculated lift and drag coefficients to the values produced by the simulation.

A summary of the data is shown in Table 4.1 and graphs in Figures 4.1 - 4.5. From this comparison, the average Mach number for Equation 2.44 and Equation 2.49 over the weight range, as well as Equation 2.44 and Equation 2.38 constantly updated as weight changes were in the top six for best fuel consumption for all altitudes. The average of Equation 2.47 and Equation 2.47 constantly updated as weight changes were both also in the top six for four of the altitudes. At altitudes less than 40,000 feet, compared to a normal cruising speed of Mach 0.78, each of the discussed methods use less fuel. At all altitudes, when the airspeed control law was used to track the airspeed on the singular arc (Equation 2.38) the fuel consumption was better than when the thrust for the arc (Equation 2.39) was used. The thrust method for the arc did not end up in the top six at any altitude, this could indicate that the simplifications proposed in [27] were not accurate for this aircraft. Figure 4.6 compares the best method at each altitude and shows that there is not only an optimum speed to fly for a given altitude, there is also an optimum altitude to fly.

The introduction of winds impacted the data as expected. The graphs in Figures 4.7 -

4.11 show the difference between the cases with and without winds. Due to the change in ground speed, with head winds the fuel consumption was worse, and with tail winds the fuel consumption was improved. When turbulence was added, the results were about the same. The numerical data for the cases with winds is included in Appendix B.

The simulation did not show a significant difference in the fuel consumption when the reference was rounded to the nearest thousandth instead of the nearest hundredth. In Table 4.2, the data with each rounding value is provided for 30,000 feet. All of the data from this simulation is also provided in Appendix B.

Several combinations of changes were made to the autothrottle control law used in these simulations to reduce throttle activity. These changes included reducing the gain and removing the trim parameter that is sent directly to the engine. By removing the trim parameter, the amount of dead zone is increased before a change of thrust is commanded. None of these changes resulted in a significant improvement to the initial results, in steady air or with winds, at several Mach numbers between 0.5 and 0.85.

Table 4.1: Fuel used (nmi/lb) for each method at each altitude

Equation	Altitude (Ft)				
	20,000	25,000	30,000	35,000	40,000
Equation 2.44	0.1744	0.1927	0.2103	0.2286	0.2491
Equation 2.44 constantly updated	0.1744	0.1931	0.2108	0.2283	0.2480
Constant thrust	0.1459	0.1588	0.1673	0.1721	0.1797
Two levels of thrust	0.1536	0.1678	0.1798	0.1844	0.1912
Equation 2.46	0.1575	0.1723	0.1792	0.1843	0.1733
Equation 2.47 average	0.1739	0.1918	0.2096	0.2277	0.1943
Equation 2.47 constantly updated	0.1740	0.1928	0.2095	0.2308	0.2145
Equation 2.49	0.1734	0.1923	0.2093	0.2298	0.2315
Equation 2.38 average	0.1699	0.1862	0.2044	0.2259	0.2186
Equation 2.38 constantly updated	0.1738	0.1921	0.2101	0.2289	0.2504
Equation 2.39	0.1729	0.1908	0.2077	0.2265	0.1959
Cruise Mach	0.1386	0.1636	0.1934	0.2258	0.2497

Table 4.2: Fuel used (nmi/lb) for each rounding method at 30,000 feet

Equation	0.01 Rounding	0.001 Rounding
Equation 2.44	0.2103	0.2110
Equation 2.44 constantly updated	0.2108	0.2107
Equation 2.46	0.1792	0.1798
Equation 2.47 average	0.2096	0.2093
Equation 2.47 constantly updated	0.2095	0.2094
Equation 2.49	0.2093	0.2098
Equation 2.38 average	0.2044	0.2040
Equation 2.38 constantly updated	0.2101	0.2106
Cruise Mach	0.1934	0.1934

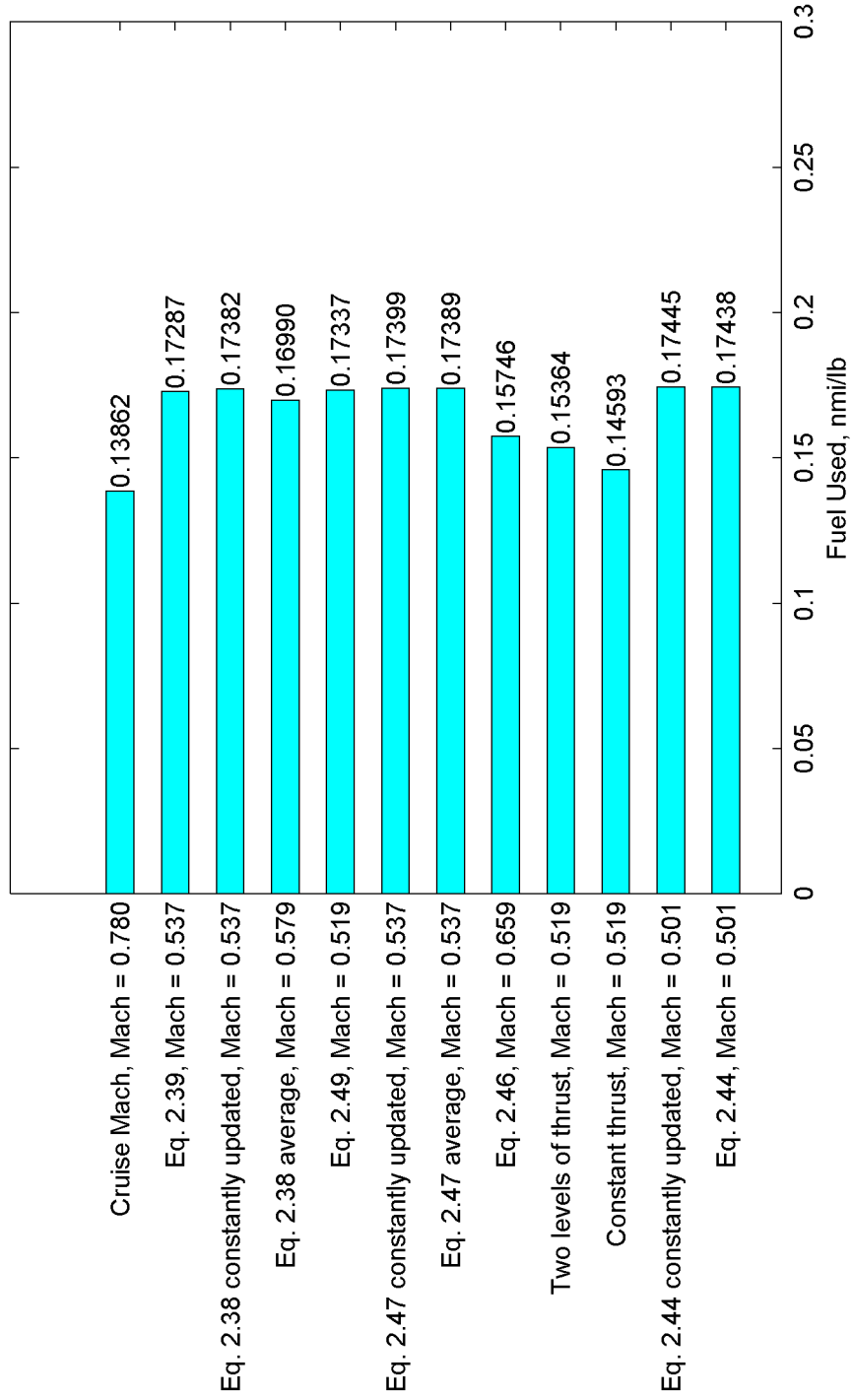


Figure 4.1: Comparison of methods at 20,000 feet

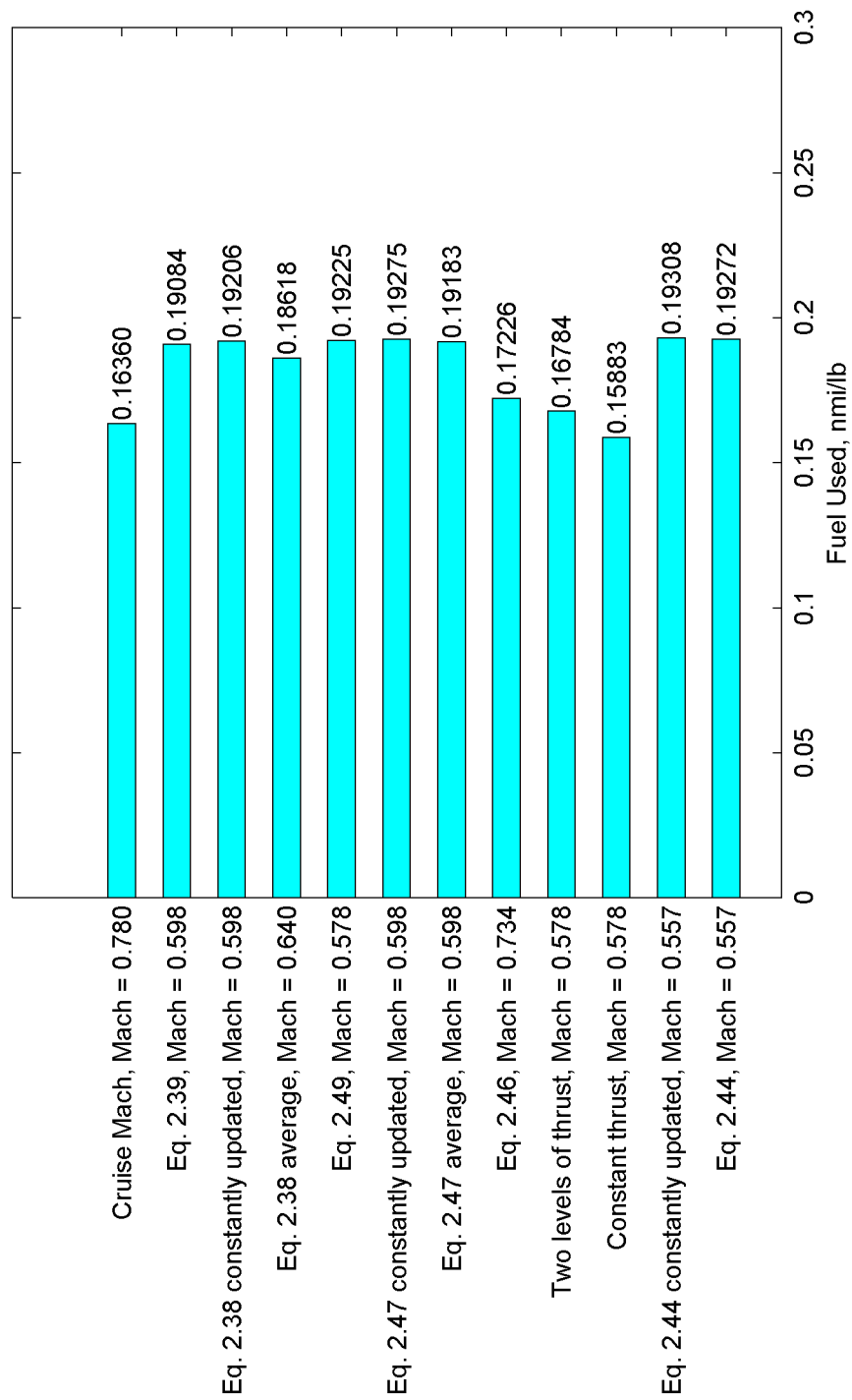


Figure 4.2: Comparison of methods at 25,000 feet

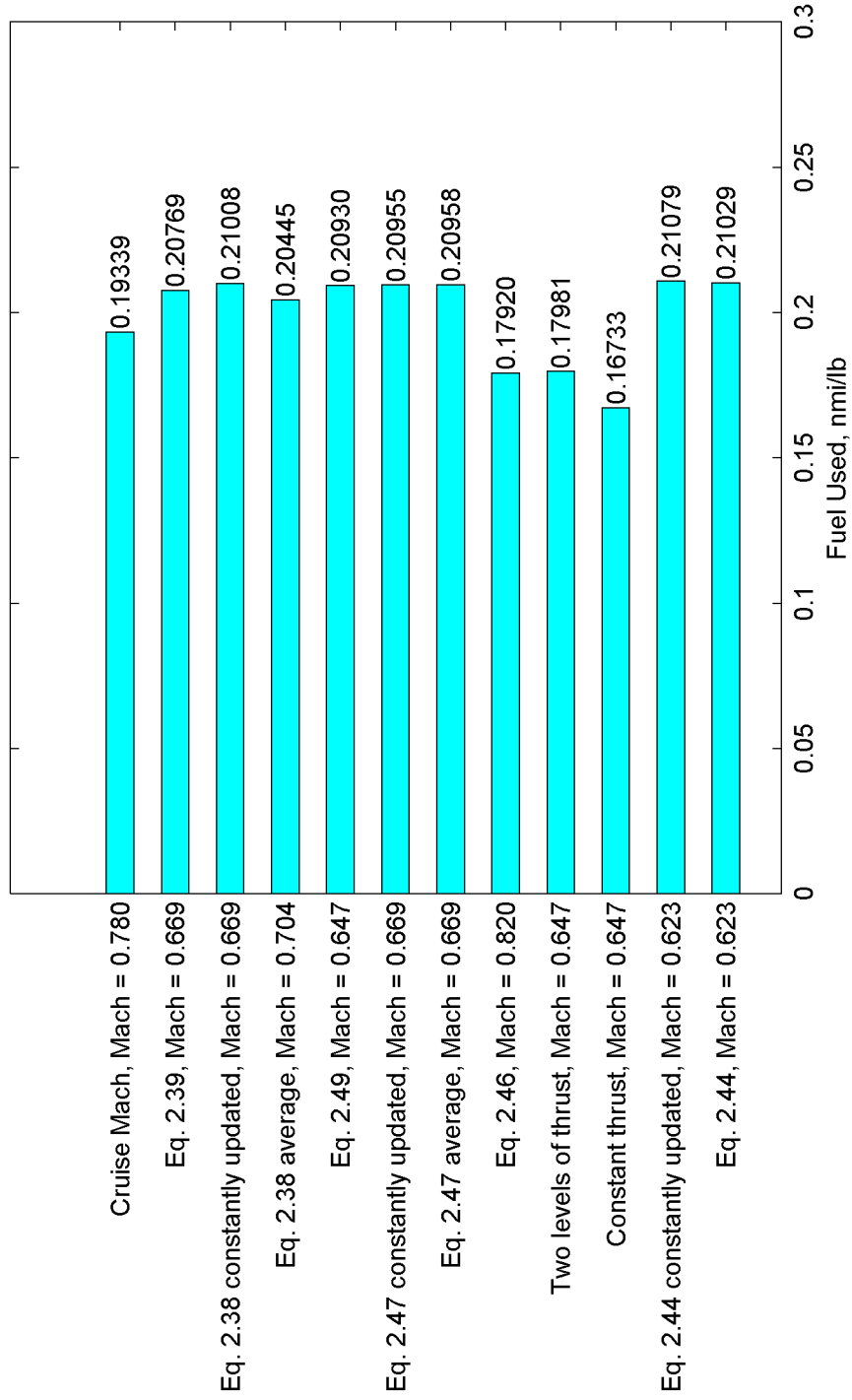


Figure 4.3: Comparison of methods at 30,000 feet

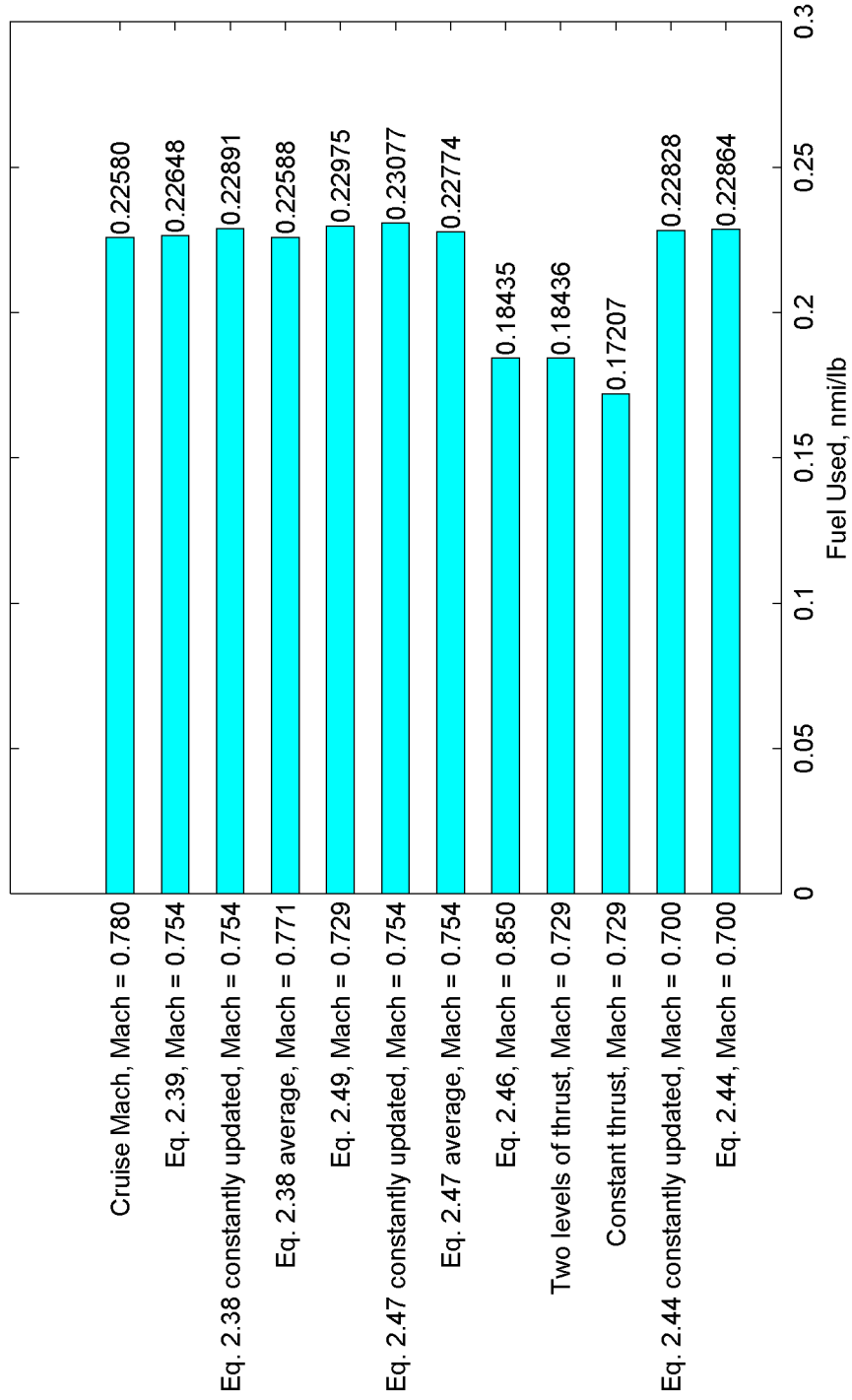


Figure 4.4: Comparison of methods at 35,000 feet

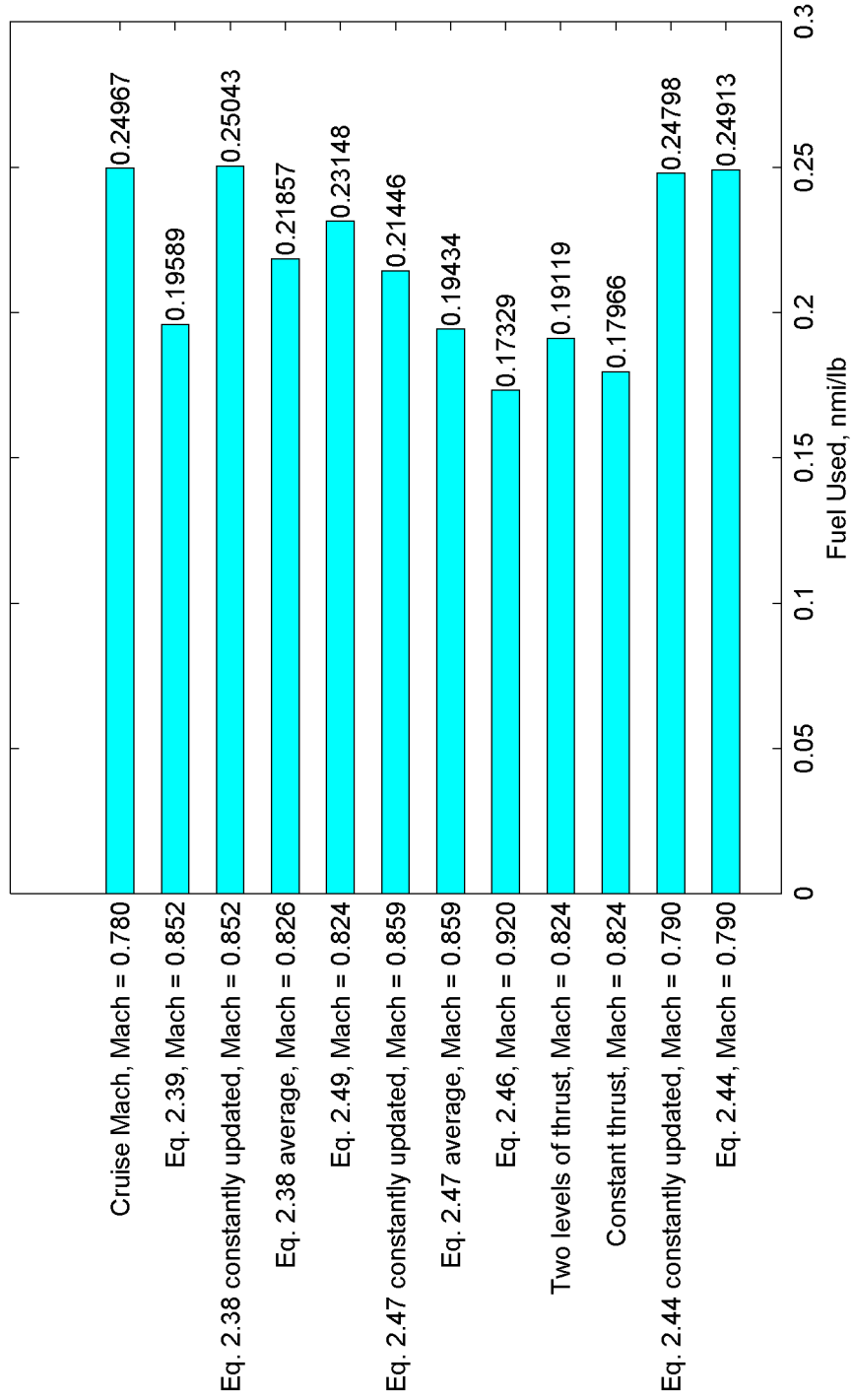


Figure 4.5: Comparison of methods at 40,000 feet

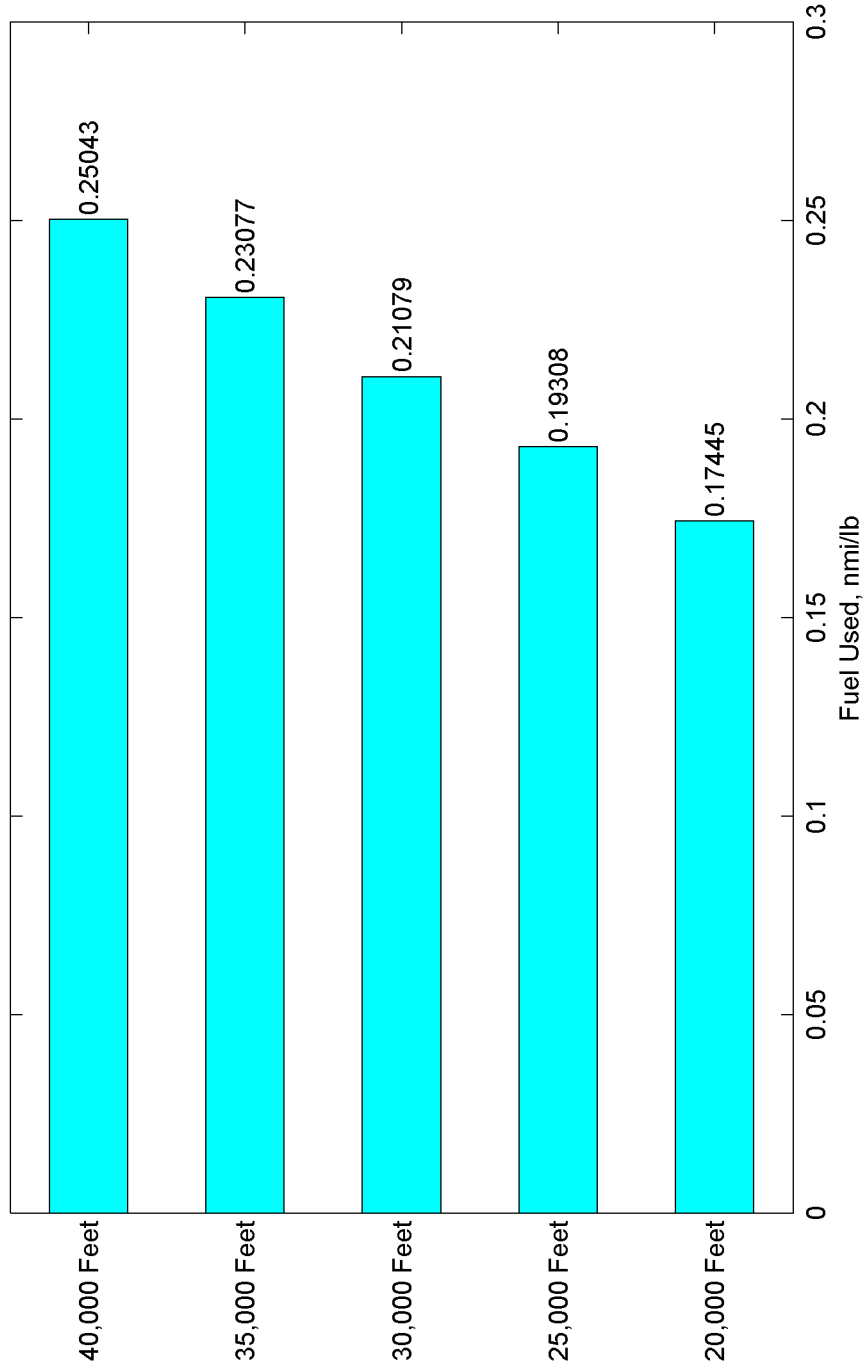


Figure 4.6: Comparison best fuel consumption at each altitude

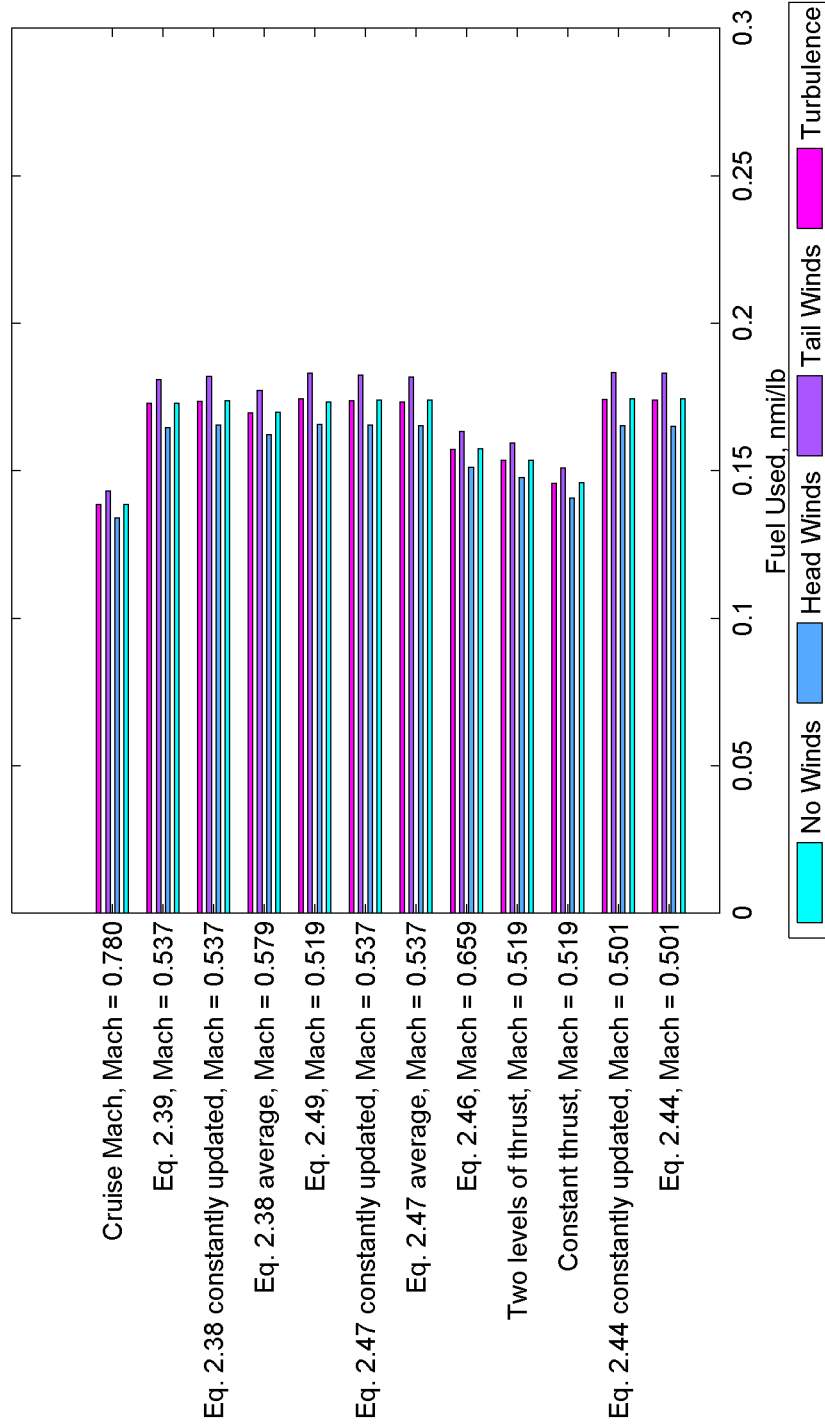


Figure 4.7: Comparison of methods with winds at 20,000 feet

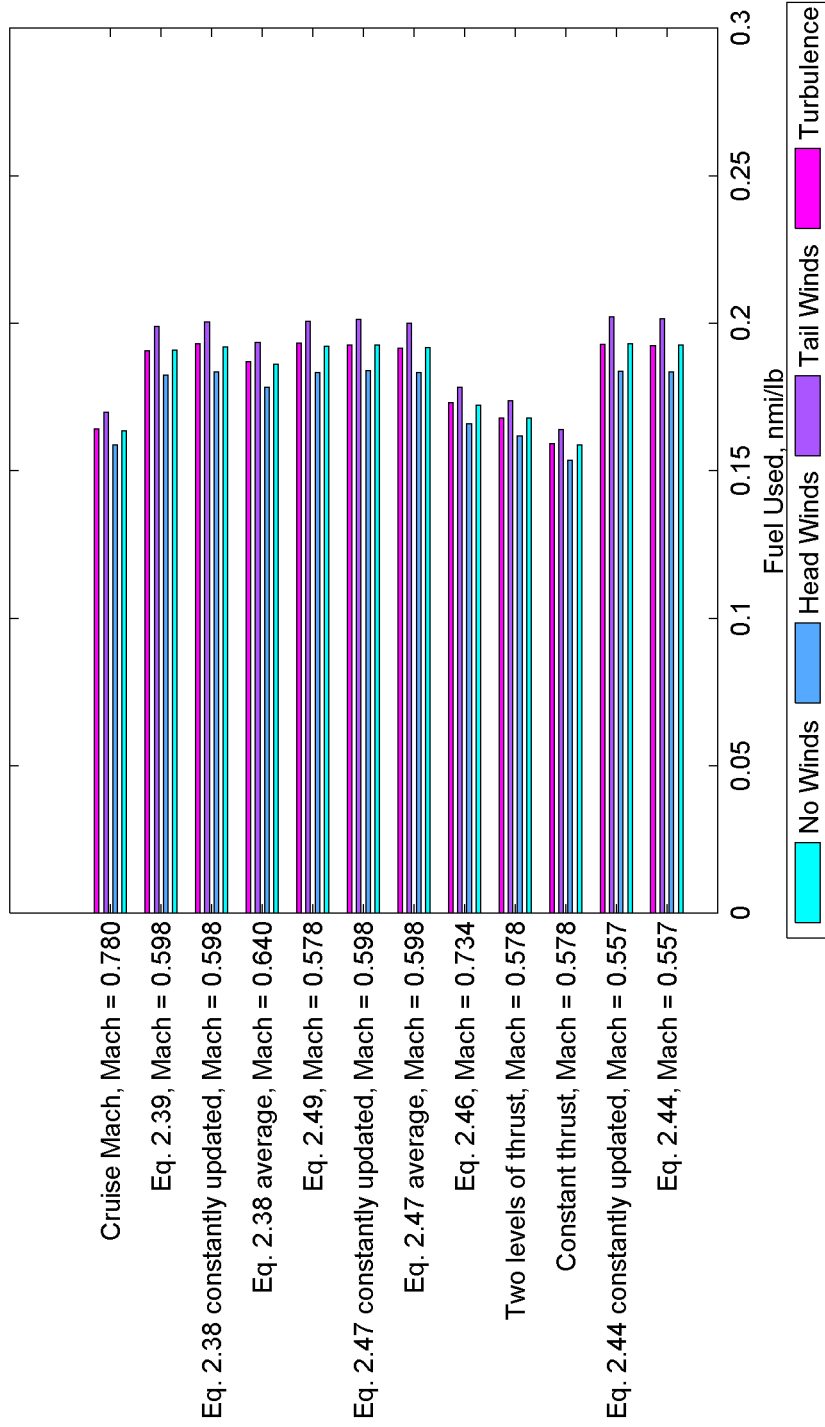


Figure 4.8: Comparison of methods with winds at 25,000 feet

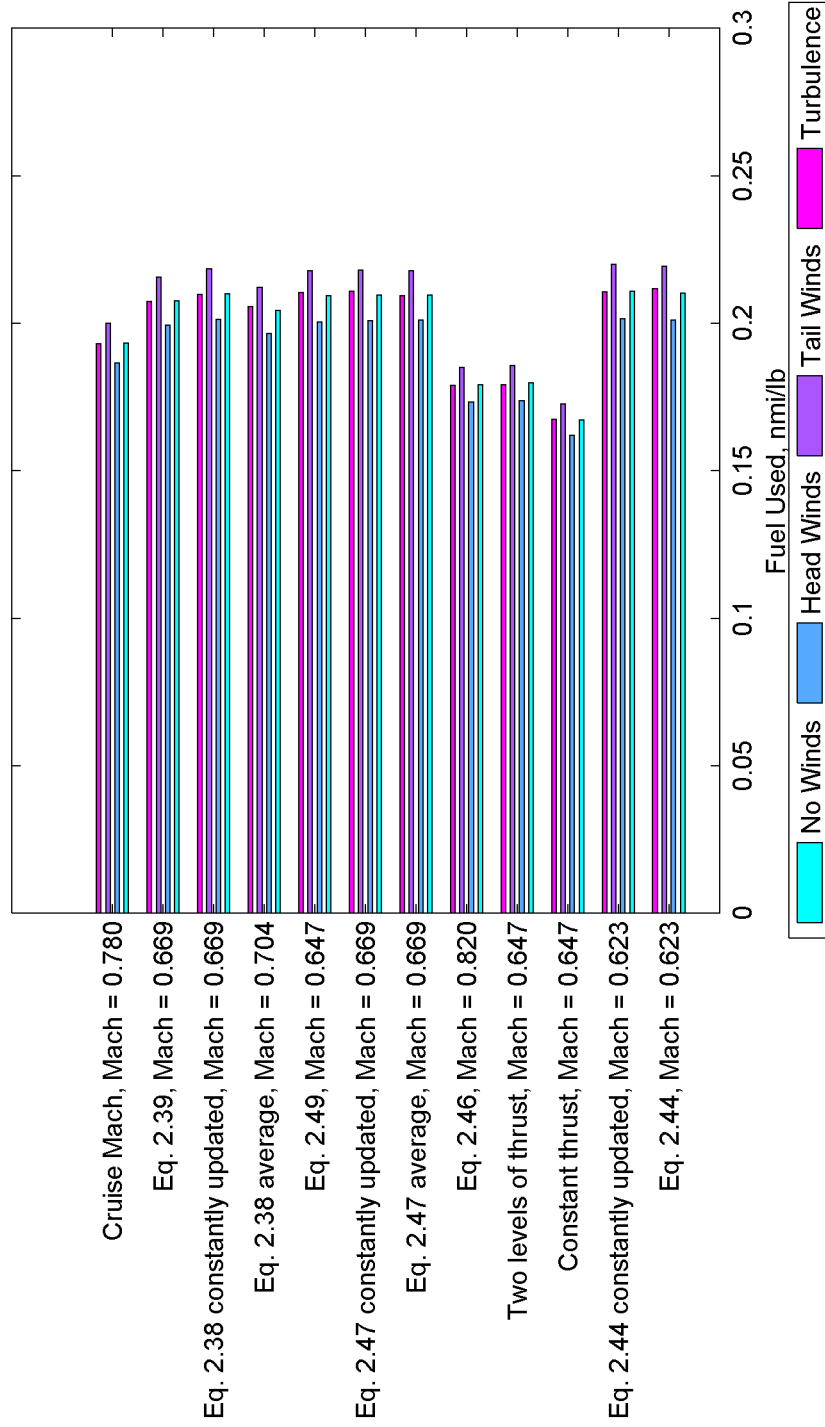


Figure 4.9: Comparison of methods with winds at 30,000 feet

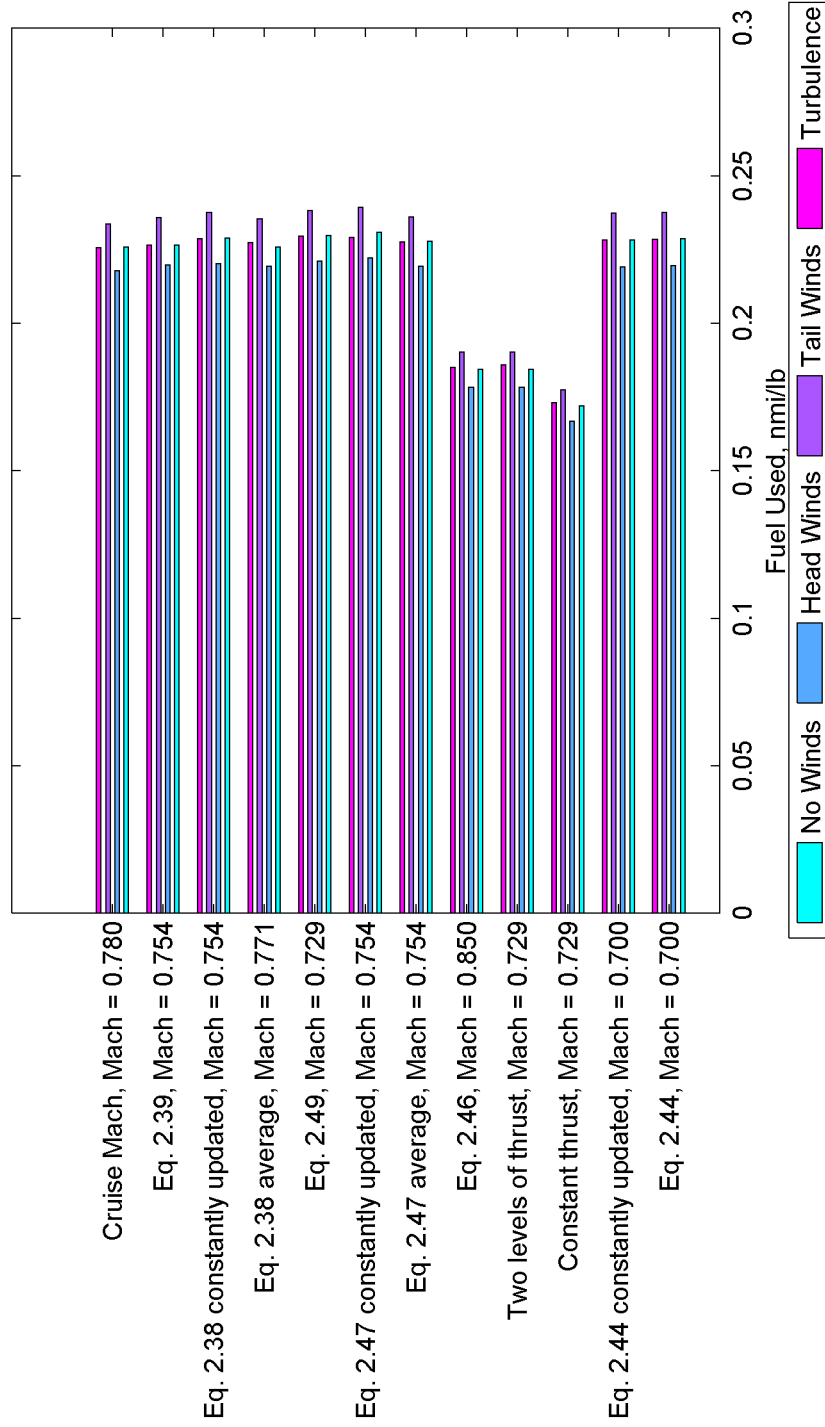


Figure 4.10: Comparison of methods with winds at 35,000 feet

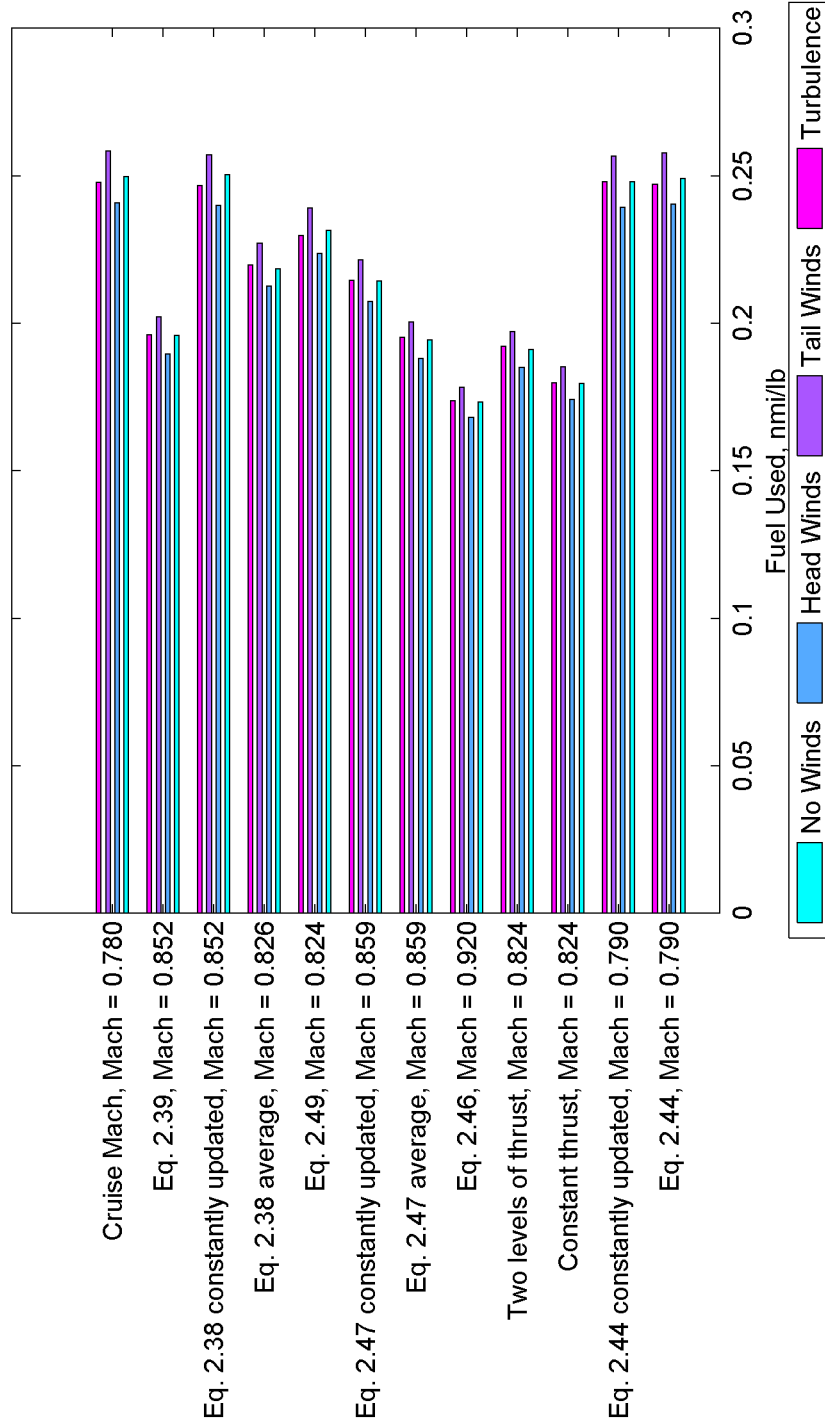


Figure 4.11: Comparison of methods with winds at 40,000 feet

CHAPTER 5. DISCUSSION AND SUMMARY

Several conclusions can be drawn from the results presented in Chapter 4. The first result is that there is at least one speed at every altitude that performed better than the standard cruise speed of Mach 0.78. While minimal throttle activity is preferred, the results show that some movement is necessary. The disturbances impacted the results as expected. The proposed method to be used on this aircraft. There were also limitations to this method that are described. Additionally the practical implementation and future work associated with this research are discussed.

5.1 Discussion

At each altitude there is at least one speed that is more efficient than the standard cruise Mach number. Table 5.1 shows the rank of the top six most efficient methods at each altitude when the reference was rounded to the nearest hundredth. In Table 5.2, the reference was rounded to the nearest thousandth. The top six were selected because, for all altitudes except 40,000 feet, these same six of the twelve total methods all appeared in various orders.

Table 5.1: Rank of top six methods at each altitude with the Mach number rounded to the nearest hundredth

Rank	20,000 Ft	25,000 Ft	30,000 Ft	35,000 Ft	40,000 Ft
1	Eq. 2.44 constantly updated	Eq. 2.44 constantly updated	Eq. 2.44 constantly updated	Eq. 2.47 constantly updated	Eq. 2.38 constantly updated
2	Eq. 2.44	Eq. 2.47 constantly updated	Eq. 2.44	Eq. 2.49	Cruise Mach number
3	Eq. 2.47 constantly updated	Eq. 2.44	Eq. 2.38 constantly updated	Eq. 2.38 constantly updated	Eq. 2.44
4	Eq. 2.47	Eq. 2.49	Eq. 2.47	Eq. 2.44	Eq. 2.44 constantly updated
5	Eq. 2.38 constantly updated	Eq. 2.38 constantly updated	Eq. 2.47 constantly updated	Eq. 2.44 constantly updated	Eq. 2.49
6	Eq. 2.49	Eq. 2.47	Eq. 2.49	Eq. 2.47	Eq. 2.38

Table 5.2: Rank of top six methods at each altitude with the Mach number rounded to the nearest thousandth

Rank	20,000 Ft	25,000 Ft	30,000 Ft	35,000 Ft	40,000 Ft
1	Eq. 2.49	Eq. 2.44	Eq. 2.44	Eq. 2.47 constantly updated	Eq. 2.38 constantly updated
2	Eq. 2.44 constantly updated	Eq. 2.49	Eq. 2.44 constantly updated	Eq. 2.49	Cruise Mach number
3	Eq. 2.38 constantly updated	Eq. 2.44 constantly updated	Eq. 2.38 constantly updated	Eq. 2.38 constantly updated	Eq. 2.44
4	Eq. 2.47 constantly updated	Eq. 2.47 constantly updated	Eq. 2.49	Eq. 2.44	Eq. 2.44 constantly updated
5	Eq. 2.47	Eq. 2.47	Eq. 2.47 constantly updated	Eq. 2.44 constantly updated	Eq. 2.49
6	Eq. 2.44	Eq. 2.38 constantly updated	Eq. 2.47	Eq. 2.47	Eq. 2.38

At 20,000 feet, the lowest altitude studied, the results from the top six methods were all within the margin of error for the simulation, and Equation 2.39 (rank 7) was also within the margin of error. Each of these methods were better than the Mach 0.78 cruising speed, which was the worst method for this altitude and the second worst method was constant thrust.

The results were very similar at altitudes between 25,000 and 35,000 feet, the worst case was constant thrust. The results of the best results showed that the top 7, 6, and 5 methods were within the margin of error for 25,000 feet, 30,000 feet, and 35,000 feet, respectively. However, at 35,000 feet, the sixth position was only 0.00303 nmi/lb lower than best method.

At 40,000 feet, only four of the top six methods remained within the margin of error of the simulation. In this case the difference between position five and one was 0.01895 nmi/lb and

the difference between six and one was 0.03186 nmi/lb, this translate to about 116 and 208 extra miles, respectively, that could have been flown during the same duration if best case was flown instead. The worst case for this altitude was Equation 2.46 and the second worst case was constant thrust. This altitude yielded a different set methods for the top six; the cruise Mach number and the average of Equation 2.38 were not in the top six for any other altitude. The cruise Mach number is probably in the top six in this case because it was within 0.15 Mach of the other speeds derived. Since the best case for this altitude was when Equation 2.38 was constantly updated, it is not entirely surprising that the average also performed pretty well. As this altitude is within about 1,000 feet of the service ceiling of the aircraft, the results may not be representative of the rest of the flight envelope.

For all altitudes there was no other method within the margin of error of the worst case. For altitudes between 25,000 feet and 35,000 feet, constant throttle was the worst case and it was the second worst case for the other two altitudes. This is expected because in the course of a three hour flight, over 5,000 lbs of fuel is consumed. As discussed in Section 3.3.3, the thrust required is directly dependent on the weight of the aircraft, so as fuel is burned and weight decreases the thrust required is also decreasing. This means that the throttle position set at the beginning of the flight is no longer appropriate.

As described in [8], minimal throttle activity is a desired design criterion for an autothrottle. However, this research shows that at least some throttle activity is needed to maintain a given speed, because the constant-thrust and dual-thrust methods were not in the top six at any altitude. The be same result would likely be seen on many airframes other than the one studied in this research.

Each of the original authors tested his proposed solution on different airframes, one a business jet [26], one an air transport sized jet [27] and one a generic transport sized aircraft [12] which is probably bigger than the aircraft considered here. In [26] the best method was achieved using the Mach number calculated with Equation 2.47. However, this data shows that, when comparing the methods from [26], at all altitudes except 35,000 feet, Equation 2.44 is more efficient than Equation 2.47. At all altitudes the difference between the best performing methods proposed in [26] were within the error of the simulation.

Since most of these methods were within the margin of error for this research, it is hard to pick one particular method that is the best. For a regional jet the normal cruise altitude range (20,000 - 30,000 feet), in this range the best method is Equation 2.44. The constant value from Equation 2.44 was also close to the top for each of these altitudes and would be a good alternative if the desired speed is to remain constant. While current ATC rules might not allow for varying speeds, the FAA is planning to role out new rules by 2025 that maybe more adaptable to flying a dynamically changing speed.

Since the speeds are so dependent on aircraft drag coefficients and engine characteristics, the best method proposed in this research might not be the same result for every airframe. The aircraft drag is quite different between a small business jet, like the Gulfstream IV and a Boeing 747 and each of these methods is dependent on the value of the drag coefficient. Additionally, the TSFC for each engine is different as is the transfer function of thrust to airspeed. Due to the difference in performance based on altitude, long haul air transport aircraft and business jets may find different results because they tend to fly at higher altitudes.

After analyzing the data from the sensitivity analysis, it was determined that for altitudes less than 35,000 feet, a variation of approximately plus or minus 0.05 Mach was still within the margin of error of the most efficient. The industry autothrottle is designed to track airspeeds to within plus or minus 0.02 Mach, therefore the autothrottle does not negatively impact the data at these altitudes. The sensitivity to slight changes in these speeds proposed seems to be minimal.

The next disturbance was winds. The head wind and tail wind disturbances had a significant impact on the fuel usage as expected. With a headwind burst the throttles would advance the throttles to compensate for the decrease in speed and then reduce the throttles once the burst had dissipated. As extra thrust is required to maintain the reference speed, the fuel usage was negatively impacted. However, the tail wind bursts had the opposite effect on the results. The impact of these bursts is unpredictable and probably cannot be avoided. To anticipate this impact, the average wind speed could be taken into consideration when flight planning. The results show that when six feet per second RMS turbulence was added the performance was not impacted. The fuel consumption for these cases was within the margin

of error of the case with no wind. This likely means that the industry autothrottle has been appropriately designed and tuned to fly through moderate turbulence.

Several combinations of changes were made to the autothrottle control law used in these simulations to reduce throttle activity. These changes included reducing the gain and removing the trim parameter that is sent directly to the engine. By removing the trim parameter, the amount of dead zone is increased before a change of thrust is commanded. None of these changes resulted in a significant improvement to the initial results, in steady air or with winds at several Mach numbers between 0.5 and 0.85. These changes were ineffective because prior to this research the autothrottle was already tuned to match this aircraft. The two gain programmers as well as the proportional and derivative gains would need to be adjusted when applied to another aircraft. As the engine characteristics directly impact the gain programmers and the dynamics of the aircraft, such as thrust-to-weight ratio, impact the other gains.

Several things were accomplished using the techniques in this research: various methods for optimizing fuel were compared using the same airframe. The speed-based methods were implemented using a practical process, however the thrust cases were more difficult to implement practically because they require a specific value of thrust which is unknown during flight. All of the practical methods were implemented using data available in a typical avionics system and using controllers in a typical industry autothrottle. The thrust methods were also implemented to determine if the performance increase warranted improvements to the system to implement this method. Finally, simulations were also run with the airspeed references constantly updated, even if that method is not practical in controlled airspace.

5.2 Limitations of the method

However, some things could not be accomplished in this study. Since the research was based on a generic regional jet simulation, exact values for C_D and C_L were unknown. If a simulation and real data for these parameters had been available from the airframe manufacturer, the data would have been more accurate for the airframe. The values calculated in this research are very specific to a particular airframe. Also, the data could not be validated with an actual flight test.

There were also things that ended up somewhat imperfectly. The greatest imperfection was the engine simulation. The resolution of the fuel flow model created 40 pound increments of weight change. These increments induced about 0.003 nmi/lb of error in the data. The accuracy of the fuel-flow model of the engine could not be verified. There are inefficiencies in the engine that can waste fuel when the fuel flow is adjusted, and the fuel flow is adjusted each time the throttle position is changed. These inefficiencies may not be accurately modeled in this simulation. Because the exact values of C_D and C_L were not available, estimates of these terms were used. As such, they are still not quite matched to the generic simulation.

5.3 Practical implementation

There are three ways that these methods could be implemented on a real airplane. The first implementation could be to add the algorithm to the FMS to continuously calculate the optimal Mach number for the autothrottle to follow. When the crew is setting up the flight plan, they could select the optimum Mach number as the speed for cruise flight. Another method would be to include these values in the flight planning software used by airlines. This would allow flight planners to consider both the altitude and speed at which each airplane is flown. Once this speed and altitude are selected by the flight planner they can be uploaded to the airplane via a data link or provided to the crew for entry into a flight plan. The latter method would be used on older aircraft. The third possibility would be to include the algorithm to calculate the optimum speed in the autothrottle. However, selection and deselection of the speed becomes more difficult to implement. Regardless of which method is used, it is essential to make it easy to deselect the speed in case the crew is directed to do so by ATC. Any of these methods could be immediately implemented in industry, given sufficient resources. Using the method of flight planning software would be easiest as it would not require recertifying the aircraft.

5.4 Future Work

In the future these equations could be applied to simulations of other airframes such as business jets or air-transport-sized aircraft to see if the same equations provide the best Mach number. Working directly with the airframe designer could also improve the results, since they would know the correct values of the constants needed to derive these values. Once the airframe is chosen, the speeds should be calculated using the constants for that airframe and the autothrottle should be tuned to match the new airframe as well. Then these same simulations could be performed, after that a method could be chosen to implement in flight worthy software and flown during in a real flight test. This flight test would validate the practical implementation discussed.

5.5 Summary

The results confirmed the first hypothesis that there is a specific speed, the optimum Mach number, that will maximize range. However this speed might not be derived the same way at each altitude. For this aircraft the recommendation is to fly the speed corresponding to the minimum thrust. If ATC will allow the aircraft to fly at these speeds, less fuel will be used. The key to making this result usable is to allow for the avionics (FMS/Autothrottle) or a ground-based database to calculate the speed for the crew. Since there are millions of flights per year in the United States alone, even small reductions in fuel consumption can have a large impact on fuel expense. Since flights using the optimum Mach number technique will require smaller fuel payloads, additional profitable payload can be added to each flight in the form of passengers or cargo. Additionally, the reductions in fuel consumption will lower greenhouse gas emissions from aircraft.

The second hypothesis was not confirmed in this study. It appears that the design of the industry autothrottle performed quite well in this simulation. However if this method is applied to other airframes, the autothrottle may need to be retuned to achieve the same performance.

APPENDIX A. NOMENCLATURE

AR	= Aspect ratio
b	= Wing Span
C_D	= Coefficient of drag
C_{D_0}	= Drag coefficient at zero lift
C_L	= Coefficient of lift
c_T	= Thrust Specific Fuel Consumption (TSFC)
c_{T_0}	= TSFC constant at a given altitude
D	= Drag
e	= Oswald span efficiency factor
E_m	= Maximum lift-to-drag ratio with cambered wing
E_{m_0}	= Maximum lift-to-drag ratio without cambered wing
g	= Gravity
h	= Altitude
K	= Induced drag factor
L	= Lift
M	= Mach number
m	= Mass
\dot{m}_{ac}	= Change of mass of the aircraft
\dot{m}_f	= Fuel mass flow rate
p	= Pressure at altitude
R	= Range
S	= Wing area
T	= Thrust

T_M = Maximum thrust

V = Velocity, true airspeed

W = Weight

β = TSFC Mach number exponent

γ = Specific heat ratio for air

δ = Throttle position

μ = ratio of the Mach number to the minimum drag Mach number

ρ = Atmospheric density

APPENDIX B. ALL RESULTS

All of the data collected for each method with the Mach number rounded to the nearest hundredth

Table B.1: Fuel used (nmi/lb) for each method with the Mach number rounded to the nearest hundredth at 20,000 feet

Equation	Mach	No Winds	Head Winds	Tail Winds	Turbulence
Eq. 2.44	0.50	0.1744	0.1651	0.1831	0.1739
Eq. 2.44 constantly updated	0.50	0.1744	0.1652	0.1833	0.1742
Constant thrust	0.52	0.1459	0.1408	0.1510	0.1459
Two levels of thrust	0.52	0.1536	0.1478	0.1595	0.1536
Eq. 2.46	0.66	0.1575	0.1511	0.1634	0.1572
Eq. 2.47 average	0.54	0.1739	0.1653	0.1819	0.1734
Eq. 2.47 constantly updated	0.54	0.1740	0.1655	0.1825	0.1738
Eq. 2.49	0.52	0.1734	0.1658	0.1830	0.1743
Eq. 2.38 average	0.58	0.1699	0.1622	0.1772	0.1697
Eq. 2.38 constantly updated	0.54	0.1738	0.1654	0.1821	0.1736
Eq. 2.39	0.54	0.1729	0.1647	0.1809	0.1728
Cruise Mach	0.78	0.1386	0.1340	0.1431	0.1385

Table B.2: Fuel used (nmi/lb) for each method with the Mach number rounded to the nearest hundredth at 25,000 feet

	Equation	Mach	No Winds	Head Winds	Tail Winds	Turbulence
	Eq. 2.44	0.56	0.1927	0.1835	0.2016	0.1923
Eq. 2.44	constantly updated	0.56	0.1931	0.1837	0.2022	0.1929
	Constant thrust	0.58	0.1588	0.1536	0.1640	0.1593
	Two levels of thrust	0.58	0.1678	0.1619	0.1737	0.1679
	Eq. 2.46	0.73	0.1723	0.1660	0.1783	0.1730
	Eq. 2.47 average	0.60	0.1918	0.1833	0.2001	0.1915
Eq. 2.47	constantly updated	0.60	0.1928	0.1840	0.2013	0.1926
	Eq. 2.49	0.58	0.1923	0.1834	0.2007	0.1933
	Eq. 2.38 average	0.64	0.1862	0.1783	0.1936	0.1871
Eq. 2.38	constantly updated	0.60	0.1921	0.1835	0.2004	0.1932
	Eq. 2.39	0.60	0.1908	0.1825	0.1989	0.1907
	Cruise Mach	0.78	0.1636	0.1588	0.1698	0.1642

Table B.3: Fuel used (nmi/lb) for each method with the Mach number rounded to the nearest hundredth at 30,000 feet

	Equation	Mach	No Winds	Head Winds	Tail Winds	Turbulence
	Eq. 2.44	0.62	0.2103	0.2011	0.2193	0.2117
Eq. 2.44	constantly updated	0.62	0.2108	0.2015	0.2199	0.2107
	Constant thrust	0.65	0.1673	0.1620	0.1727	0.1674
	Two levels of thrust	0.65	0.1798	0.1738	0.1857	0.1791
	Eq. 2.46	0.82	0.1792	0.1733	0.1850	0.1790
	Eq. 2.47 average	0.67	0.2096	0.2011	0.2179	0.2093
Eq. 2.47	constantly updated	0.67	0.2095	0.2009	0.2180	0.2110
	Eq. 2.49	0.65	0.2093	0.2006	0.2178	0.2105
	Eq. 2.38 average	0.70	0.2044	0.1966	0.2121	0.2056
Eq. 2.38	constantly updated	0.67	0.2101	0.2014	0.2186	0.2099
	Eq. 2.39	0.67	0.2077	0.1995	0.2157	0.2075
	Cruise Mach	0.78	0.1934	0.1866	0.1999	0.1932

Table B.4: Fuel used (nmi/lb) for each method with the Mach number rounded to the nearest hundredth at 35,000 feet

	Equation	Mach	No Winds	Head Winds	Tail Winds	Turbulence
	Eq. 2.44	0.70	0.2286	0.2196	0.2375	0.2285
Eq. 2.44	constantly updated	0.70	0.2283	0.2192	0.2374	0.2282
	Constant thrust	0.73	0.1721	0.1667	0.1775	0.1731
	Two levels of thrust	0.73	0.1844	0.1784	0.1903	0.1859
	Eq. 2.46	0.85	0.1843	0.1784	0.1902	0.1852
	Eq. 2.47 average	0.75	0.2277	0.2194	0.2360	0.2276
Eq. 2.47	constantly updated	0.75	0.2308	0.2222	0.2392	0.2291
	Eq. 2.49	0.73	0.2298	0.2211	0.2383	0.2296
	Eq. 2.38 average	0.77	0.2259	0.2193	0.2355	0.2273
Eq. 2.38	constantly updated	0.75	0.2289	0.2202	0.2375	0.2287
	Eq. 2.39	0.75	0.2265	0.2197	0.2359	0.2265
	Cruise Mach	0.78	0.2258	0.2178	0.2336	0.2256

Table B.5: Fuel used (nmi/lb) for each method with the Mach number rounded to the nearest hundredth at 40,000 feet

	Equation	Mach	No Winds	Head Winds	Tail Winds	Turbulence
	Eq. 2.44	0.79	0.2491	0.2404	0.2578	0.2472
Eq. 2.44	constantly updated	0.79	0.2480	0.2392	0.2568	0.2479
	Constant thrust	0.82	0.1797	0.1742	0.1852	0.1798
	Two levels of thrust	0.82	0.1912	0.1851	0.1973	0.1921
	Eq. 2.46	0.92	0.1733	0.1681	0.1784	0.1738
	Eq. 2.47 average	0.86	0.1943	0.1881	0.2005	0.1953
Eq. 2.47	constantly updated	0.86	0.2145	0.2074	0.2215	0.2145
	Eq. 2.49	0.82	0.2315	0.2236	0.2392	0.2299
	Eq. 2.38 average	0.83	0.2186	0.2125	0.2271	0.2198
Eq. 2.38	constantly updated	0.85	0.2504	0.2400	0.2572	0.2467
	Eq. 2.39	0.85	0.1959	0.1896	0.2022	0.1961
	Cruise Mach	0.78	0.2497	0.2409	0.2585	0.2477

All of the data collected for each method with the Mach number rounded to the nearest thousandth

Table B.6: Fuel used (nmi/lb) for each method with the Mach number rounded to the nearest thousandth at 20,000 feet

	Equation	Mach	No Winds	Head Winds	Tail Winds	Turbulence
	Eq. 2.44	0.501	0.1734	0.1643	0.1820	0.1743
Eq. 2.44	constantly updated	0.501	0.1741	0.1651	0.1833	0.1741
	Eq. 2.46	0.659	0.1572	0.1517	0.1632	0.1578
	Eq. 2.47 average	0.537	0.1737	0.1652	0.1818	0.1746
Eq. 2.47	constantly updated	0.537	0.1738	0.1653	0.1823	0.1738
	Eq. 2.49	0.519	0.1743	0.1655	0.1827	0.1740
	Eq. 2.38 average	0.579	0.1695	0.1628	0.1778	0.1702
Eq. 2.38	constantly updated	0.537	0.1739	0.1655	0.1820	0.1737
	Cruise Mach	0.780	0.1387	0.1340	0.1431	0.1385

Table B.7: Fuel used (nmi/lb) for each method with the Mach number rounded to the nearest thousandth at 25,000 feet

	Equation	Mach	No Winds	Head Winds	Tail Winds	Turbulence
	Eq. 2.44	0.557	0.1931	0.1838	0.2021	0.1928
Eq. 2.44	constantly updated	0.557	0.1929	0.1836	0.2020	0.1929
	Eq. 2.46	0.578	0.1589	0.1537	0.1641	0.1592
	Eq. 2.47 average	0.598	0.1922	0.1837	0.2004	0.1919
Eq. 2.47	constantly updated	0.598	0.1926	0.1839	0.2011	0.1925
	Eq. 2.49	0.578	0.1930	0.1841	0.2016	0.1927
	Eq. 2.38 average	0.640	0.1859	0.1792	0.1945	0.1868
Eq. 2.38	constantly updated	0.598	0.1920	0.1834	0.2003	0.1932
	Cruise Mach	0.780	0.1636	0.1587	0.1698	0.1642

Table B.8: Fuel used (nmi/lb) for each method with the Mach number rounded to the nearest thousandth at 30,000 feet

	Equation	Mach	No Winds	Head Winds	Tail Winds	Turbulence
	Eq. 2.44	0.623	0.2110	0.2018	0.2200	0.2107
Eq. 2.44	constantly updated	0.623	0.2107	0.2015	0.2199	0.2108
	Eq. 2.46	0.647	0.1668	0.1615	0.1721	0.1673
	Eq. 2.47 average	0.647	0.1790	0.1730	0.1849	0.1797
Eq. 2.47	constantly updated	0.669	0.2094	0.2009	0.2179	0.2109
	Eq. 2.49	0.647	0.2098	0.2011	0.2184	0.2111
	Eq. 2.38 average	0.704	0.2040	0.1961	0.2116	0.2052
Eq. 2.38	constantly updated	0.669	0.2106	0.2019	0.2191	0.2104
	Cruise Mach	0.780	0.1934	0.1866	0.1999	0.1932

Table B.9: Fuel used (nmi/lb) for each method with the Mach number rounded to the nearest thousandth at 35,000 feet

	Equation	Mach	No Winds	Head Winds	Tail Winds	Turbulence
	Eq. 2.44	0.700	0.2283	0.2193	0.2372	0.2281
Eq. 2.44	constantly updated	0.700	0.2280	0.2190	0.2371	0.2281
	Eq. 2.46	0.729	0.1715	0.1662	0.1769	0.1715
	Eq. 2.47 average	0.729	0.1845	0.1786	0.1904	0.1845
Eq. 2.47	constantly updated	0.850	0.1844	0.1784	0.1903	0.1852
	Eq. 2.49	0.729	0.2294	0.2208	0.2380	0.2293
	Eq. 2.38 average	0.771	0.2259	0.2193	0.2354	0.2273
Eq. 2.38	constantly updated	0.754	0.2286	0.2199	0.2373	0.2286
	Cruise Mach	0.780	0.2258	0.2178	0.2336	0.2256

Table B.10: Fuel used (nmi/lb) for each method with the Mach number rounded to the nearest thousandth at 40,000 feet

	Equation	Mach	No Winds	Head Winds	Tail Winds	Turbulence
	Eq. 2.44	0.790	0.2491	0.2404	0.2578	0.2472
Eq. 2.44	constantly updated	0.790	0.2479	0.2391	0.2566	0.2479
	Eq. 2.46	0.824	0.1797	0.1742	0.1852	0.1797
	Eq. 2.47 average	0.824	0.1912	0.1851	0.1973	0.1921
Eq. 2.47	constantly updated	0.920	0.1733	0.1681	0.1784	0.1738
	Eq. 2.49	0.859	0.1959	0.1896	0.2022	0.1969
	Eq. 2.38 average	0.826	0.2229	0.2168	0.2317	0.2242
Eq. 2.38	constantly updated	0.852	0.2504	0.2417	0.2590	0.2467
	Cruise Mach	0.780	0.2497	0.2409	0.2584	0.2477

All of the data collected for each Mach number variation with the Mach number rounded to the nearest hundredth

Table B.11: Fuel used (nmi/lb) for three methods with small Mach variations from the calculated value rounded to the nearest hundredth at 20,000 Feet

Eq. 2.47		Eq. 2.49		Eq. 2.38	
Mach	Fuel Used	Mach	Fuel Used	Mach	Fuel Used
0.537	0.1739	0.519	0.1734	0.579	0.1699
0.337	0.1514	0.319	0.1513	0.379	0.1514
0.362	0.1513	0.344	0.1512	0.404	0.1600
0.387	0.1544	0.369	0.1513	0.429	0.1677
0.412	0.1626	0.394	0.1543	0.454	0.1712
0.437	0.1689	0.419	0.1653	0.479	0.1739
0.487	0.1735	0.469	0.1731	0.529	0.1743
0.512	0.1739	0.494	0.1734	0.554	0.1734
0.527	0.1743	0.509	0.1738	0.569	0.1713
0.547	0.1734	0.529	0.1742	0.589	0.1675
0.562	0.1730	0.544	0.1738	0.604	0.1662
0.587	0.1677	0.569	0.1714	0.629	0.1619
0.637	0.1602	0.619	0.1629	0.679	0.1542

Table B.12: Fuel used (nmi/lb) for three methods with small Mach variations from the calculated value rounded to the nearest hundredth at 25,000 Feet

Eq. 2.47		Eq. 2.49		Eq. 2.38	
Mach	Fuel Used	Mach	Fuel Used	Mach	Fuel Used
0.598	0.1918	0.578	0.1923	0.640	0.1862
0.398	0.1654	0.378	0.1655	0.440	0.1753
0.423	0.1655	0.403	0.1654	0.465	0.1818
0.448	0.1795	0.428	0.1682	0.490	0.1887
0.473	0.1842	0.453	0.1794	0.515	0.1916
0.498	0.1909	0.478	0.1865	0.540	0.1931
0.548	0.1922	0.528	0.1927	0.590	0.1927
0.573	0.1931	0.553	0.1921	0.615	0.1910
0.588	0.1927	0.568	0.1918	0.630	0.1880
0.608	0.1910	0.588	0.1927	0.650	0.1843
0.623	0.1901	0.603	0.1918	0.665	0.1825
0.648	0.1843	0.628	0.1881	0.690	0.1788
0.698	0.1773	0.678	0.1803	0.740	0.1711

Table B.13: Fuel used (nmi/lb) for three methods with small Mach variations from the calculated value rounded to the nearest hundredth at 30,000 Feet

Eq. 2.47		Eq. 2.49		Eq. 2.38	
Mach	Fuel Used	Mach	Fuel Used	Mach	Fuel Used
0.669	0.2096	0.647	0.2093	0.704	0.2044
0.469	0.1803	0.447	0.1803	0.504	0.1968
0.494	0.1944	0.472	0.1803	0.529	0.2032
0.519	0.2010	0.497	0.1968	0.554	0.2090
0.544	0.2070	0.522	0.2010	0.579	0.2114
0.569	0.2112	0.547	0.2090	0.604	0.2116
0.619	0.2103	0.597	0.2117	0.654	0.2092
0.644	0.2106	0.622	0.2103	0.679	0.2083
0.659	0.2095	0.637	0.2107	0.694	0.2070
0.679	0.2083	0.657	0.2094	0.714	0.2033
0.694	0.2070	0.672	0.2096	0.729	0.2000
0.719	0.2010	0.697	0.2045	0.754	0.1981
0.769	0.1952	0.747	0.1970	0.804	0.1868

Table B.14: Fuel used (nmi/lb) for three methods with small Mach variations from the calculated value rounded to the nearest hundredth at 35,000 Feet

Eq. 2.47		Eq. 2.49		Eq. 2.38	
Mach	Fuel Used	Mach	Fuel Used	Mach	Fuel Used
0.754	0.2277	0.729	0.2298	0.771	0.2259
0.554	0.2116	0.529	0.1942	0.571	0.2173
0.579	0.2192	0.554	0.2115	0.596	0.2229
0.604	0.2249	0.579	0.2192	0.621	0.2284
0.629	0.2283	0.604	0.2249	0.646	0.2279
0.654	0.2278	0.629	0.2283	0.671	0.2274
0.704	0.2286	0.679	0.2272	0.721	0.2283
0.729	0.2297	0.704	0.2286	0.746	0.2278
0.744	0.2296	0.719	0.2282	0.761	0.2276
0.764	0.2276	0.739	0.2295	0.781	0.2258
0.779	0.2258	0.754	0.2277	0.796	0.2157
0.804	0.2157	0.779	0.2258	0.821	0.2045
0.850	0.1843	0.829	0.1968	0.850	0.1843

Table B.15: Fuel used (nmi/lb) for three methods with small Mach variations from the calculated value rounded to the nearest hundredth at 40,000 Feet

Eq. 2.47		Eq. 2.49		Eq. 2.38	
Mach	Fuel Used	Mach	Fuel Used	Mach	Fuel Used
0.859	0.1943	0.824	0.2315	0.826	0.2186
0.659	0.2338	0.624	0.2234	0.626	0.2233
0.684	0.2429	0.649	0.2284	0.651	0.2285
0.709	0.2436	0.674	0.2373	0.676	0.2429
0.734	0.2446	0.699	0.2421	0.701	0.2440
0.759	0.2451	0.724	0.2431	0.726	0.2446
0.809	0.2397	0.774	0.2464	0.776	0.2497
0.834	0.2185	0.799	0.2469	0.801	0.2469
0.849	0.2005	0.814	0.2396	0.816	0.2300
0.869	0.1887	0.834	0.2185	0.836	0.2096
0.884	0.1852	0.849	0.2005	0.851	0.2005
0.909	0.1752	0.874	0.1896	0.876	0.1852
0.920	0.1733	0.920	0.1733	0.920	0.1733

All of the data collected for each Mach number variation with the Mach number rounded to the nearest thousandth

Table B.16: Fuel used (nmi/lb) for three methods with small Mach variations from the calculated value rounded to the nearest thousandth at 20,000 Feet

Eq. 2.47		Eq. 2.49		Eq. 2.38	
Mach	Fuel Used	Mach	Fuel Used	Mach	Fuel Used
0.537	0.1737	0.519	0.1743	0.579	0.1695
0.437	0.1685	0.319	0.1511	0.379	0.1511
0.337	0.1511	0.344	0.1511	0.404	0.1613
0.362	0.1511	0.369	0.1511	0.429	0.1668
0.387	0.1519	0.394	0.1574	0.454	0.1722
0.412	0.1629	0.419	0.1647	0.479	0.1733
0.487	0.1733	0.469	0.1727	0.529	0.1736
0.512	0.1742	0.494	0.1736	0.554	0.1731
0.527	0.1742	0.509	0.1735	0.569	0.1709
0.547	0.1733	0.529	0.1739	0.589	0.1681
0.562	0.1722	0.544	0.1739	0.604	0.1662
0.587	0.1686	0.569	0.1712	0.629	0.1615
0.637	0.1609	0.619	0.1628	0.679	0.1545

Table B.17: Fuel used (nmi/lb) for three methods with small Mach variations from the calculated value rounded to the nearest thousandth at 25,000 Feet

Eq. 2.47		Eq. 2.49		Eq. 2.38	
Mach	Fuel Used	Mach	Fuel Used	Mach	Fuel Used
0.598	0.1922	0.578	0.1930	0.640	0.1859
0.398	0.1654	0.378	0.1654	0.440	0.1748
0.423	0.1655	0.403	0.1655	0.465	0.1818
0.448	0.1782	0.428	0.1678	0.490	0.1883
0.473	0.1848	0.453	0.1807	0.515	0.1914
0.498	0.1897	0.478	0.1857	0.540	0.1928
0.548	0.1925	0.528	0.1918	0.590	0.1923
0.573	0.1923	0.553	0.1917	0.615	0.1909
0.588	0.1917	0.568	0.1925	0.630	0.1878
0.608	0.1913	0.588	0.1920	0.650	0.1840
0.623	0.1895	0.603	0.1914	0.665	0.1825
0.648	0.1846	0.628	0.1887	0.690	0.1785
0.698	0.1775	0.678	0.1798	0.740	0.1708

Table B.18: Fuel used (nmi/lb) for three methods with small Mach variations from the calculated value rounded to the nearest thousandth at 30,000 Feet

Eq. 2.47		Eq. 2.49		Eq. 2.38	
Mach	Fuel Used	Mach	Fuel Used	Mach	Fuel Used
0.669	0.2093	0.647	0.2098	0.704	0.2040
0.469	0.1802	0.447	0.1802	0.504	0.1980
0.494	0.1962	0.472	0.1805	0.529	0.2041
0.519	0.2007	0.497	0.1973	0.554	0.2102
0.544	0.2067	0.522	0.2018	0.579	0.2106
0.569	0.2109	0.547	0.2079	0.604	0.2110
0.619	0.2099	0.597	0.2106	0.654	0.2102
0.644	0.2104	0.622	0.2110	0.679	0.2092
0.659	0.2106	0.637	0.2097	0.694	0.2052
0.679	0.2080	0.657	0.2099	0.714	0.2029
0.694	0.2055	0.672	0.2087	0.729	0.2007
0.719	0.2020	0.697	0.2050	0.754	0.1977
0.769	0.1949	0.747	0.1985	0.804	0.1855

Table B.19: Fuel used (nmi/lb) for three methods with small Mach variations from the calculated value rounded to the nearest thousandth at 35,000 Feet

Eq. 2.47		Eq. 2.49		Eq. 2.38	
Mach	Fuel Used	Mach	Fuel Used	Mach	Fuel Used
0.754	0.2273	0.729	0.2294	0.771	0.2259
0.554	0.2132	0.529	0.1941	0.571	0.2173
0.579	0.2189	0.554	0.2132	0.596	0.2230
0.604	0.2244	0.579	0.2189	0.621	0.2284
0.629	0.2279	0.604	0.2244	0.646	0.2279
0.654	0.2274	0.629	0.2279	0.671	0.2275
0.704	0.2282	0.679	0.2286	0.721	0.2282
0.729	0.2294	0.704	0.2282	0.746	0.2295
0.744	0.2291	0.719	0.2296	0.761	0.2276
0.764	0.2272	0.739	0.2292	0.781	0.2258
0.779	0.2255	0.754	0.2274	0.796	0.2184
0.804	0.2128	0.779	0.2255	0.821	0.2045
0.850	0.1843	0.829	0.1976	0.850	0.1843

Table B.20: Fuel used (nmi/lb) for three methods with small Mach variations from the calculated value rounded to the nearest thousandth at 40,000 Feet

Eq. 2.47		Eq. 2.49		Eq. 2.38	
Mach	Fuel Used	Mach	Fuel Used	Mach	Fuel Used
0.859	0.1959	0.824	0.2252	0.826	0.2229
0.659	0.2312	0.624	0.2230	0.626	0.2237
0.684	0.2420	0.649	0.2280	0.651	0.2288
0.709	0.2429	0.674	0.2408	0.676	0.2414
0.734	0.2436	0.699	0.2436	0.701	0.2424
0.759	0.2444	0.724	0.2444	0.726	0.2432
0.809	0.2407	0.774	0.2476	0.776	0.2483
0.834	0.2166	0.799	0.2483	0.801	0.2472
0.849	0.2022	0.814	0.2360	0.816	0.2334
0.869	0.1901	0.834	0.2156	0.836	0.2135
0.884	0.1840	0.849	0.2024	0.851	0.2007
0.909	0.1764	0.874	0.1876	0.876	0.1871
0.920	0.1732	0.920	0.1732	0.920	0.1732

APPENDIX C. MATLAB CODE

Matlab function used to calculate the singular arc

```

function [Warc, Marc] = singularArcFunction(altitudeSelection)
%This function calculates the singular arc
%based on an altitude selection.
%The altitude is selected according to the following
%enumeration:
%altitudeSelection      Altitude (Ft)
%1                       20,000
%2                       25,000
%3                       30,000
%4                       35,000
%5                       40,000

%parameters
S = 760;      %ft^2, wing area
b = 76.25;   %ft, wing span
AR = b^2/S;  %Aspect ratio
fuelLoadMax = 19450;    %lbs
effFac = 0.85;         %assumed Oswald span efficiency
f = 11.5;
CD0 = f/S;             %drag coefficient @ zero lift
K = 1/pi/effFac/AR;   %induced drag factor

sqrtKOverCD0 = sqrt(K/CD0);

maxTkoWeight = 75750;    %lbs
maxFuel = 19450;        %lbs
maxFuelGal = maxFuel/6.84; %gal
%lbs, approximation of cruise weight
cruiseWeight = maxTkoWeight * 0.955;

altValues = [20000, 25000, 30000, 35000, 40000];
m1AltValues = [1036.9, 1016.1, 994.8, 973.1, 968.1];
ctalphaValues = [0.3639, 0.3632, 0.3624, 0.3609, 0.3609];
alphaValues = [1.201, 1.1807, 1.1598, 1.1413, 1.1357];
Vmin = [550, 600, 650, 700, 750];
Vmax = [650, 700, 750, 800, 850];

```

```

W = 72300;           %lbs , rounded value of cruiseWeight
h = altValues(altitudeSelection);
V = 0;
V = Vmin(altitudeSelection):5:Vmax(altitudeSelection);
Marc = V./m1AltValues(altitudeSelection);

%Atmospheric density from nasa
if h < 36152
    T = 59 - 0.00356*h;           %deg F, temperature
    P = 2116 * ((T+459.7)/518.6)^5.256; %lbf/ft ^2, pressure
else
    T = -70;           %deg F, temperature
    P = 473.1 * exp(1.73-0.000048 * h); %lbf/ft ^2, pressure
end

rho = P/ (1718 * (T + 459.7));    %slugs/ft ^3, density

A = CD0 * rho*S/2;
B = 2*K/rho/S;
C_T = 0;
C_TV = 0;
Warc = 0;
for speedLoop = 1:length(V)
    C_T = ctalphaValues(altitudeSelection)*...
        exp(alphaValues(altitudeSelection)*...
            V(speedLoop)/m1AltValues(altitudeSelection));
    C_TV = ctalphaValues(altitudeSelection)*...
        alphaValues(altitudeSelection)/...
        m1AltValues(altitudeSelection)*...
        exp(alphaValues(altitudeSelection)*...
            V(speedLoop)/m1AltValues(altitudeSelection));
    Warc(speedLoop) = V(speedLoop)^2*...
        sqrt(A*(1+C_TV*V(speedLoop)/C_T)/...
            (B*(3-C_TV*V(speedLoop)/C_T)));
end

```

Matlab script used to run the simulation of each method

```

%Simulation Script
%This script will setup and run the aircraft simulation
%with each control and disturbance in the test matrix.
runTime = 3600*3;
%Run the initializaton script
atSimulationInit

```

```
%Calculate the desired Mach numbers from the Myose Paper
%Outputs Temp, MminThrust, and Mmax_CICd for each altitude
MyosePaperCalc
```

```
%The following arrays are the Mach numbers
%calculated for other scenarios in the Myose paper
```

```
%Mach number for Max V(L/D)/TSFC at 72300 lbs
initalMach = [0.536668, 0.597958, 0.669305, ...
0.754096, 0.858998];
```

```
%Mach number for Max V(L/D)/TSFC at 63118 lbs
finalMach = [0.501433, 0.558699, 0.625362, ...
0.704586, 0.796061];
```

```
%Average Mach number Max V(L/D)/TSFC
avgMach = [0.561749, 0.625904, 0.700585, ...
0.789339, 0.885789];
```

```
%Mach number for Max (L/D)
maxLDMach = [0.519051, 0.578329, 0.647333, ...
0.729341, 0.824030];
```

```
%Approximate TLA values for the Thrust Required
%at each altitude used for setting the constant
%Thrust from the Myose paper
tlaValues = [58, 58.5, 59, 60, 63];
```

```
%Average Mach number from Cavcar Paper
avgMachC = [0.51906817, 0.57836632, 0.64735469, ...
0.72938882, 0.82446515];
```

```
%Calculation of Singular Arc from Pargett Paper
startMach = [0.53666787, 0.59795812, 0.66930484, ...
0.75409557, 0.851999];
endMach = [0.50143317, 0.55869944, 0.62536192, ...
0.70458575, 0.79606091];
```

```
loopNum = 0;
```

```
%Altitudes under test
altValues = [20000, 25000, 30000, 35000, 40000];
```

```
for altLoop = 1:length(altValues)
    Ic_Alt = altValues(altLoop);
    Ic_Weight = 72300; %pounds
```

```
    for controlLoop = 1:11
        asRefCalulated = 0;
```

```

asRefMinThrustReq = 0;
asRefMax = 0;
constantTla = 0;
External_Throttle_Input = 0;
switch controlLoop
  case 1
    controlType = 'Myose: V_{minThrust} -...
    Init Value';
    Ic_Mach = MminThrust(altLoop);
    MachReference = Ic_Mach;
    IcMachReference = Ic_Mach;
  case 2
    controlType = 'Myose: V_{minThrust} -...
    Constant Update';
    asRefCalculated = 1;
    asRefMinThrustReq = 1;
    Ic_Mach = MminThrust(altLoop);
    MachReference = Ic_Mach;
    IcMachReference = Ic_Mach;
  case 3
    controlType = 'Myose: Constant Thrust';
    Ic_Mach = maxLDMach(altLoop);
    MachReference = Ic_Mach;
    IcMachReference = Ic_Mach;
    constantTla = 1;
    External_Throttle_Input = 1;
    leftThrottleStepTime = 3600;
    leftThrottleInitial = tlaValues(altLoop);
    leftThrottleFinal = tlaValues(altLoop);
    rightThrottleStepTime = 3600;
    rightThrottleInitial = tlaValues(altLoop);
    rightThrottleFinal = tlaValues(altLoop);
  case 4
    controlType = 'Myose: Dual Thrust';
    constantTla = 1;
    External_Throttle_Input = 1;
    leftThrottleStepTime = runTime/2;
    leftThrottleInitial = tlaValues(altLoop);
    leftThrottleFinal = tlaValues(altLoop)-5;
    rightThrottleStepTime = runTime/2;
    rightThrottleInitial = tlaValues(altLoop);
    rightThrottleFinal = tlaValues(altLoop)-5;
  case 5
    controlType = 'Myose: Max V(L/D)';
    Ic_Mach = Mmax_ClCd(altLoop);
    MachReference = Ic_Mach;

```

```

IcMachReference = Ic_Mach;

case 6
controlType = 'Myose: Max V(L/D)/...
TSFC-Average';
Ic_Mach = initalMach(altLoop);
MachReference = Ic_Mach;
IcMachReference = Ic_Mach;

case 7
controlType = 'Myose: Max V(L/D)/...
TSFC-Constant Update';
asRefCalulated = 1;
asRefMax = 1;
Ic_Mach = avgMach(altLoop);
MachReference = Ic_Mach;
IcMachReference = Ic_Mach;
Ic_Mach = initalMach(altLoop);
maxMach = [finalMach(altLoop),...
           initalMach(altLoop)];

case 8
controlType = 'Cavcar: Average Mach';
Ic_Mach = avgMachC(altLoop);
MachReference = Ic_Mach;
IcMachReference = Ic_Mach;

case 9
controlType = 'Pargett: Average Mach';
[Warc, Marc] = singularArcFunction(altLoop);
Ic_Mach = mean(Marc);
MachReference = Ic_Mach;
IcMachReference = Ic_Mach;

case 10
controlType = 'Pargett: Singular Arc';
[Warc, Marc] = singularArcFunction(altLoop);
asRefCalulated = 1;
Ic_Mach = startMach(altLoop);
MachReference = Ic_Mach;
IcMachReference = Ic_Mach;

case 11
controlType = 'Cruise Mach';
Ic_Mach = 0.78;
MachReference = Ic_Mach;
IcMachReference = Ic_Mach;

end %switch - control

```

```

if Ic_Alt > 37000
    mmoSim = 0.92;
else
    mmoSim = 0.85;
end

if Ic_Mach > mmoSim
    Ic_Mach = mmoSim;
end

% Trim the aircraft to the specific IC conditions
Ic_Tas=ias2tas ([Ic_Mach ,Ic_Alt ]);
Trim_Mode_Req = 1;
sim('fcssimAutothrottleAirspeedCruise',5); %
Trim_Mode_Req = 0;

for distLoop = 1:4
    windsTime = [0, 1000, 1060, 4660, 4720, ...
        6500, 6501, 8500, 8560, runTime];
    windsSpeed = [0, 0, 0, 0, 0, ...
        0, 0, 0, 0, 0];
    windsEnbLngGust=0;
    windsEnbLatGust=0;
    windsEnbVrtGust=0;
    switch distLoop

        case 1
            distTxt = 'None';

        case 2
            distTxt = 'Head Winds';
            windsTime = [0, 1000, 1060, 4660, 4720, ...
                6500, 6501, 8500, 8560, runTime];
            windsSpeed = [0, 0, 30, 30, 0, ...
                0, 30, 30, 0, 0]*1.6878;

        case 3
            distTxt = 'Tail Winds';
            windsTime = [0, 1000, 1060, 4660, 4720, ...
                6500, 6501, 8500, 8560, runTime];
            windsSpeed = [0, 0, 30, 30, 0, ...
                0, 30, 30, 0, 0]*-1.6878;
    end

```

```

case 4
    distTxt = 'Turbulence';
    windsEnbLngGust=1;
    windsEnbLatGust=1;
    windsEnbVrtGust=1;

end %switch - control

% Run the simulation
tic
sim('fcssimAutothrottleAirspeedCruise',runTime);
toc

% Save the data
fileName=sprintf('autothrottleAirspeedTest_%d_%d_%d',...
    altLoop,controlLoop,distLoop)
save(fileName,'plotout','Ic_Alt','Ic_Mach',...
    'distTxt','controlType');

% Extract the label names
plotoutLabelNames = extractLabelNamesFunction(plotout);

% Plot the results
titleName=strrep(fileName,'_','\ ');
figure(1)
orient landscape;

subplot(6,1,1)
plot(plotout.time,plotout.signals.values(:,3));
hold on;
plot(plotout.time,plotout.signals.values(:,4),'m—');
ylabel(plotoutLabelNames(3));
xlabel(sprintf('%s shown in Pink — Line',...
    plotoutLabelNames{4}))
title(sprintf('%s: Alt = %d Ft, Control Type = %s, ...
    Disturbance = %s\nMach = %0.3g, X-Dist %5.3f nmi, ...
    Weight Final = %5.0f lbs',...
    titleName,Ic_Alt,controlType,distTxt,Ic_Mach,...
    max(plotout.signals.values(:,16))/6076.11549,...
    plotout.signals.values(length(plotout.time),17)));
ylim([min(plotout.signals.values(:,3))-0.01,...
    max(plotout.signals.values(:,3))+0.01]);
xlim([0,max(plotout.time)]);
set(gca,'xticklabel',[]);
grid on; hold off;

```

```

subplot(6,1,2)
plot(plotout.time, plotout.signals.values(:,1));
hold on;
plot(plotout.time, plotout.signals.values(:,2), 'm—');
ylabel(plotoutLabelNames(1));
xlabel(sprintf('%s shown in Pink — Line', ...
    plotoutLabelNames{2}))
xlim([0, max(plotout.time)]);
set(gca, 'xticklabel', []);
grid on; hold off;

subplot(6,1,3)
plot(plotout.time, plotout.signals.values(:,22));
hold on;
plot(plotout.time, plotout.signals.values(:,23), 'm—');
ylabel(plotoutLabelNames(22));
xlabel(sprintf('%s shown in Pink — Line', ...
    plotoutLabelNames{23}))
ylim([min([plotout.signals.values(:,22);...
    plotout.signals.values(:,23)]) - 1, ...
    max([plotout.signals.values(:,22);...
    plotout.signals.values(:,23)]) + 1]);
xlim([0, max(plotout.time)]);
set(gca, 'xticklabel', []);
grid on; hold off;

subplot(6,1,4)
plot(plotout.time, plotout.signals.values(:,7));
hold on;
plot(plotout.time, plotout.signals.values(:,5), 'm—');
ylabel(sprintf('%s\n', plotoutLabelNames{7}));
xlabel(sprintf('%s shown in Pink — Line', ...
    plotoutLabelNames{5}))
xlim([0, max(plotout.time)]);
set(gca, 'xticklabel', []);
grid on; hold off;

subplot(6,1,5)
plot(plotout.time, plotout.signals.values(:,9));
hold on;
plot(plotout.time, plotout.signals.values(:,11), 'm—');
ylabel(sprintf('%s\n', plotoutLabelNames{9}));
if controlLoop == 3
    desiredThrust=0;
    desiredThrust(1:length(plotout.time))=...
        thrustForLDMax/2;

```



```

    plot(plotout.time,desiredThrust,'c-');
    xlabel(sprintf('%s in Pink — Line and Thrust...
        for max L/D in Cyan — Line'...
        ,plotoutLabelNames{11}));
else
    xlabel(sprintf('%s in Pink — Line',...
        plotoutLabelNames{11}));
end
ylim([min([plotout.signals.values...
        (50:length(plotout.time),9)];...
        plotout.signals.values(...
        50:length(plotout.time),11)])-100,...
    max([plotout.signals.values...
        (50:length(plotout.time),9)];...
        plotout.signals.values...
        (50:length(plotout.time),11)]+100)]
xlim([0,max(plotout.time)]);
set(gca,'xticklabel',[]);
grid on; hold off;

subplot(6,1,6)
plot(plotout.time,plotout.signals.values(:,20));
hold on;
plot(plotout.time,plotout.signals.values(:,24),'m-');
ylabel(plotoutLabelNames(20));
xlabel(sprintf('Time (Sec)\n...
    %s shown in Pink — Line',...
    plotoutLabelNames{24}));
ylim([min([plotout.signals.values...
        (2:length(plotout.time),20)];...
        plotout.signals.values...
        (2:length(plotout.time),24)])-10,...
    max([plotout.signals.values...
        (2:length(plotout.time),20)];...
        plotout.signals.values...
        (2:length(plotout.time),24)]+10)]);
xlim([0,max(plotout.time)]);
grid on; hold off;

if altLoop == 1 && controlLoop == 1 && distLoop == 1
    print('-dpsc','-r600','atAirspeedPlot1');
else
    print('-dpsc','-r600','-append','atAirspeedPlot1');
end

```

```

figure (2)
orient landscape;

subplot (5,1,1)
rhoCalc = 0;
cl = 0;
cd = 0;
clcdcalc = 0;
clcd = 0;
rhoCalc = plotout.signals.values(:,18)/ ...
    (1718 * (Temp(altLoop) + 459.7));
cl = plotout.signals.values(:,17)./(.5*S*rhoCalc.*...
    (plotout.signals.values(:,19).*1.6878).^2);
plot (plotout.time, plotout.signals.values(:,15));
hold on;
plot (plotout.time, cl, 'm—');
ylabel (sprintf ('CL'));
xlabel (sprintf ('Estimated CL in Pink — Line'));
title (sprintf ('%s: Alt = %d Ft, Control Type = %s, ...
    Disturbance = %s, Mach = %0.3g, X-Dist %7.5f nmi, ...
    Weight Final = %5.0f lbs', ...
    titleName, Ic_Alt, controlType, distTxt, Ic_Mach, ...
    max(plotout.signals.values(:,16))/6076.11549, ...
    plotout.signals.values(length(plotout.time),17)));
xlim ([0, max(plotout.time)]);
grid on; hold off;

subplot (5,1,2)
cd = CD0+K.*cl.^2;
plot (plotout.time, plotout.signals.values(:,14));
hold on;
plot (plotout.time, cd, 'm—');
ylabel (sprintf ('CD'));
xlabel (sprintf ('Estimated CD in Pink — Line'))

xlim ([0, max(plotout.time)]);
grid on; hold off;

subplot (5,1,3)
clcdcalc = cl./cd;
clcd = plotout.signals.values(:,15)./...
    plotout.signals.values(:,14);
plot (plotout.time, clcd); hold on;
plot (plotout.time, clcdcalc, 'm—');

```

```

ylabel('C_L\\C_D');
xlabel('Estimated C_L\\C_D in Pink — Line');
xlim([0,max(plotout.time)]);
set(gca,'xticklabel',[]);
grid on; hold off;

subplot(5,1,4)
tsfcLeft = plotout.signals.values(:,9)./...
    plotout.signals.values(:,11);
tsfcRight = plotout.signals.values(:,10)./...
    plotout.signals.values(:,12);
plot(plotout.time,tsfcLeft); hold on;
plot(plotout.time,tsfcRight,'m—');
ylabel('TSFC Left');
xlabel(sprintf('TSFC Right in Pink — Line'));
xlim([0,max(plotout.time)]);
grid on; hold off;

subplot(5,1,5)
uclcdtsfc = 0;
uclcdtsfcCalc = 0;
uclcdtsfc = plotout.signals.values(:,19)...
    .*1.6878.*cld./(tsfcLeft);
uclcdtsfcCalc = plotout.signals.values(:,19)...
    .*1.6878.*cldcalc./(tsfcLeft);
plot(plotout.time,uclcdtsfc); hold on;
plot(plotout.time,uclcdtsfcCalc,'m—');
ylabel(sprintf('V(L/D)/TSFC'));
xlabel(sprintf('
    ('Time (Sec)\nEstimated V(L/D)/TSFC...
    in Pink — Line')));
xlim([0,max(plotout.time)]);
grid on; hold off;

loopNum = loopNum+1;
resultData{loopNum,1}=sprintf('
    (%s: Alt = %d Ft, Control Type = %s,...
    Disturbance = %s, Mach = %4.3f,...
    X-Dist %5.3f nmi,...
    Weight Final = %5.0f lbs',...
    fileName,Ic_Alt,controlType,distTxt,Ic_Mach,...
    max(plotout.signals.values(:,16))/6076.11549,...
    plotout.signals.values(length(plotout.time),17));

if altLoop == 1 && controlLoop == 1 && distLoop == 1

```

```
        print( '-dpsc ', '-r600 ', 'atAirspeedPlot2 ');
    else
        print( '-dpsc ', '-r600 ', '-append ', 'atAirspeedPlot2 ');
    end

        end %distLoop
    end %controlLoop
end %altLoop

save( 'atAirspeedTestCaseData ', 'resultData ');
```

BIBLIOGRAPHY

- [1] Earth atmosphere model - imperial units. <http://www.grc.nasa.gov/WWW/K-12/airplane/atmos.html>, July 11 2008.
- [2] Specific heats. <http://www.grc.nasa.gov/WWW/K-12/airplane/specheat.html>, July 11 2008.
- [3] Speed of sound. <http://www.grc.nasa.gov/WWW/K-12/airplane/sound.html>, July 11 2008.
- [4] December 2008 airline traffic data: System traffic down 5.7 percent in December from 2007 and down 3.7 percent in 2008. http://www.bts.gov/press_releases/2009/bts012_09/html/bts012_09.html, 2009.
- [5] December 2009 airline traffic data: System traffic down 0.6 percent from December 2008. http://www.bts.gov/press_releases/2010/bts012_10/html/bts012_10.html, 2009.
- [6] Movements of an airplane. <http://visual.merriam-webster.com/transport-machinery/air-transport/movements-an-airplane.php>, 2010.
- [7] A. M. Shevtchenko A. P. Kurdjov, G. N. Natchinkina. Energy approach to flight control. In AIAA Guidance, Navigation, and Control Conference and Exhibit. AIAA, 1998.
- [8] Douglas L. Bader. Automatic throttle control for business and commuter aircraft. In 9th Digital Avionics Systems Conference, pages 205–211, Virginia Beach, VA, USA, 1990. IEEE, Piscataway, NJ, USA.
- [9] Charles W. Bert. Prediction of range and endurance of jet aircraft at constant altitude. Journal of Aircraft, 18(10):890–892, 1981. Compilation and indexing terms, Copyright 2008 Elsevier Inc. 82060005845 0021-8669.
- [10] Aydan Cavcar and Mustafa Cavcar. Approximate solutions of range for constant altitude - constant high subsonic speed flight of transport aircraft. Aerospace Science and Technology, 8(6):557–567, 2004.
- [11] Aydan Cavcar and Mustafa Cavcar. Impact of aircraft performance differences on fuel consumption of aircraft in air of management environment. Aircraft Engineering and Aerospace Technology, 76(5):502–515, 2004. Compilation and indexing terms, Copyright 2008 Elsevier Inc. 04508712658 0002-2667 Aircraft performance differences Aviation fuel Airworthiness.
- [12] Mustafa Cavcar and Aydan Cavcar. Comparison of generalized approximate cruise range solutions for turbojet/fan aircraft. Journal of Aircraft, 40(5):891–895, 2003.

- [13] Lee Chapman. Transport and climate change: a review. Journal of Transport Geography, 15(5):354 – 367, 2007.
- [14] Alison Duquette. Fact sheet, nextgen goal: Performance-based navigation. http://www.faa.gov/news/fact_sheets/news_story.cfm?newsId=8768, April 24, 2009.
- [15] Federal Aviation Administration. Advisory Circular 25.1329-1B: Approval of Flight Guidance Systems, July 17, 2006.
- [16] Federal Aviation Administration. Aeronautical Information Manual: Official Guide to Basic Flight Information and ATC Procedures, February 11, 2010.
- [17] Antonio Filippone. Operational aspects of transport aircraft on carbon-dioxide emissions. In 46th AIAA Aerospace Sciences Meeting and Exhibit; Reno, NV; USA; 7-10 Jan. 2008, number AIAA Paper 2008-195. American Institute of Aeronautics and Astronautics, 1801 Alexander Bell Drive, Suite 500, Reston, VA, 20191-4344, USA, 2008.
- [18] W. Grimm, K. H. Well, and H. J. Oberle. Periodic control for minimum-fuel aircraft trajectories. Journal of Guidance, Control, and Dynamics, 9(2):169–174, 1986.
- [19] John Griswold. Integrated flight and propulsion control system design for a business jet. In AIAA Guidance, Navigation, and Control Conference and Exhibit. AIAA, 2000.
- [20] G.P. Jayaraman. Modeling and design of an autothrottle speed control system. In Control and Automation, 2009. MED '09. 17th Mediterranean Conference on, pages 1190 –1195, June 2009.
- [21] Hassan K. Khalil. Nonlinear Systems. Prentice Hall, Upper Saddle River, NJ, third edition, 2002.
- [22] Donald E. Kirk. Optimal Control Theory: An Introduction. Dover Publications, Inc., 31 East 2nd Street, Mineola, NY 11501, 2004.
- [23] Steve Last and Martin Alder. British airways airbus a320 pilots' autothrust survey. pages 51 – 63, Long Beach, CA, USA, 1991.
- [24] Frank L. Lewis and Vassilis L. Syrmos. Optimal Control. John Wiley & Sons, Inc., 1995.
- [25] Andrew Macintosh and Lailey Wallace. International aviation emissions to 2025: Can emissions be stabilised without restricting demand? Energy Policy, 37(1):264 – 273, 2009.
- [26] Roy Myose, Trevor Young, and Gordon Sim. Comparison of business jet performance using different strategies for flight at constant altitude. In Collection of Technical Papers - AIAA 5th ATIO and the AIAA 16th Lighter-than-Air Systems Technology Conference and Balloon Systems Conference, volume 1, pages 254–265, Reston, VA 20191-4344, United States, 2005. American Inst. Aeronautics and Astronautics Inc.
- [27] Douglas M. Pargett and Mark D. Ardema. Flight path optimization at constant altitude. Journal of Guidance, Control, and Dynamics, 30(4):1197–1201, 2007.

- [28] Jan Roskam. Airplane Flight Dynamics and Automatic Flight Controls, Part 1. Design, Analysis and Research Corporation, Lawrence, KS 66044, 1998.
- [29] Jan Roskam. Airplane Flight Dynamics and Automatic Flight Controls, Part 2. Design, Analysis and Research Corporation, Lawrence, KS 66044, 2003.
- [30] Wilson J. Rugh and Jeff S. Shamma. Research on gain scheduling. Automatica, 36(10):1401 – 1425, 2000.